Genetic analysis of resistance to Fusarium stalk rot in sorghum (*Sorghum bicolor* (L) Moench)

by

Kinde Nouh Ketema

B.S., Haramaya University, 2006
M.S., Hawassa University, 2012

AN ABSTRACT OF A DISSERTATION

submitted in partial fulfillment of the requirements for the degree

DOCTOR OF PHILOSOPHY

Department of Agronomy
College of Agriculture

KANSAS STATE UNIVERSITY
Manhattan, Kansas

2023

Abstract

Sorghum is a climate-resilient C4 plant best suited for the drier areas of the world. It is the fifth most widely cultivated cereal for food, feed, and biofuel production. Fusarium stalk rot, caused by *Fusarium thapsinum,* is among the predominant sorghum diseases in Kansas, affecting economic traits including grain yield, sugar yield, quality, and biomass. Resistant variety is the most viable way to manage the disease and minimize the associated losses. Adequate knowledge of genetic mechanisms associated with the development of the disease is a prerequisite for progress toward developing resistant hybrids. This dissertation comprises three separate experiments aimed at understanding the genetics of stalk rot resistance in sorghum, identifying genes and/or genomic regions associated with the disease, understanding molecular pathways responsible for resistance, and assessing the potential of selected resistant lines as parents for resistance breeding.

The first experiment focuses on mapping QTLs associated with disease resistance and dissecting the QTL by environment interactions. Two hundred and thirty-three recombinant inbred lines (RILs) developed from crosses of BTx3042 (susceptible) × SC599 (resistant) were evaluated for reaction to infection by *F. thapsinum* in the 2018, 2019, and 2020 field seasons. The genotypes were artificially inoculated by *F. thapsinum,* and disease development was rated as lesion length and the number of diseased nodes. Flowering time, plant height, and lodging data were recorded. The RILs were genotyped using genotyping-by-sequencing, and 3297 polymorphic SNP markers were used for linkage mapping and QTL analysis. The analysis of phenotypic data showed significant differences and transgressive segregation for disease parameters. Heritability was 66% for major lesion length and 92% for plant height. The SNPs covered 3070.8 cM with an average distance of 1.8 cM between markers. Inclusive composite interval mapping detected four stable

additive QTLs across environments on chromosomes 1, 3, 5, and 9 for major lesion length. The results from this study may serve as a basis for future mapping studies on Fusarium stalk rot to aid resistant germplasm development through breeding.

In the second experiment, the RIL founder parents, SC599 (resistant) and BTx3042 (susceptible), were used for the transcriptome analysis to investigate genes regulating disease resistance and identify the molecular basis of host plant resistance. Early activation of the defense response was observed in the resistant line at 24 hours post-infection (hpi). Differentially expressed genes (DEGs) such as nucleotide-binding site leucine-rich repeat (SbRWRKY1, SbLRx4, and Sobic.005G226400), pathogenesis-related (PR10 Sobic.001G401200), disease resistance-response (Sobic.009G021300), wall-associated kinase (Sobic.008G170800 and Sobic.002G249600), peroxidase (*SbPrx34* and *SbPrx30),* chalcone synthase (*SbCHS1* and *SbCHS5*), and flavonoid synthase genes (*SbDFR3*) were upregulated in the resistant and downregulated in the susceptible genotypes at 24 hpi. The resistant genotype displayed a time-regulated transcriptome response showing that defense regulation might be related to the pathogen's hemi-biotrophic nature. This result provides a foundation for future studies to understand genes and pathways involved in the molecular mechanisms of Fusarium stalk rot resistance in sorghum.

The third experiment aimed to identify the genetic mechanisms associated with stalk rot resistance, lodging, and agronomic traits and pinpoint key traits related to stalk rot resistance. Sixty-one lines from the BTx3042 (susceptible) × SC599 (resistant) RIL population representing the susceptible, intermediate, and resistant categories were crossed with three standard seed parents in a factorial mating design to generate 183 F1 hybrids. The hybrids and 64 inbred parents

were grown in an alpha lattice incomplete block design in three replications at four environments in Kansas. Data were collected on days to flowering, plant height, major lesion length, total lesion length, number of diseased nodes, grain yield, and stalk lodging. Significant differences were observed between entries for all traits. Likewise, the male and female effects and their interaction with the environment were significant for most traits, indicating that the general combining ability (GCA) effect had a large role in regulating plant response to *F. thapsinum* infection. The male-by-female interaction effect also known as the specific combining ability (SCA) was also significant. Grain yield had a negative genotypic correlation with all disease traits and lodging, indicating that stalk rot infection does affect yield performance.

Genetic analysis of resistance to Fusarium stalk rot (*Fusarium thapsinum*) in sorghum (*Sorghum bicolor* (L) Moench)

by

Kinde Nouh Ketema

B.S., Haramaya University, 2006
M.S., Hawassa University, 2012

A DISSERTATION

submitted in partial fulfillment of the requirements for the degree

DOCTOR OF PHILOSOPHY

Department of Agronomy
College of Agriculture

KANSAS STATE UNIVERSITY
Manhattan, Kansas

2023

Approved by:

Co-Major Professor
Dr. Ramasamy Perumal

Approved by:

Co-Major Professor
Dr. Tesfaye Tesso

Copyright

Abstract

Sorghum is a climate-resilient C4 plant best suited for the drier areas of the world. It is the fifth most widely cultivated cereal for food, feed, and biofuel production. Fusarium stalk rot, caused by *Fusarium thapsinum*, is among the predominant sorghum diseases in Kansas, affecting economic traits including grain yield, sugar yield, quality, and biomass. Resistant variety is the most viable way to manage the disease and minimize the associated losses. Adequate knowledge of genetic mechanisms associated with the development of the disease is a prerequisite for progress toward developing resistant hybrids. This dissertation comprises three separate experiments aimed at understanding the genetics of stalk rot resistance in sorghum, identifying genes and/or genomic regions associated with the disease, understanding molecular pathways responsible for resistance, and assessing the potential of selected resistant lines as parents for resistance breeding.

The first experiment focuses on mapping QTLs associated with disease resistance and dissecting the QTL by environment interactions. Two hundred and thirty-three recombinant inbred lines (RILs) developed from crosses of BTx3042 (susceptible) × SC599 (resistant) were evaluated for reaction to infection by *F. thapsinum* in the 2018, 2019, and 2020 field seasons. The genotypes were artificially inoculated by *F. thapsinum*, and disease development was rated as lesion length and the number of diseased nodes. Flowering time, plant height, and lodging data were recorded. The RILs were genotyped using genotyping-by-sequencing, and 3297 polymorphic SNP markers were used for linkage mapping and QTL analysis. The analysis of phenotypic data showed significant differences and transgressive segregation for disease parameters. Heritability was 66% for major lesion length and 92% for plant height. The SNPs covered 3070.8 cM with an average distance of 1.8 cM between markers. Inclusive composite interval mapping detected four stable

additive QTLs across environments on chromosomes 1, 3, 5, and 9 for major lesion length. The results from this study may serve as a basis for future mapping studies on Fusarium stalk rot to aid resistant germplasm development through breeding.

In the second experiment, the RIL founder parents, SC599 (resistant) and BTx3042 (susceptible), were used for the transcriptome analysis to investigate genes regulating disease resistance and identify the molecular basis of host plant resistance. Early activation of the defense response was observed in the resistant line at 24 hours post-infection (hpi). Differentially expressed genes (DEGs) such as nucleotide-binding site leucine-rich repeat (SbRWRKY1, SbLRx4, and Sobic.005G226400), pathogenesis-related (PR10 Sobic.001G401200), disease resistance-response (Sobic.009G021300), wall-associated kinase (Sobic.008G170800 and Sobic.002G249600), peroxidase (*SbPrx34* and *SbPrx30),* chalcone synthase (*SbCHS1* and *SbCHS5*), and flavonoid synthase genes (*SbDFR3*) were upregulated in the resistant and downregulated in the susceptible genotypes at 24 hpi. The resistant genotype displayed a time-regulated transcriptome response showing that defense regulation might be related to the pathogen's hemi-biotrophic nature. This result provides a foundation for future studies to understand genes and pathways involved in the molecular mechanisms of Fusarium stalk rot resistance in sorghum.

The third experiment aimed to identify the genetic mechanisms associated with stalk rot resistance, lodging, and agronomic traits and pinpoint key traits related to stalk rot resistance. Sixty-one lines from the BTx3042 (susceptible) × SC599 (resistant) RIL population representing the susceptible, intermediate, and resistant categories were crossed with three standard seed parents in a factorial mating design to generate 183 F1 hybrids. The hybrids and 64 inbred parents

were grown in an alpha lattice incomplete block design in three replications at four environments in Kansas. Data were collected on days to flowering, plant height, major lesion length, total lesion length, number of diseased nodes, grain yield, and stalk lodging. Significant differences were observed between entries for all traits. Likewise, the male and female effects and their interaction with the environment were significant for most traits, indicating that the general combining ability (GCA) effect had a large role in regulating plant response to *F. thapsinum* infection. The male-by-female interaction effect also known as the specific combining ability (SCA) was also significant. Grain yield had a negative genotypic correlation with all disease traits and lodging, indicating that stalk rot infection does affect yield performance.

Table of Contents

List of Figures

List of Tables

Acknowledgments

My stay at K-State was not smooth. It had difficulties. This work would not have been successful without the support of many colleagues, classmates, family, and friends. I am deeply thankful to my advisers, Dr. Tesfaye Tesso and Dr. Ramasamy Perumal, for their advice, support, encouragement, and constructive critique. I would also like to thank my committee members for their editorial input to my draft dissertation and assistance throughout my research. In addition, Dr. Sanzhen Liu advised on the experimental procedures and provided codes for the analysis of RNA-seq, and Dr. Christopher Little assisted with several issues and continuously supplied pathogen inoculum. My special gratitude goes to Dr. Sandeep Marla for technical support in the data analysis and edition, encouragement, and providing helpful comments. I am thankful to Dr. Alina Akhunova and her team, Dr. Gui Bai and his team, Natalie Waite, and Dr. Afsana Noor for their support at various stages of my work.

Dr. Vara Prasad, thanks for the support on my GBS genotyping. I am thankful to Kansas Grain Sorghum Commission for the financial support of this study. I am also thankful to the Computing and Information Sciences Department, Kansas State University, for availing the Beocat computing cluster for storing and analyzing genomic data. Thanks to my lab mates, Dr. Dereje Dugassa, Mr. Diriba Chere, Dr. Yemane Belaineh, and Mr. Daniel Hopper, for the support and good moments. Thank you! I express my deepest gratitude to Mr. Robert Berry, Mrs. Teresa Wille, Mrs. Nancy Williams, and Mrs. Karlene Teske for their help during my stay.

Finally, my wife, the strongest woman in my life, without her support, I would not be able complete this work. Thanks, Tigist Setegn, Miki, Mara, and Kalo, for your support, encouragement, and understanding. Thanks, Gashe and Eto, for the support and prayers. We did it all together!

Dedication

This work is dedicated to the most important people in my life: my loving wife, Tigist Setegn, our brave children, and my parents, Worknesh Yeda and Nouh Ketema.

CHAPTER 1 – LITERATURE REVIEW

Sorghum is a climate-resilient C4 plant best suited for the drier areas of the world. The crop is mainly produced as a major source of food and feed; recently, it has found a new application as a feedstock source for biofuel production. The crop is believed to have originated in northeastern Africa in a vast region recognized today as Sudan, Eritrea, and Ethiopia (Doggett, 1970). However, currently, it is cultivated in both tropical and temperate regions. The cultivated sorghum belongs to the Poaceae family, the genus *Sorghum*, and the species *bicolor*. Cultivated sorghum is classified into five botanical and ten intermediate races primarily based on spikelet and panicle architecture and grain attributes (Harlan and de Wet, 1972). The five primary races of sorghum include *bicolor, guinea, kafir, caudatum,* and *durra*. These races are distributed throughout sorghum-growing regions based on adaptive features and racial characteristics. For example, the guinea sorghum's full glume coverage and bending peduncles is considered an adaptation mechanism in high rainfall areas where grain molding pathogens are prevalent. Likewise, the compact-headed *dura* is dominant in dry areas not only for its drought adaptation but also because it is not suitable for wet environments due to the compact head retaining moisture and exposing the grain to molding pathogens.

1.1 Overview of sorghum production and productivity

Sorghum is the fifth most widely cultivated cereal globally. In 2020, 58.7 million tons of sorghum was produced from 40 million hectares globally, with average productivity of 1.5 tons per hectare (t/ha) (FAO, 2021). It is produced on all continents inhabited by humans. According to the FAOSTAT (2021), 47% of the global grain sorghum is produced in Africa, 16% in North America,

and another 16% in Asia. However, the higher production in Africa and Asia is primarily due to the larger area planted to the crop. In North America, higher production is due to higher productivity (Figure 1.1). On average, the productivity in North America, East Asia, and Europe (4.5 t/ha) was remarkably high, while Africa and South Asia have the lowest average yield of about 1 t/ha (Figure 1; FAO, 2021). Several reasons can be cited for this difference, but one conspicuous factor is that low-yielding non-hybrid cultivars dominate the production landscape in Africa and South Asia while the other regions have fully adopted hybrid technology. Other factors, such as improved crop management, may also have contributed to the yield difference that goes along with the adoption of hybrids. Despite that, sorghum yields in countries such as Sudan and Niger are among the lowest in the world, where it is grown as a staple food crop on large acres. Environmental stresses, especially drought, appear to be the major limiting factor.

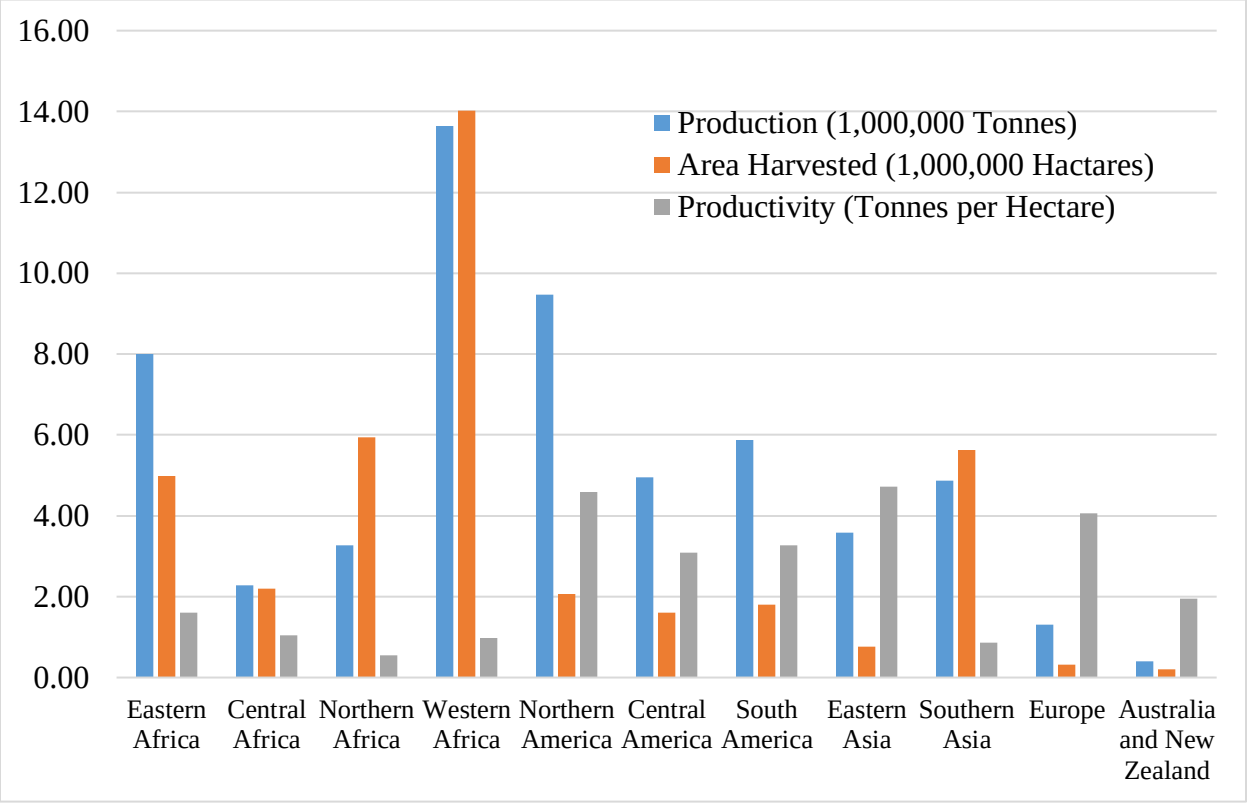

Figure 1-1. Regional sorghum production, area harvested, and productivity (Source: FAO,2021)

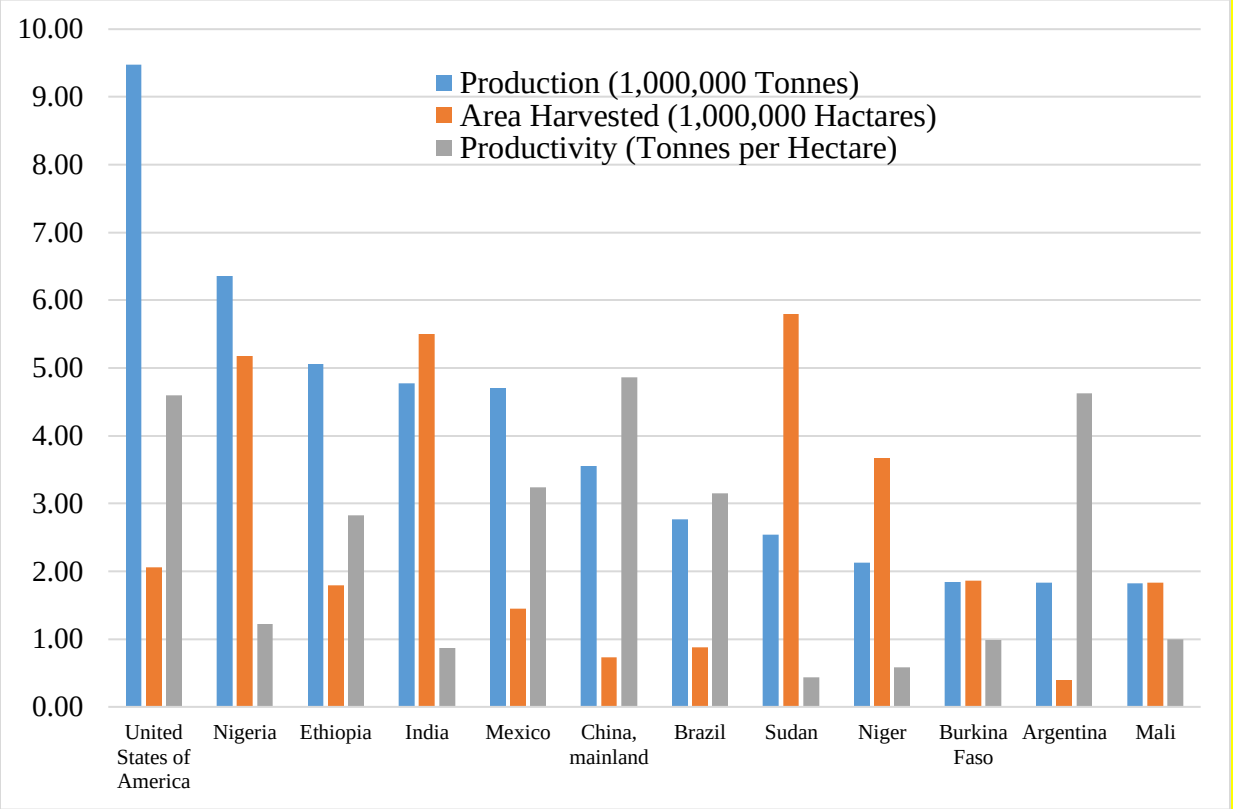

Figure 1-2. Sorghum production, area harvested, and productivity for the top sorghum producing countries of the world (Source: FAO,2021)

1.2 Stalk rot diseases and the economic importance

Stalk rots, as the name implies, are diseases of the stalks and roots caused by several groups of pathogens. Many crops, including sorghum, suffer from these diseases. Under severe conditions, infection by stalk rots can lead to crop lodging, poor grain fill, and even plant death, resulting in significant economic losses (Claflin and Giorda, 2008; Tesso et al., 2005). In sorghum, stalk rots are caused by a variety of fungal pathogens. The major stalk rot diseases of sorghum are charcoal rot caused by *Macrophomina phaseolina* (Tassi) Goidanich and Fusarium stalk rot caused by

different *Fusarium spp.* In addition, these pathogens cause several other diseases in different crops, including seedling blight in maize and sorghum; grain mold in sorghum; leaf spots, ear and kernel rot in maize; Fusarium wilt, sudden death syndrome, and pod rot in soybean (Leslie, 1990). Fusarium stalk rot caused by *F. thapsinum* is among the predominant type of stalk rots in Kansas (Jardine & Leslie, 1992), and the pathogen is the most virulent species affecting sorghum (Leslie et al., 2005; Tesso et al., 2010).

Infection by Fusarium stalk rot pathogens is favored by cool, wet weather followed by hot, dry conditions (Zummo, 1984; Tesso et al., 2012). The symptoms caused by different *Fusarium* species are similar, and they are visible when infected stalks are split longitudinally (Jardine, 2006). Stalk rot pathogens infect susceptible hosts at any growth stage (Claflin & Giorda, 2008). However, the disease remains latent and begins to develop several weeks after pollination, with the infected regions developing a characteristic dark red or purple discoloration or shredded tan lesions (Claflin and Giorda, 2008). The infected plants are often characterized by a weak stem, which easily crashes when pressed by hand or breaks when pushed lightly (Jardine, 2006). Fusarium stalk rot is different from charcoal rot in that it spreads slowly with less tissue disintegration and reduced intensity of pigmentation (Zummo, 1984). Environmental stresses like drought or heat often weaken the plant immunity and increase disease severity favoring secondary infection, the impact of which could be devastating (Zummo, 1984; Tesso et al., 2012). Generally, stalk rot disease development occurs late in the season after pollination and seed set though the infection could have started early. The disease develops when the host condition is weakened due to the remobilization of water and nutrients during grain filling or exposure to a stressful environment (Leslie et al., 2005).

The impact of stalk rot diseases is not limited to grain yield. It can also affect biomass and sugar yield in sweet sorghums, significantly reducing stover and sugar quality and quantity (Das et al., 2008; Bandara et al., 2017). Older reports show that the average grain loss due to Fusarium stalk rot was about 4%, but the loss can reach 50% in locations with a higher incidence of the disease (Jardine and Leslie, 1992). In the United States, stalk rot-induced lodging in high-yielding hybrids can reach as high as 60% during severe weather conditions, and the resulting economic loss can surpass $15 million annually (Jardine, 2006). This loss, which could become even higher under adverse weather conditions, warrants investment to develop hybrids resistant to stalk rot pathogens. Unfortunately, breeding efforts to develop hybrids with horizontal resistance were minimal, and thus the crop's economic potential was not fully exploited (Jardine & Leslie, 1992; Tesso et al., 2004). The slow nature of breeding for polygenic traits and the tedious and time-consuming artificial inoculation and disease-scoring procedure for germplasm screening caused a delay in the development of resistant hybrids. Indirect selection for traits associated with stalk rot resistance, such as stay-green, might help enhance standability (Funnell-Harris et al., 2014; Adeyanju et al., 2015). Brown midrib traits, though they can suppress the development of the disease due to higher stalk sugar, may not be of much use since the traits also contribute to weaker stalks due to reduced lignification. Nevertheless, chlorophyll content and leaf temperature (indicators of crop drought response) were not associated with stalk rot disease resistance and yield (Perumal et al., 2020).

1.3 Genetic improvement and its progress in sorghum

Compared to the global average of 1.5 t/ha, the average sorghum yield (4.6 t/ha) in the United States is significantly higher, which may be attributed to various causes. The historical national

yield data recorded over 61 years (1930-1990) showed that sorghum yield in the United States increased by 50 kg per hectare per year (Eghball & Power, 1995). Simply stated, sorghum yield has improved by 3 tons over the last six decades to reach today's yield level of 4.6 t/ha (Eghball & Power, 1995). Improved crop genetics, especially the adoption of hybrid cultivars, is one of the factors that drove yield increases. However, reports of genetic improvement's contribution are inconsistent across the board. Miller & Kebede (1984) reported that 40% yield improvement gained up until that time was due to genetics. A later report indicated that out of a total of 139 % yield increase from 1956 to 1997, 93% was due to improved management and associated factors, and the remaining 46% was due to genetic improvement (Unger & Baumhardt, 1999). On the other hand, Assefa and Staggenborg (2011) reported that the contribution of genetic improvement to sorghum grain yield over the last sixty years was 60 to 65%. This agrees with the latest report by Pfeiffer et al. (2019), where genetic improvement was shown to have contributed about 60% to sorghum yield increase since the 1950s with an average annual increase of 0.121 t/ha. Moreover, genetic improvement is a continuous process, unlike agronomic management, which is more or less fixed.

However, genetic improvement of sorghum, especially hybrid breeding, is not straightforward. Sorghum hybrid seed production is more complicated than that of maize. Sorghum hybrid development is based on cytoplasmic male sterility and involves three parental lines (Rooney, 2004), the A-lines (cytoplasmic male sterile females) and B-lines (female maintainers) as part of the seed parents, and the R-lines a the male or pollen parents (Lambright, 2019). Sorghum hybrid breeding, therefore, starts with improving and identifying the most suitable B and R lines and then converting the B line into the corresponding sister A-line (Lambright, 2019; Rooney, 2004). Then hybrids are synthesized by intercrossing the A and R lines. The testcross

hybrids are evaluated to see the performance of the parental lines in a hybrid combination known as combining ability, an important genetic parameter defining the value of a line as a breeding parent. After multiple years of evaluation, hybrids are selected and recommended for production in environments they deem fit. Sorghum hybrid development also requires the continued maintenance of the three parent systems.

Therefore, the two most important activities in hybrid crop breeding are finding agronomically suitable parental lines and evaluating them in hybrid combinations across environments to select the best combination of hybrids for commercial deployment. The two essential genetic elements defining the value of lines and crosses in plant breeding are general combining ability (GCA) and specific combining ability (SCA). GCA is the mean performance of a line in a hybrid combination with several other lines. It is a measure of additive genetic effect, and lines with higher GCA are often preferred as breeding parents. On the other hand, SCA is the performance of a given cross relative to the mean performance of several other crosses. Two lines that provide the best SCA in cross combination with each other may or may not express the same performance when crossed to other lines. Hence, unlike lines with good GCA that can generate superior hybrids in combination with several other lines, a good SCA may or may not be repeated in other crosses. Heterosis, also known as hybrid vigor, is a relative superiority of a hybrid over its parents (Hallauer et al., 2010). In sorghum, genetic improvement in the inbred parent was slower than the gain in hybrids observed in the long-term selection, showing a significant role of heterosis for hybrid performance (Pfeiffer et al., 2019). Nevertheless, the genetic basis of heterosis is not yet clear. Dominance, overdominance, and epistasis-based hypotheses were reported in different crops (Schnell & Cockerham, 1992)

Despite the impressive yield gains through developing high-yielding hybrids, significant yield losses also occur due to lodging caused by various factors like stalk rot diseases. Post-flowering drought stress also aggravates stalk rot diseases, especially in high-yielding hybrids that tend to pull a higher proportion of assimilates from the stalk, resulting in stalk collapse. Although the degree may vary, almost all hybrids suffer from lodging (Jardine, 2006). Despite the significant genetic variation for the trait (Adeyanju et al., 2015; Perumal et al., 2020), the classical breeding method for stalk rot resistance is generally slow for various reasons such as the lack of high throughput disease phenotyping procedure, and the influence of environment on disease development. Though not associated to stalk rot resistance, direct selection for stalk strength may contribute to standability. It is a heritable trait, and selection for stalk strength has positively contributed to lodging resistance in both maize and sorghum (Gomez et al., 2020; Wang et al., 2022). The inheritance of both stalk rot resistance and stalk strength appears to be quantitative (Das et al., 2008). Therefore, breeding efforts to improve stalk strength and rot resistance simultaneously can significantly improve standability. However, given the polygenic nature of both traits, such an endeavor may not be straightforward. Marker technologies may help overcome such difficulty, provided such tools are available. Next-generation sequencing (NGS) technology has provided an opportunity for scanning the entire genome of organisms. Combined with emerging data science, the new technology may help get close to specific genomic regions associated with traits of interest (Elshire et al., 2011; Jamann et al., 2015). One of the focuses of this dissertation is to map genomic regions associated with stalk rot resistance in sorghum.

1.4 Genetic mapping and QTL analysis

Various molecular tools have been developed to map quantitative trait loci (QTL) for different traits in several crops. A QTL is a chromosomal region containing genes influencing the expression of quantitative traits. QTL analysis is a statistical procedure used to find a specific chromosomal region that has a genetic effect on the variability of specific traits of interest by associating the trait value with genotypic data (Lynch and Walsh, 1998). It combines DNA marker data and phenotypic information from the target mapping population to find a correlation between a DNA marker and phenotype data. In addition to its use in marker-assisted selection, QTL maps can be further resolved by adding more markers and can eventually lead to the discovery of the causal gene. A high-density genetic map is vital for identifying those chromosomal regions that control quantitative traits (Collard et al., 2005; Doerge, 2002). Several major effects QTL have been used in breeding programs in marker-assisted selection in different crops. Some of such QTLs or genes used for genetic improvement in sorghum include $Ma_{1\text{-}6}$ controlling flowering time, the *lgs* QTL for *Striga* resistance, and stay-green QTLs for post-flowering drought tolerance (Childs et al., 1997; Kebede et al., 2001; Haussmann et al., 2004; Satish et al., 2012).

In QTL mapping and marker-assisted breeding, F_2, double haploid, recombinant inbred lines (RILs), nested association mapping (NAM), multi-parent advanced generation intercross (MAGIC), backcross populations, and near-isogenic lines (NILs) can be used as a mapping population. Such populations should involve two or more parents contrasting for the trait(s) of interest to provide sufficient segregation for the trait (Myles & Wayne, 2008). In sorghum, various mapping resources have been developed by public programs at different times. For example, a

NAM population involving ten founder parents with diverse genetic backgrounds that vary for traits, including yield, grain quality, and abiotic and biotic stress tolerance, has been developed (Perumal et al., 2021). Moreover, a highly robust sorghum MAGIC population developed through multiple generations of random mating has become available for trait dissection (Ongom & Ejeta, 2018). At the same time, various types of recombinant inbred populations have been developed to study QTLs underlying specific traits such as post-flowering drought tolerance, cold tolerance, and stalk rot resistance. In addition, near-isogenic lines (NILs) were developed and used to identify and characterize anthracnose resistance genes (Mewa et al., 2022). Other unique RILs were used for genetic analysis to discover and characterize molecular components of food crops that influence the human gut microbiome (Yang et al., 2022).

In addition to a robust population, QTL mapping and gene identification also require appropriate genotyping techniques that allow for the detection of polymorphisms. These tools and techniques have evolved over the last few decades, each advancement adding power and reducing cost. Today, single nucleotide polymorphic (SNP) markers developed through genotyping-by-sequencing (GBS) techniques are routinely utilized for mapping and molecular marker development studies. SNP markers are preferred over all other marker systems in that they can detect polymorphisms at the nucleotide level (Brookes, 1999; Elshire et al., 2011). They are ubiquitous in the genome, reproducible, and cost-effective (Brookes, 1999; Elshire et al., 2011).

Over the years, many advances have been made in QTL mapping and the development of new statistical methods to identify significant QTL trait associations. These include single marker analysis (Haley & Knott, 1992), simple interval mapping (Zeng, 1993), composite interval mapping (Kao et al., 1999; Li et al., 2007), inclusive composite interval mapping, and multiple

QTL mapping (Meng et al., 2015). Single marker analysis involves testing the association between a single genetic marker and a trait of interest, which is useful when the marker effect is expected to be strong (Haley & Knott, 1992). Simple interval mapping is used to identify QTLs based on the location of genetic markers relative to a trait of interest and is preferred when the number of QTL affecting the trait is small, and the effect of each QTL is moderate to strong (Zeng, 1993). Composite interval mapping is a method that combines the strengths of single marker analysis and simple interval mapping to increase the accuracy of QTL mapping (Kao et al., 1999). Finally, inclusive composite interval mapping is a modification of composite interval mapping that accounts for the effects of other QTLs while mapping a particular QTL (Li et al., 2007). It is primarily applicable when multiple QTLs affect the trait, and their effects are correlated (Li et al., 2007). Various statistical tools are used to detect the association between markers and the trait and determine the degree to which such associations occur. The common statistical methods are regression, maximum likelihood, and Bayesian models (Li et al., 2007; Meng et al., 2015).

1.5 Genetic mechanism and mapping for stalk rot resistance in sorghum

The use of resistant varieties is the most viable approach to reduce sorghum yield losses incurred due to stalk rot diseases. However, the lack of efficient inoculation and disease scoring procedures makes the resistance breeding effort complicated and cumbersome. Both procedures are tedious and challenging to apply to large numbers of breeding materials. The use of modern genetic markers, if available, may simplify the breeding process and accelerate the effort. Stalk rot resistance in sorghum appears to be quantitative with a dominant mode of inheritance (Thakur et al., 1996; Tesso et al., 2005; Adeyanju et al., 2015). However, Pecina-Quintero et al. (1999) reported both additive and nonadditive effects contributing to charcoal rot resistance.

Adeyanju et al. (2015) conducted a genome-wide association analysis on the global sorghum association panel (SAP) to discover and map loci associated with resistance to stalk rot diseases and identified multiple candidate genes associated with resistance to *F. thapsinum*. They discovered two stable QTLs (Sb09g029260 and Sb09g029260) on chromosome 9 and ten location-specific QTLs. The same study also reported four additional SNPs associated with resistance genes in chromosomes 2, 7, 8, and 9. In addition, Reddy et al. (2008) reported three stable QTLs for charcoal rot (*Macrophomina phaseolina*) resistance across locations. Similarly, Patil et al. (2012) identified morphological and biochemical traits associated with QTL for charcoal rot resistance. Similarly, Mahmoud et al. (2018) reported 13 QTL significantly associated with charcoal rot resistance. Wang et al. (2020) reported 12 QTLs for lodging resistance and claimed that they were identical to the QTLs reported by Reddy et al. (2008) and Adeyanju et al. (2015) on charcoal and Fusarium stalk rots.

1.6 Transcriptome and functional analysis of stress response reaction in plants

RNA-seq is one of the next-generation sequencing (NGS) technologies that revolutionized transcriptome profiling to measure gene expression by utilizing cDNA obtained from the reverse transcription of mRNA (Wang et al., 2009; Metzker, 2010). RNA-seq helps to identify, quantify, characterize gene expression, and validate the gene annotation and prediction in a functional study (de Sá et al., 2018). In addition, RNA-seq provides information on alternative splicing and non-coding RNAs (Conesa et al., 2016; Costa-Silva et al., 2017). The typical steps in RNA-seq analysis after the conversion into cDNA are adapter ligation, single-end (uni-directional) or paired-end (bi-directional) sequencing, alignment into reference genome or de novo assembly, and statistical analysis (Wang et al., 2009). Data processing, statistical procedures, and software to process the

data may vary based on the type of data (sample, gene, transcript, and exon levels) and study objectives (Costa-Silva et al., 2017; Li et al., 2019). RNA-seq data analysis involves quality control, gene expression profiling, transcriptome profiling, functional profiling, visualization, and data integration (Conesa et al., 2016; Costa-Silva et al., 2017; Garg, 2021). Differential expression analysis is one of the most widely applied methods in RNA-seq studies that utilize gene and transcript expression values compared among paired samples (Conesa et al., 2016; Stark et al., 2019; Garg, 2021). In addition, functional profiling through different methods like gene ontology (GO) and pathway enrichment analysis characterizes the biological processes, molecular function, and cellular components in which differentially expressed genes are involved (Thomas, 2017).

RNA-seq studies in plant stress responses quantify and compare differentially expressed upstream and downstream genes and transcripts associated with stress responses that include different defense mechanisms. In a typical plant host defense reaction, multiple response mechanisms are involved. Many authors conducted RNA-seq analysis in sorghum to study disease reactions and other environmental stresses. For example, Gelli et al. (2014, 2016, 2017) studied the response to nitrogen (N) stress between high and low nitrogen use efficiency (NUE) recombinant inbred lines. Fracasso et al. (2016) studied drought response gene expression between genotypes with contrasting water use efficiency, and Marla et al. (2017) conducted transcriptome analysis to understand the molecular signature of chilling tolerance in tolerant and susceptible genotypes. Similarly, Fu et al. (2020), Cui et al. (2021), and Natarajan et al. (2021) performed differential gene expression analysis for anthracnose in sorghum genotypes with contrasting disease reactions that showed MAMP-triggered reactive oxygen species (ROS) and transcriptional responses. Likewise, Adhikari et al. (2021) conducted transcriptional analysis on maize and sorghum in response to the fungal pathogen *Exserohilum turcicum* infection to examine the

differential expression of orthologs in both hosts. Nida et al. (2021) studied sorghum's global transcription profile to understand the genetic, molecular, and biochemical components of grain mold resistance. Serba et al. (2021) conducted a transcriptome analysis to explain the molecular mechanisms underlying sugarcane aphid resistance. These works contributed to a body of knowledge on sorghum by unraveling pathways for discovering novel abiotic stress and disease-resistance genes.

However, only a few gene expression studies have been conducted on sorghum stalk rot disease response. Sharma et al. (2014) studied the role of defense genes, chitinase, and stilbene synthase in resistant and susceptible sorghum genotypes infected with *M. phaseolina*. The result showed a higher level of expression of the genes in the resistant genotypes over the susceptible ones. Bandara et al. (2018) reported an increased expression of cell-wall-degrading enzymes (pectin methylesterase, polygalacturonase, cellulase, endoglucanase, and glycosyl hydrolase) in *M. phaseolina* susceptible sorghum genotypes compared to the resistant genotypes. In a study by Funnell-Harris et al. (2019), over-expressing genes of monolignol biosynthesis introgressed *bmr* lines tested for their reaction to infection by two stalk rot pathogens (*F. thapsinum* and *M. phaseolina*) from greenhouse and field evaluations and showed a higher level of resistance gene expression when compared to wild-type lines.

1.7 Molecular mechanisms involved in quantitative disease resistance against *Fusarium* spp.

Plant pathogenic fungi could be biotrophic, necrotrophic, or hemi-biotrophic based on their lifestyle after infection. Biotrophic pathogens depend on living host cells and tissues for nutrients and often produce lesser amounts of cell wall degrading enzymes and effectors to suppress the

host immunity (Stergiopoulos and De Wit, 2009; Wang et al., 2014). In contrast, necrotrophic fungal pathogens depend on the dead host tissues due to pathogenesis and induced cell necrosis through the secretion of phytotoxins and increased levels of ROS (Horbach et al., 2011). However, hemi-biotrophic fungal pathogens have both the nature of biotrophs in the early stages and necrotrophy in the later stage of their lifecycle, where they produce toxins to kill the host tissues to obtain nutrients (Horbach et al., 2011). *Fusarium* spp. is a hemi-biotrophic pathogen with biotrophic properties during the initial stages of infection and changes to necrotrophy in later stages (Lyons et al., 2015; Robles-Barrios et al., 2022).

In a typical plant host defense reaction, multiple response mechanisms are involved. They are broadly classified into qualitative and quantitative disease resistance (Roux et al., 2014; French et al., 2016; Corwin and Kliebenstein, 2017; Delplace et al., 2020). Qualitative disease resistance is a complete resistance controlled by a single or few major resistance (R) genes (often nucleotide-binding domain leucine-rich repeat (NLR) receptors) with a significant effect (Roux et al., 2014; Delplace et al., 2020). Quantitative disease resistance (QDR), an incomplete resistance controlled by several genes with minor effects, has durable broad-spectrum resistance that regulates most host-pathogen interactions (Roux et al., 2014; Niks et al., 2015; Corwin and Kliebenstein, 2017). There is no clear distinction between qualitative and quantitative disease resistance except for the degree to which the genes regulate resistance (Poland et al., 2009). Incomplete MTI or ETI resistance can be considered QDR (Kushalappa et al., 2016). Although this classification does not always indicate the mode of inheritance (Mendelian/qualitative and quantitative), it shows the level of resistance phenotypically (Niks et al., 2015). Some qualitatively inherited genes can be involved in quantitative resistance (Niks et al., 2015).

There is a two-tiered innate initial defense system in plants considered to have qualitative disease resistance when they bring complete immunity (Zhang et al., 2013; Kushalappa et al., 2016; Corwin and Kliebenstein, 2017). The first is the frontline defense, pathogen or microbe-associated molecular patterns (P/MAMP)-triggered immunity (P/MTI (Roux et al., 2014; Segonzac and Zipfel, 2011). Transmembrane pattern recognition receptors (PRRs) recognize P/MAMPs and activate P/MTI (Jones & Dangl, 2006). However, some pathogen secretes effectors to suppress PTI, and the plant perceives those effectors and activates the effector-triggered immunity (ETI) as the second defense layer (Monaghan and Zipfel, 2012; Roux et al., 2014; Kushalappa et al., 2016; Patin et al., 2019). Qualitative disease resistance often results in cell and tissue death due to the hypersensitive response (HR) and is effective against biotrophs (Zhang et al., 2013). In addition, the defense system against biotrophic pathogens follows salicylic acid (SA) dependent signaling and defense pathways, which initiates systemic acquired resistance (SAR) (Glazebrook, 2005). This defense mechanism might be necessary for Fusarium stalk rot to reduce infection during the early infection cycle while the pathogen is in its biotrophic life cycle. However, in the later stage, increased HR would contribute to successful pathogenesis and susceptibility as the pathogen's life cycle becomes necrotrophic. Programmed cell death in the host is a perfect method for acquiring nutrients for the pathogen (Basavaraju et al., 2009; Sharma et al., 2014; Nida et al., 2021). R-gene-mediated qualitative resistance is rarely reported in necrotrophic pathogens (Poland et al., 2009). Nevertheless, the pathogen could often overcome R-gene-mediated resistance through an evolutionary arm race (Roux et al., 2014).

Partial resistance or reduced susceptibility due to incomplete suppression of PTI by pathogen effectors, weaker immunity by PTI or ETI, and permitting pathogen progression is referred to as quantitative disease resistance (QDR) (Niks et al., 2015). It is durable as the pathogen

pressure is countered by several minor effect genes (Niks et al., 2015). QDR is effective against hemi-biotrophic and necrotrophic pathogens (Zipfel, 2009; Segonzac & Zipfel, 2011; Balint-Kurti, 2019). Hence, the QDR mechanism would be effective against *Fusarium* spp., as it is a hemi-biotrophic pathogen. Unlike qualitative resistance, QDR involves several small or moderate effect genes with a continuous distribution of phenotypes involved in the pathogen perception, signal transduction, and defense responses (Poland et al., 2009; St.Clair, 2010; Roux et al., 2014; Niks et al., 2015; Corwin & Kliebenstein, 2017). In pathogen perception and signaling, larger effect loci/genes like MAMPs, RLKs, and NLRs are quantitatively involved and linked to downstream defense response pathways which are regulated by polygenic minor effect loci (Corwin & Kliebenstein, 2017).

During infection, the upstream perception and signaling mechanisms initiated in the cell wall are involved in cell growth and development and provide a physical and biochemical defense (Engelsdorf et al., 2018). Cell wall is composed of cellulose, hemicellulose, lignin, and pectin. During infection, pathogens produce enzymes that trigger cell wall components' lignification (Höfte & Voxeur, 2017). However, resistant genotypes produce lignan, which inhibits pathogen enzymes such as cellulases, polygalacturonases, glucosidases, and laccases used for cell wall degradation (Paniagua et al., 2017). In addition, lignin embodies a barrier against pathogens to limit pathogen toxins and enzymes, giving stability and hydrophobicity to the plant vascular system (Miedes et al., 2014). Increased concentration of lignan and lignin during early pathogen infection has been reported (Akiyama et al., 2007; Mohr & Cahill, 2007). Disease resistance-responsive (dirigent-like protein) family protein (DIR) and peroxidases in the cell wall are involved in lignan and lignin biosynthesis (Halls et al., 2004; Paniagua et al., 2017). Plants produce these proteins during pathogen exposure or wounding to avoid physical penetration into the cell

wall (Kohorn & Kohorn, 2012). The host cell wall's lower physical and chemical barriers in response to pathogen stimuli may contribute to susceptibility by facilitating penetration and infection in sorghum by the stalk rot pathogen, *M. phaseolina* (Bandara et al., 2018).

Additionally, cell wall strength and HR are regulated by the accumulation of ROS, such as hydrogen peroxide (H_2O_2), through activation of the *Peroxidase superfamily protein (SbPrx)* immediately in response to infection (Basavaraju et al., 2009; Gechev & Hille, 2005; Shetty et al., 2008). ROS must be produced in low amounts by the plant system during normal physiological processes and after stress responses, as they are toxic and increase cell death (Huang et al., 2019; Mittler, 2017). Elevated expression of ROS in susceptible wheat germplasm infected by the necrotrophic fungus, *Rhizoctonia solani* has been reported (Foley et al., 2016). In sorghum, early accumulation is related to resistance, and late accumulation contributes to pathogenesis by stressing the plant for anthracnose infection (Basavaraju et al., 2009) and aphid resistance (Pant & Huang, 2021; Scully et al., 2016). In addition, the biochemical response induces lignin biosynthesis due to cell wall damage through elevated reactive oxygen species (ROS), oxidative burst, and activation of calcium (Ca^{2+}) based signaling (Denness et al., 2011; Hamann et al., 2009). Moreover, cell wall lignification and breakage by pathogen enzymes bring fragments of cell wall components like oligogalacturonides (OG) that are recognized by wall-associated kinase-like (WAKs) proteins, providing a signal of pathogen intrusion into the cell hence activating a defense response (Ferrari et al., 2013; Wolf, 2017). In addition to cell wall-associated signal transduction, nucleotide-binding domain leucine-rich repeat (NBS-LRR) genes are the largest among the disease resistance genes found in clusters in the genome and are involved in recognition and signal transduction after pathogen infection in sorghum (Mchale et al., 2006; Mace et al., 2014).

QDR's downstream defense response mechanisms include defensins, pathogen-related proteins, and secondary metabolic enzymes (Corwin & Kliebenstein, 2017). So far, 17 families of pathogenesis-related (PR) proteins (PR-1 to PR-17) have been reported based on their sequence similarity or other functions (Sinha et al., 2014). PR *Bet v I* family protein belongs to the PR-10 family and is also known as *Betallergen* (Wen et al., 1997; Radauer et al., 2008). In addition, *Bet_v_1*/*PYR1* were reported to be abscisic acid receptors and play an essential role in plant resistance to biotic and abiotic stresses in different crops (Dupeux, et al., 2009; Nishimura et al., 2009; Rodrigues, et al., 2009). In this regard, there are several reports in sorghum about the PR-10 expression in defense response to different fungal pathogen infections (Lo et al., 2007; Katilé et al., 2010; Cui et al., 2021; Nida et al., 2021). Likewise, the PR-5 family proteins, thaumatin superfamily proteins (*Tyr*), or thaumatin-like proteins (*TLP*) were also reported to be involved in plant defense against pathogen infection (Liu et al., 2010; de Jesús-Pires et al., 2020).

The regulation of chalcone and stilbene synthase family (CHS/STS) and bifunctional dihydroflavonol 4-reductase/dihydroflavonol 4-reductase (DFR3) are reported to be involved in QDR downstream defense responses. Most of the chalcones (CHS) and stilbene synthase (STS) family proteins were cloned *(SbCHS1 to SbCHS8)* and characterized in sorghum for their function in defense against pathogen infection (Lo et al., 1999; Lo et al., 2002; Yu et al., 2005; Dao et al., 2011; Sharma et al., 2014; Bhavsar et al., 2019). They are plant polyketide synthase superfamily (PKS III) members. PKS IIIs are involved in the metabolism of antimicrobial phytoalexins, such as the biosynthesis of flavonoids and isoflavonoids (Springob et al., 2003; Yu et al., 2005; Dao et al., 2011). Lo et al. (2002) reported a cluster of CHS closely linked, highly conserved genes on chromosome 5, all having a single intron and sharing 97.5% amino acid sequence identity, to be closely related to maize C2 and *WHP* genes. They are only induced by pathogen infection, except

SbCHS5, which is activated by a light signal in addition to fungal infection signals (Liu et al., 2010). Early accumulation of 3-deoxyanthocyanidins and induction of genes encoding CHS synthase in a resistant cultivar were reported to be the principal mechanism of resistance in sorghum against *Colletotrichum sublineolum* (Lo et al., 1999). Sharma et al. (2014) studied the differential expression of chitinase (SbChit) and stilbene (SbSTS1) synthase genes in sorghum against the stalk rot fungal pathogen, *M. phaseolina* and reported lower and delayed expression in the susceptible cultivar. Similarly, Adeyanju et al. (2015) reported the chalcone and stilbene synthase protein family gene in chromosome 9 as one of the candidate genes in their genome-wide association study on resistance to *M. phaseolina* and *F. thapsinum* in sorghum.

The plant system regularly produces flavonoids or secondary metabolites for normal metabolism. However, some genes are involved in the biosynthesis of an important class of flavonoids whose biosynthesis is directly regulated by biotic stress. *SbDFR3* is an enzyme induced during 3-deoxyanthocyanidin accumulation due to fungal infection, which is unique to sorghum, where it is synthesized into anthocyanidins (Liu et al., 2010). Antifungal proteins and secondary metabolites such as 3-deoxyanthocyanidin flavonoids kill both the plant cell under fungal attack and the pathogen to limit further colonization (Snyder & Nicholson, 1990). However, cell death caused by the plant defense system might benefit a hemi-biotrophic pathogen with a necrotrophic stage, and the pathogen kills additional tissues leading to an increased lesion length which in turn affects the overall plant system as it affects the plant fluid and nutrient transport through the stem/stalk (Glazebrook, 2005). The necrotrophic pathogens are opportunists that utilize the plant's HR responses and effective pathogenesis making the host susceptible (Govrin & Levine, 2000; Bandara et al., 2018). Additionally, the flavonoids are not only involved in early defense but in the later stages, these phytoalexins are involved in antioxidant activities where they scavenge ROS

produced as a result of infection by both the plant and the pathogen to reduce further damage by ROS to the host (Treutter, 2005; Agati et al., 2012; Mierziak et al., 2014). They also regulate auxin activity towards reinforcing plant tissues and overall structure (Beckman, 2000; Treutter, 2005; Mierziak et al., 2014).

References

Adeyanju, A., Little, C., Yu, J., & Tesso, T. (2015). Genome-wide association study on resistance to stalk rot diseases in grain sorghum. G3: Genes, Genomes, Genetics, 5(6), 1165–1175. https://doi.org/10.1534/g3.114.016394

Adhikari, P., Mideros, S. X., & Jamann, T. M. (2021). Differential Regulation of Maize and Sorghum Orthologs in Response to the Fungal Pathogen *Exserohilum turcicum*. Frontiers in Plant Science, 12. https://doi.org/10.3389/fpls.2021.675208

Agati, G., Azzarello, E., Pollastri, S., & Tattini, M. (2012). Flavonoids as antioxidants in plants: Location and functional significance. Plant Science : An International Journal of Experimental Plant Biology, 196, 67–76. https://doi.org/10.1016/J.PLANTSCI.2012.07.014

Akiyama, K., Maruyama, M., Yamauchi, S., Nakashima, Y., Nakato, T., Tago, R., Sugahara, T., Kishida, T., & Koba, Y. (2007). Antimicrobiological Activity of Lignan: Effect of Benzylic Oxygen and Stereochemistry of 2,3-Dibenzyl-4-butanolide and 3,4-Dibenzyltetrahydrofuran Lignans on Activity. Bioscience, Biotechnology, and Biochemistry, 71(7), 1745–1751. https://doi.org/10.1271/bbb.70168

Balint-Kurti, P. (2019). The plant hypersensitive response: Concepts, control and consequences. Molecular Plant Pathology, 20(8), 1163–1178. https://doi.org/10.1111/mpp.12821

Bandara, Y. M. A. Y., Weerasooriya, D. K., Liu, S., & Little, C. R. (2018). The necrotrophic fungus *Macrophomina phaseolina* promotes charcoal rot susceptibility in grain sorghum through induced host cell-wall-degrading enzymes. Phytopathology, 108(8), 948–956. https://doi.org/10.1094/PHYTO-12-17-0404-R

Bandara, Y. M. A. Y., Weerasooriya, D. K., Tesso, T. T., & Little, C. R. (2017). Stalk Rot Diseases Impact Sweet Sorghum Biofuel Traits. Bioenergy Research, 10(1), 26–35. https://doi.org/10.1007/S12155-016-9775-6/FIGURES/2

Basavaraju, P., Shetty, N. P., Shetty, S. H., De Neergaard, E., & Jørgensen, H. J. L. (2009). Infection biology and defence responses in sorghum against *Colletotrichum sublineolum*. Journal of Applied Microbiology, 107(2), 404–415. https://doi.org/10.1111/J.1365-2672.2009.04234.X

Beckman, C. H. (2000). Phenolic-storing cells: Keys to programmed cell death and periderm formation in wilt disease resistance and in general defence responses in plants. Physiological and Molecular Plant Pathology, 57(3), 101–110. https://doi.org/10.1006/PMPP.2000.0287

Bhavsar, B., Patel, M. I., & Kalaria, R. K. (2019). Molecular and in silico identification of chalcone synthase gene-2 (CHS-2) in sorghum (*Sorghum bicolor* L.) against anthracnose. International Journal of Chemical Studies, 7(4), 839–844.

Brookes, A. J. (1999). The essence of SNPs. Gene, 234(2), 177–186. https://doi.org/10.1016/S0378-1119(99)00219-X

Childs, K. L., Miller, F. R., Cordonnier-Pratt, M. M., Pratt, L. H., Morgan, P. W., & Mullet, J. E. (1997). The sorghum photoperiod sensitivity gene, *Ma3*, encodes a phytochrome B. Plant Physiology, 113(2), 611–619.

Claflin, L. E., & Giorda, L. M. (2008). Stalk Rots of Sorghum. Sorghum and Millets Diseases, 185–190. https://doi.org/10.1002/9780470384923.ch33

Collard, B. C. Y., Jahufer, M. Z. Z., Brouwer, J. B., & Pang, E. C. K. (2005). An introduction to markers, quantitative trait loci (QTL) mapping and marker-assisted selection for crop improvement: The basic concepts. Euphytica, 142(1–2), 169–196. https://doi.org/10.1007/s10681-005-1681-5

Conesa, A., Madrigal, P., Tarazona, S., Gomez-Cabrero, D., Cervera, A., McPherson, A., Szcześniak, M. W., Gaffney, D. J., Elo, L. L., Zhang, X., & Mortazavi, A. (2016). A survey of best practices for RNA-seq data analysis. Genome Biology, 17(1), 1–19. https://doi.org/10.1186/s13059-016-0881-8

Corwin, J. A., & Kliebenstein, D. J. (2017). Quantitative Resistance: More Than Just Perception of a Pathogen. The Plant Cell, 29(4), 655. https://doi.org/10.1105/TPC.16.00915

Costa-Silva, J., Domingues, D., & Lopes, F. M. (2017). RNA-Seq differential expression analysis: An extended review and a software tool. PLoS ONE, 12(12), 1–18. https://doi.org/10.1371/journal.pone.0190152

Cui, Y., Chen, D., Jiang, Y., Xu, D., Balint-Kurti, P., & Stacey, G. (2021). Variation in gene expression between two *Sorghum bicolor* lines differing in innate immunity response. Plants, 10(8). https://doi.org/10.3390/plants10081536

Dao, T. T. H., Linthorst, H. J. M., & Verpoorte, R. (2011). Chalcone synthase and its functions in plant resistance. Phytochemistry Reviews, 10(3), 397. https://doi.org/10.1007/S11101-011-9211-7

Das, I. K., Prabhakar, & Indira, S. (2008). Role of stalk-anatomy and yield parameters in development of charcoal rot caused by *Macrophomina phaseolina* in winter sorghum. Phytoparasitica 2008 36:2, 36(2), 199–208. https://doi.org/10.1007/BF02981332

de Jesús-Pires, C., Ferreira-Neto, J. R. C., Pacifico Bezerra-Neto, J., Kido, E. A., de Oliveira Silva, R. L., Pandolfi, V., Wanderley-Nogueira, A. C., Binneck, E., da Costa, A. F., Pio-Ribeiro, G., Pereira-Andrade, G., Sittolin, I. M., Freire-Filho, F., & Benko-Iseppon, A. M. (2020). Plant Thaumatin-like Proteins: Function, Evolution and Biotechnological Applications. Current Protein & Peptide Science, 21(1), 36–51. https://doi.org/10.2174/1389203720666190318164905

de Sá, P. H. C. G., Guimarães, L. C., das Graças, D. A., de Oliveira Veras, A. A., Barh, D., Azevedo, V., da Costa da Silva, A. L., & Ramos, R. T. J. (2018). Next-generation sequencing and data analysis: Strategies, tools, pipelines and protocols. Omics Technologies and Bio-Engineering: Academic Press, 1, 191–207. https://doi.org/10.1016/B978-0-12-804659-3.00011-7

Delplace, F., Huard-Chauveau, C., Dubiella, U., Khafif, M., Alvarez, E., Langin, G., Roux, F., Peyraud, R., & Roby, D. (2020). Robustness of plant quantitative disease resistance is provided by a decentralized immune network. Proceedings of the National Academy of

Sciences of the United States of America, 117(30), 18099–18109. https://doi.org/10.1073/PNAS.2000078117

Denness, L., McKenna, J. F., Segonzac, C., Wormit, A., Madhou, P., Bennett, M., Mansfield, J., Zipfel, C., & Hamann, T. (2011). Cell wall damage-induced lignin biosynthesis is regulated by a reactive oxygen species- and jasmonic acid-dependent process in arabidopsis. Plant Physiology, 156(3), 1364–1374. https://doi.org/10.1104/pp.111.175737

Doerge, R. W. (2002). Mapping and analysis of quantitative trait loci in experimental populations. Nature Reviews Genetics, 3(1), 43–52. https://doi.org/10.1038/nrg703

Doggett, H. (1970). Sorghum. Longmans.

Eghball, B., & Power, J. F. (1995). Fractal description of temporal yield variability of 10 crops in the United States. Agronomy Journal, 87(2), 152–156. https://doi.org/10.2134/AGRONJ1995.00021962008700020003X

Elshire, R. J., Glaubitz, J. C., Sun, Q., Poland, J. A., Kawamoto, K., Buckler, E. S., & Mitchell, S. E. (2011). A robust, simple genotyping-by-sequencing (GBS) approach for high diversity species. PLoS ONE, 6(5), 1–10. https://doi.org/10.1371/journal.pone.0019379

Engelsdorf, T., Gigli-Bisceglia, N., Veerabagu, M., McKenna, J. F., Vaahtera, L., Augstein, F., Van der Does, D., Zipfel, C., & Hamann, T. (2018). The plant cell wall integrity maintenance and immune signaling systems cooperate to control stress responses in *Arabidopsis thaliana*. Science Signaling, 11(536). https://doi.org/10.1126/SCISIGNAL.AAO3070

FAO. (2021). World Food and Agriculture – Statistical Yearbook 2021. Rome. https://doi.org/10.4060/CB4477EN

Ferrari, S., Savatin, D., Sicilia, F., Gramegna, G., Cervone, F., & De Lorenzo, G. (2013). Oligogalacturonides: Plant damage-associated molecular patterns and regulators of growth and development. Frontiers in Plant Science, 4. https://www.frontiersin.org/articles/10.3389/fpls.2013.00049

Foley, R. C., Kidd, B. N., Hane, J. K., Anderson, J. P., & Singh, K. B. (2016). Reactive oxygen species play a role in the infection of the necrotrophic fungi, *Rhizoctonia solani* in wheat. PLoS ONE, 11(3). https://doi.org/10.1371/JOURNAL.PONE.0152548

Fracasso, A., Trindade, L. M., & Amaducci, S. (2016). Drought stress tolerance strategies revealed by RNA-Seq in two sorghum genotypes with contrasting WUE. BMC Plant Biology, 16(1), 1–18. https://doi.org/10.1186/s12870-016-0800-x

French, E., Kim, B. S., & Iyer-Pascuzzi, A. S. (2016). Mechanisms of quantitative disease resistance in plants. Seminars in Cell & Developmental Biology, 56, 201–208. https://doi.org/10.1016/J.SEMCDB.2016.05.015

Fu, F., Girma, G., & Mengiste, T. (2020). Global mRNA and microRNA expression dynamics in response to anthracnose infection in sorghum. BMC Genomics, 21(1), 1–16. https://doi.org/10.1186/s12864-020-07138-0

Funnell-Harris, D. L., Sattler, S. E., & Pedersen, J. F. (2014). Response of *Fusarium thapsinum* to Sorghum brown midrib Lines and to Phenolic Metabolites. Plant Disease, 98(10), 1300–1308. https://doi.org/10.1094/PDIS-09-13-0980-RE

Garg, M. (2021). RNA sequencing. In Advances in Animal Genomics. Elsevier Inc. https://doi.org/10.1016/b978-0-12-820595-2.00005-9

Gechev, T. S., & Hille, J. (2005). Hydrogen peroxide as a signal controlling plant programmed cell death. The Journal of Cell Biology, 168(1), 17. https://doi.org/10.1083/JCB.200409170

Gelli, M., Duo, Y., Konda, A. R., Zhang, C., Holding, D., & Dweikat, I. (2014). Identification of differentially expressed genes between sorghum genotypes with contrasting nitrogen stress tolerance by genome-wide transcriptional profiling. BMC Genomics, 15(1), 1–16. https://doi.org/10.1186/1471-2164-15-179

Gelli, M., Konda, A. R., Liu, K., Zhang, C., Clemente, T. E., Holding, D. R., & Dweikat, I. M. (2017). Validation of QTL mapping and transcriptome profiling for identification of candidate genes associated with nitrogen stress tolerance in sorghum. BMC Plant Biology, 17(1), 1–18. https://doi.org/10.1186/s12870-017-1064-9

Gelli, M., Mitchell, S. E., Liu, K., Clemente, T. E., Weeks, D. P., Zhang, C., Holding, D. R., & Dweikat, I. M. (2016). Mapping QTLs and association of differentially expressed gene transcripts for multiple agronomic traits under different nitrogen levels in sorghum. BMC Plant Biology, 16(1). https://doi.org/10.1186/s12870-015-0696-x

Glazebrook, J. (2005). Contrasting mechanisms of defense against biotrophic and necrotrophic pathogens. Annu. Rev. Phytopathol, 43, 205–232. https://doi.org/10.1146/annurev.phyto.43.040204.135923

Gomez, F. E., Mullet, J. E., Muliana, A. H., Niklas, K. J., & Rooney, W. L. (2020). The genetic architecture of biomechanical traits in sorghum. Crop Science, 60(1), 82–99. https://doi.org/10.1002/csc2.20049

Govrin, E. M., & Levine, A. (2000). The hypersensitive response facilitates plant infection by the necrotrophic pathogen *Botrytis cinerea*. Current Biology, 10(13), 751–757. https://doi.org/10.1016/S0960-9822(00)00560-1

Haley, C. S., & Knott, S. A. (1992). A simple regression method for mapping quantitative trait loci in line crosses using flanking markers. Heredity, 69:4, 69(4), 315–324. https://doi.org/10.1038/hdy.1992.131

Halls, S. C., Davin, L. B., Kramer, D. M., & Lewis, N. G. (2004). Kinetic study of coniferyl alcohol radical binding to the (+)-pinoresinol forming dirigent protein. Biochemistry, 43(9), 2587–2595. https://doi.org/10.1021/bi035959o

Hamann, T., Bennett, M., Mansfield, J., & Somerville, C. (2009). Identification of cell-wall stress as a hexose-dependent and osmosensitive regulator of plant responses. The Plant Journal, 57(6), 1015–1026. https://doi.org/10.1111/j.1365-313X.2008.03744.x

Harlan, J. R., & de Wet, J. M. J. (1972). A Simplified Classification of Cultivated Sorghum. Crop Science, 12(2). https://doi.org/10.2135/cropsci1972.0011183X001200020005x

Haussmann, B. I. G., Hess, D. E., Omanya, G. O., Folkertsma, R. T., Reddy, B. V. S., Kayentao, M., Welz, H. G., & Geiger, H. H. (2004). Genomic regions influencing resistance to the parasitic weed *Striga hermonthica* in two recombinant inbred populations of sorghum.

Theoretical and Applied Genetics, 109(5), 1005–1016. https://doi.org/10.1007/s00122-004-1706-9

Höfte, H., & Voxeur, A. (2017). Plant cell walls. Current Biology , 27(17), R865–R870. https://doi.org/10.1016/J.CUB.2017.05.025

Horbach, R., Navarro-Quesada, A. R., Knogge, W., & Deising, H. B. (2011). When and how to kill a plant cell: Infection strategies of plant pathogenic fungi. Journal of Plant Physiology, 168(1), 51–62. https://doi.org/10.1016/j.jplph.2010.06.014

Huang, H., Ullah, F., Zhou, D. X., Yi, M., & Zhao, Y. (2019). Mechanisms of ROS Regulation of Plant Development and Stress Responses. Frontiers in Plant Science, 10. https://doi.org/10.3389/FPLS.2019.00800

Jamann, T. M., Balint-Kurti, P. J., & Holland, J. B. (2015). QTL mapping using high-throughput sequencing. In Plant Functional Genomics: Methods and Protocols: Second Edition. https://doi.org/10.1007/978-1-4939-2444-8_13

Jardine, D. J. (2006). Stalk Rots of Corn and Sorghum (p. 6). Kansas State University.

Jardine, D. J., & Leslie, J. F. (1992). Aggressiveness of *Gibberella fujikuroi* (*Fusarium moniliforme*) isolates to grain sorghum under greenhouse conditions. Plant Disease, 76(9), 897. https://doi.org/10.1094/pd-76-0897

Jones, J. D. G., & Dangl, J. L. (2006). The plant immune system. Nature, 444(7117). https://doi.org/10.1038/nature05286

Kao, C. H., Zeng, Z. B., & Teasdale, R. D. (1999). Multiple interval mapping for quantitative trait loci. Genetics, 152(3), 1203–1216. https://doi.org/10.1093/GENETICS/152.3.1203

Katilé, S. O., Perumal, R., Rooney, W. L., Prom, L. K., & Magill, C. W. (2010). Expression of pathogenesis-related protein PR-10 in sorghum floral tissues in response to inoculation with *Fusarium thapsinum* and *Curvularia lunata*. Molecular Plant Pathology, 11(1), 93–103. https://doi.org/10.1111/J.1364-3703.2009.00580.X

Kebede, H., Subudhi, P., Rosenow, D., & Nguyen, H. (2001). Quantitative trait loci influencing drought tolerance in grain sorghum (*Sorghum bicolor* L. Moench). Theoretical and Applied Genetics, 103, 266–276.

Kohorn, B. D., & Kohorn, S. L. (2012). The cell wall-associated kinases, WAKs, as pectin receptors. Frontiers in Plant Science, 3, 88. https://doi.org/10.3389/FPLS.2012.00088/BIBTEX

Kushalappa, A. C., Yogendra, K. N., & Karre, S. (2016). Plant innate immune response: Qualitative and quantitative resistance. Critical Reviews in Plant Sciences, 35(1), 38–55. https://doi.org/10.1080/07352689.2016.1148980

Lambright, L. (2019). Hybrid sorghum product development and production. Methods in Molecular Biology, 1931, 3–9. https://doi.org/10.1007/978-1-4939-9039-9_1/COVER

Leslie, J. F. (1990). Fusarium spp. From Corn, Sorghum, and Soybean Fields in the Central and Eastern United States. Phytopathology, 80(4), 343. https://doi.org/10.1094/phyto-80-343

Leslie, J. F., Zeller, K. A., Lamprecht, S. C., Rheeder, J. P., & Marasas, W. F. O. (2005). Toxicity, pathogenicity, and genetic differentiation of five species of Fusarium from sorghum and millet. Phytopathology, 95(3), 275–283. https://doi.org/10.1094/PHYTO-95-0275

Li, H., Ye, G., & Wang, J. (2007). A Modified Algorithm for the Improvement of Composite Interval Mapping. Genetics, 175(1), 361–374. https://doi.org/10.1534/GENETICS.106.066811

Li, W. V., & Li, J. J.L. (2018). Modeling and analysis of RNA-seq data: a review from a statistical perspective. Quantitate Biology, 6(3), 195–209. https://doi.org/10.1007/s40484-018-0144-7.

Liu, H., Du, Y., Chu, H., Shih, C. H., Wong, Y. W., Wang, M., Chu, I. K., Tao, Y., & Lo, C. (2010). Molecular dissection of the pathogen-inducible 3-deoxyanthocyanidin biosynthesis pathway in sorghum. Plant & Cell Physiology, 51(7), 1173–1185. https://doi.org/10.1093/PCP/PCQ080

Liu, J. J., Sturrock, R., & Ekramoddoullah, A. K. M. (2010). The superfamily of thaumatin-like proteins: Its origin, evolution, and expression towards biological function. Plant Cell Reports, 29:5, 29(5), 419–436. https://doi.org/10.1007/S00299-010-0826-8

Lo, C., Coolbaugh, R. C., & Nicholson, R. L. (2002). Molecular characterization and in silico expression analysis of a chalcone synthase gene family in *Sorghum bicolor*. Physiological and Molecular Plant Pathology, 61(3), 179–188. https://doi.org/10.1006/PMPP.2002.0428

Lo, S. C. C., De Verdier, K., & Nicholson, R. L. (1999). Accumulation of 3-deoxyanthocyanidin phytoalexins and resistance to *Colletotrichum sublineolum* in sorghum. Physiological and Molecular Plant Pathology, 55(5), 263–273. https://doi.org/10.1006/PMPP.1999.0231

Lo, S. C. C., Hipskind, J. D., & Nicholson, R. L. (1999). cDNA Cloning of a sorghum pathogenesis-related protein (PR-10) and differential expression of defense-related genes following inoculation with *Cochliobolus heterostrophus* or *Colletotrichum sublineolum*. Molecular Plant-Microbe Interactions, 12(6), 479–489. https://doi.org/10.1094/MPMI.1999.12.6.479

Lynch, M., & Walsh, B. (1998). Genetics and Analysis of Quantitative Traits (Vol. 1). Sinauer.

Lyons, R., Stiller, J., Powell, J., Rusu, A., Manners, J. M., & Kazan, K. (2015). *Fusarium oxysporum* triggers tissue-specific transcriptional reprogramming in *Arabidopsis thaliana*. PLoS ONE, 10(4). https://doi.org/10.1371/JOURNAL.PONE.0121902

Mace, E., Tai, S., Innes, D., Godwin, I., Hu, W., Campbell, B., Gilding, E., Cruickshank, A., Prentis, P., Wang, J., & Jordan, D. (2014). The plasticity of NBS resistance genes in sorghum is driven by multiple evolutionary processes. BMC Plant Biology, 14(1), 1–14. https://doi.org/10.1186/s12870-014-0253-z

Mahmoud, A. F., Abou-Elwafa, S. F., & Shehzad, T. (2018). Identification of charcoal rot resistance QTLs in sorghum using association and in silico analyses. Journal of Applied Genetics, 59(3), 243–251. https://doi.org/10.1007/s13353-018-0446-5

Marla, S. R., Shiva, S., Welti, R., Liu, S., Burke, J. J., & Morris, G. P. (2017). Comparative transcriptome and lipidome analyses reveal molecular chilling responses in chilling-

tolerant sorghums. The Plant Genome, 10(3), 1–16. https://doi.org/10.3835/plantgenome2017.03.0025

Mchale, L., Tan, X., Koehl, P., & Michelmore, R. W. (2006). Plant NBS-LRR proteins: Adaptable guards. Genome Biology, 7, 212. https://doi.org/10.1186/gb-2006-7-4-212

Meng, L., Li, H., Zhang, L., & Wang, J. (2015). QTL IciMapping: Integrated software for genetic linkage map construction and quantitative trait locus mapping in biparental populations. The Crop Journal, 3(3), 269–283. https://doi.org/10.1016/J.CJ.2015.01.001

Metzker, M. L. (2010). Sequencing technologies the next generation. Nature Reviews Genetics, 11(1), 31–46. https://doi.org/10.1038/nrg2626

Mewa, D. B., Lee, S., Liao, C.-J., Souza, A. M., Adeyanju, A., Helm, M., Lisch, D., & Mengiste, T. (2022). *ANTHRACNOSE RESISTANCE GENE2* confers fungal resistance in sorghum. The Plant Journal, 113(2), 308-326. https://doi.org/10.1111/tpj.16048

Miedes, E., Vanholme, R., Boerjan, W., & Molina, A. (2014). The role of the secondary cell wall in plant resistance to pathogens. Frontiers in Plant Science, 5. https://www.frontiersin.org/articles/10.3389/fpls.2014.00358

Mierziak, J., Kostyn, K., & Kulma, A. (2014). Flavonoids as important molecules of plant interactions with the environment. molecules, 19(10), 16240. https://doi.org/10.3390/MOLECULES191016240

Miller, F. R., & Kebede, Y. (1984). Genetic contributions to yield gains in sorghum, 1950 to 1980. CSSA Special Publications, 33, 1–14. https://doi.org/10.2135/CSSASPECPUB7.C1

Mittler, R. (2017). ROS are good. Trends in Plant Science, 22(1), 11–19. https://doi.org/10.1016/J.TPLANTS.2016.08.002

Mohr, P. G., & Cahill, D. M. (2007). Suppression by ABA of salicylic acid and lignin accumulation and the expression of multiple genes in Arabidopsis infected with *Pseudomonas syringae* pv. Tomato. Functional & Integrative Genomics, 7(3), 181–191. https://doi.org/10.1007/s10142-006-0041-4

Monaghan, J., & Zipfel, C. (2012). Plant pattern recognition receptor complexes at the plasma membrane. Current Opinion in Plant Biology, 15(4), 349–357. https://doi.org/10.1016/j.pbi.2012.05.006

Myles, C., & Wayne, M. (2008). Quantitative trait locus (QTL) analysis. Nature Education, 208(1). https://www.nature.com/scitable/topicpage/quantitative-trait-locus-qtl-analysis-53904/

Natarajan, P., Ahn, E., Reddy, U. K., Perumal, R., Prom, L. K., & Magill, C. (2021). RNA-Sequencing in resistant (QL3) and susceptible (Theis) sorghum cultivars inoculated with johnsongrass isolates of *Colletotrichum sublineola*. Frontiers in Genetics, 12. https://doi.org/10.3389/fgene.2021.722519

Nida, H., Lee, S., Li, Y., & Mengiste, T. (2021). Transcriptome analysis of early stages of sorghum grain mold disease reveals defense regulators and metabolic pathways associated with resistance. BMC Genomics, 22(1), 1–17. https://doi.org/10.1186/s12864-021-07609-y

Niks, R. E., Qi, X., & Marcel, T. C. (2015). Quantitative resistance to biotrophic filamentous plant pathogens: Concepts, misconceptions, and mechanisms. Annual Review of

Phytopathology, 53, 445–470. https://doi.org/10.1146/ANNUREV-PHYTO-080614-115928

Nishimura, N., Hitomi, K., Arvai, A. S., Rambo, R. P., Hitomi, C., Cutler, S. R., Schroeder, J. I., & Getzoff, E. D. (2009). Structural mechanism of abscisic acid binding and signaling by dimeric *PYR1*. Science, 326(5958), 1373. https://doi.org/10.1126/SCIENCE.1181829

Ongom, P. O., & Ejeta, G. (2018). Mating design and genetic structure of a multi-parent advanced generation intercross (MAGIC) population of sorghum (*Sorghum bicolor* (L.) Moench). G3: Genes, Genomes, Genetics, 8(1), 331–341. https://doi.org/10.1534/G3.117.300248/-/DC1/FILES1.DOCX

Paniagua, C., Bilkova, A., Jackson, P., Dabravolski, S., Riber, W., Didi, V., Houser, J., Gigli-Bisceglia, N., Wimmerova, M., Budínská, E., Hamann, T., & Hejatko, J. (2017). Dirigent proteins in plants: Modulating cell wall metabolism during abiotic and biotic stress exposure. Journal of Experimental Botany, 68(13), 3287–3301. https://doi.org/10.1093/JXB/ERX141

Pant, S., & Huang, Y. (2021). Elevated production of reactive oxygen species is related to host plant resistance to sugarcane aphid in sorghum. Plant Signaling & Behavior, 16(2). https://doi.org/10.1080/15592324.2020.1849523

Patil, A., Fakrudin, B., Salimath, P. M., & Rajkumar. (2012). Genome-wide molecular mapping and QTL analysis, validated across locations and years for charcoal rot disease incidence traits in *Sorghum bicolor* (L.) Moench. Indian Journal of Genetics and Plant Breeding, 72(3), 296–302.

Patin, E. C., Thompson, A., & Orr, S. J. (2019). Pattern recognition receptors in fungal immunity. Seminars in Cell and Developmental Biology, 89, 24–33. https://doi.org/10.1016/j.semcdb.2018.03.003

Pecina-Quintero, V., Williams-Alanis, H., & Vandemark, G. J. (1999). Diallel Analysis of Resistance to *Macrophomina phaseolina* in Sorghum. Cereal Research Communications 27:1, 27(1), 99–106. https://doi.org/10.1007/BF03543925

Perumal, R., Tesso, T. T., Morris, G. P., Jagadish, S. V. K., Little, C. R., Bean, S. R., Yu, J., Prasad, P. V. V., & Tuinstra, M. R. (2021). Registration of the sorghum nested association mapping (NAM) population in RTx430 background. Journal of Plant Registrations, 15(2), 395–402. https://doi.org/10.1002/PLR2.20110

Perumal, R., Tomar, S. S., Bandara, A., Maduraimuthu, D., Tesso, T. T., Prasad, P. V. V., Upadhyaya, H. D., & Little, C. R. (2020). Variation in stalk rot resistance and physiological traits of sorghum genotypes in the field under high temperature. Journal of General Plant Pathology, 86(5), 350–359. https://doi.org/10.1007/s10327-020-00940-4

Pfeiffer, B. K., Pietsch, D., Schnell, R. W., & Rooney, W. L. (2019). Long-term selection in hybrid sorghum breeding programs. Crop Science, 59(1), 150–164. https://doi.org/10.2135/CROPSCI2018.05.0345

Poland, J. A., Balint-Kurti, P. J., Wisser, R. J., Pratt, R. C., & Nelson, R. J. (2009). Shades of gray: The world of quantitative disease resistance. Trends in Plant Science, 14(1), 21–29. https://doi.org/10.1016/J.TPLANTS.2008.10.006

Radauer, C., Lackner, P., & Breiteneder, H. (2008). The Bet v 1 fold: An ancient, versatile scaffold for binding of large, hydrophobic ligands. BMC Evolutionary Biology, 8(1). https://doi.org/10.1186/1471-2148-8-286

Robles-Barrios, F., Ramírez-Granillo, A., Medina-Canales, M. G., Gómez-Lim, M., Loske, A. M., Rodríguez-Tovar, A. V., & Pérez, N. O. (2022). *Fusarium temperatum* shows a hemibiotrophic infection process and differential pathogenicity over different maize breeds from Mexico. Journal of Phytopathology, 170(1), 21–33. https://doi.org/10.1111/JPH.13052

Rooney, W. L. (2004). Sorghum improvement-integrating traditional and new technology to produce improved genotypes. Advances in Agronomy, 83. https://doi.org/10.1016/S0065-2113(04)83002-5

Roux, F., Voisin, D., Badet, T., Balagué, C., Barlet, X., Huard-Chauveau, C., Roby, D., & Raffaele, S. (2014). Resistance to phytopathogens e tutti quanti: Placing plant quantitative disease resistance on the map. Molecular Plant Pathology, 15(5), 427–432. https://doi.org/10.1111/MPP.12138

Santiago, J., Dupeux, F., Round, A., Antoni, R., Park, S. Y., Jamin, M., Cutler, S. R., Rodriguez, P. L., & Márquez, J. A. (2009). The abscisic acid receptor PYR1 in complex with abscisic acid. Nature, 462(7273), 665–668. https://doi.org/10.1038/NATURE08591

Santiago, J., Rodrigues, A., Saez, A., Rubio, S., Antoni, R., Dupeux, F., Park, S. Y., Márquez, J. A., Cutler, S. R., & Rodriguez, P. L. (2009). Modulation of drought resistance by the abscisic acid receptor PYL5 through inhibition of clade A PP2Cs. Plant Journal, 60(4), 575–588. https://doi.org/10.1111/J.1365-313X.2009.03981.X

Satish, K., Gutema, Z., Grenier, C., Rich, P. J., & Ejeta, G. (2012). Molecular tagging and validation of microsatellite markers linked to the low germination stimulant gene (lgs) for Striga resistance in sorghum [*Sorghum bicolor* (L.) Moench]. TAG. Theoretical and Applied Genetics, 124(6), 989–1003. https://doi.org/10.1007/s00122-011-1763-9

Schnell, F. W., & Cockerham, C. C. (1992). Multiplicative Vs. Arbitrary Gene Action in Heterosis. Genetics, 131(2), 461. https://doi.org/10.1093/GENETICS/131.2.461

Scully, E. D., Donze-Reiner, T., Wang, H., Eickhoff, T. E., Baxendale, F., Twigg, P., Kovacs, F., Heng-Moss, T., Sattler, S. E., & Sarath, G. (2016). Identification of an orthologous clade of peroxidases that respond to feeding by greenbugs *(Schizaphis graminum*) in C4 grasses. Functional Plant Biology, 43(12), 1134–1148. https://doi.org/10.1071/FP16104

Segonzac, C., & Zipfel, C. (2011). Activation of plant pattern-recognition receptors by bacteria. Current Opinion in Microbiology, 14(1), 54–61. https://doi.org/10.1016/j.mib.2010.12.005

Serba, D. D., Meng, X., Schnable, J., Bashir, E., Michaud, J. P., Vara Prasad, P. V., & Perumal, R. (2021). Comparative transcriptome analysis reveals genetic mechanisms of sugarcane aphid resistance in grain sorghum. International Journal of Molecular Sciences, 22(13). https://doi.org/10.3390/ijms22137129

Sharma, I., Kumari, N., & Sharma, V. (2014). Defense gene expression in Sorghum bicolor against *Macrophomina phaseolina* in leaves and roots of susceptible and resistant cultivars. Journal of Plant Interactions, 9(1), 315–323. https://doi.org/10.1080/17429145.2013.832425

Shetty, N. P., Jørgensen, H. J. L., Jensen, J. D., Collinge, D. B., & Shetty, H. S. (2008). Roles of reactive oxygen species in interactions between plants and pathogens. European Journal of Plant Pathology, 121(3), 267–280. https://doi.org/10.1007/S10658-008-9302-5/FIGURES/2

Sinha, M., Singh, R. P., Kushwaha, G. S., Iqbal, N., Singh, A., Kaushik, S., Kaur, P., Sharma, S., & Singh, T. P. (2014). Current overview of allergens of plant pathogenesis-related protein families. The Scientific World Journal, 2014. https://doi.org/10.1155/2014/543195

Snyder, B. A., & Nicholson, R. L. (1990). Synthesis of phytoalexins in sorghum as a site-specific response to fungal ingress. Science, 248(4963), 1637–1639. https://doi.org/10.1126/SCIENCE.248.4963.1637

Springob, K., Nakajima, J. I., Yamazaki, M., & Saito, K. (2003). Recent advances in the biosynthesis and accumulation of anthocyanins. Natural Product Reports, 20(3), 288–303. https://doi.org/10.1039/B109542K

Srinivasa Reddy, P., Fakrudin, B., Rajkumar, Punnuri, S. M., Arun, S. S., Kuruvinashetti, M. S., Das, I. K., & Seetharama, N. (2008). Molecular mapping of genomic regions harboring QTLs for stalk rot resistance in sorghum. Euphytica, 159(1–2), 191–198. https://doi.org/10.1007/s10681-007-9472-9

Stark, R., Grzelak, M., & Hadfield, J. (2019). RNA sequencing: The teenage years. Nature Reviews Genetics, 20(11), 631–656. https://doi.org/10.1038/s41576-019-0150-2

St.Clair, D. A. (2010). Quantitative disease resistance and quantitative resistance loci in breeding. Annual Review of Phytopathology, 48(1), 247–268. https://doi.org/10.1146/annurev-phyto-080508-081904

Stergiopoulos, I., & De Wit, P. J. G. M. (2009). Fungal effector proteins. Annual Review of Phytopathology, 47, 233–263. https://doi.org/10.1146/ANNUREV.PHYTO.112408.132637

Tesso, T. T., Claflin, L. E., & Tuinstra, M. R. (2004). Estimation of combining ability for resistance to Fusarium stalk rot in grain sorghum. Crop Science, 44(4), 1195–1199. https://doi.org/10.2135/cropsci2004.1195

Tesso, T. T., Claflin, L. E., & Tuinstra, M. R. (2005). Analysis of stalk rot resistance and genetic diversity among drought tolerant sorghum genotypes. Crop Science, 45(2), 645–652. https://doi.org/10.2135/cropsci2005.0645

Tesso, T. T., Ochanda, N., Little, C. R., Claflin, L., & Tuinstra, M. R. (2010). Analysis of host plant resistance to multiple Fusarium species associated with stalk rot disease in sorghum [*Sorghum bicolor* (L.) Moench]. Field Crops Research, 118(2), 177–182. https://doi.org/10.1016/j.fcr.2010.05.010

Tesso, T. T., Perumal, R., Little, C. R., Adeyanju, A., Radwan, G. L., Prom, L. K., & Magill, C. W. (2012). Sorghum pathology and biotechnology—A fungal disease perspective: Part II. Anthracnose, stalk Rot, and downy mildew. The European Journal of Plant Science and Biotechnology, 6, 31–44.

Thakur, R., Frederiksen, R., Murty, D., Reddy, B., Bandyopadhyay, R., Giorda, L., Odvody, G., & Claflin, L. (1996). Breeding for disease resistance in sorghum. Proceedings of the International Conference on Genetic Improvement of Sorghum and Pearl Millet, 22–27.

Thomas, P. D. (2017). The gene ontology and the meaning of biological function. In The gene ontology handbook. Humana Press, New York, NY., 1446, 15–24. https://doi.org/10.1007/978-1-4939-3743-1

Treutter, D. (2005). Significance of flavonoids in plant resistance and enhancement of their biosynthesis. Plant Biology, 7(6), 581–591. https://doi.org/10.1055/S-2005-873009

Unger, P. W., & Baumhardt, R. L. (1999). Factors related to dryland grain sorghum yield increases: 1939 through 1997. Agronomy Journal, 91(5), 870–875. https://doi.org/10.2134/AGRONJ1999.915870X

Wang, X., Chen, Y., Sun, X., Li, J., Zhang, R., Jiao, Y., Wang, R., Song, W., & Zhao, J. (2022). Characteristics and candidate genes associated with excellent stalk strength in maize (*Zea mays* L.). Frontiers in Plant Science, 13. https://www.frontiersin.org/articles/10.3389/fpls.2022.957566

Wang, X., Jiang, N., Liu, J., Liu, W., & Wang, G. L. (2014). The role of effectors and host immunity in plant–necrotrophic fungal interactions. Virulence, 5(7), 722. https://doi.org/10.4161/VIRU.29798

Wang, X., Mace, E., Tao, Y., Cruickshank, A., Hunt, C., Hammer, G., & Jordan, D. (2020). Large-scale genome-wide association study reveals that drought-induced lodging in grain sorghum is associated with plant height and traits linked to carbon remobilization. Theoretical and Applied Genetics, 133(11), 3201–3215. https://doi.org/10.1007/s00122-020-03665-2

Wang, Z., Gerstein, M., & Snyder, M. (2009). RNA-Seq: A revolutionary tool for transcriptomics. Nature Reviews Genetics, 10(1), 57–63. https://doi.org/10.1038/nrg2484

Wen, J., Vanek-Krebitz, M., Hoffmann-Sommergruber, K., Scheiner, O., & Breiteneder, H. (1997). The potential of Betv1 homologues, a nuclear multigene family, as phylogenetic markers in flowering plants. Molecular Phylogenetics and Evolution, 8(3), 317–333. https://doi.org/10.1006/MPEV.1997.0447

Wolf, S. (2017). Plant cell wall signalling and receptor-like kinases. The Biochemical Journal, 474(4), 471–492. https://doi.org/10.1042/BCJ20160238

Yang, Q., Van Haute, M., Korth, N., Sattler, S. E., Toy, J., Rose, D. J., Schnable, J. C., & Benson, A. K. (2022). Genetic analysis of seed traits in *Sorghum bicolor* that affect the human gut microbiome. Nature Communications, 13(1), 1–15. https://doi.org/10.1038/s41467-022-33419-1

Yu, C. K. Y., Springob, K., Schmidt, J., Nicholson, R. L., Chu, I. K., Wing, K. Y., & Lo, C. (2005). A Stilbene synthase gene (SbSTS1) is involved in host and nonhost defense responses in sorghum. Plant Physiology, 138(1), 393. https://doi.org/10.1104/PP.105.059337

Zeng, Z. B. (1993). Theoretical basis for separation of multiple linked gene effects in mapping quantitative trait loci. Proceedings of the National Academy of Sciences of the United States of America, 90(23), 10976. https://doi.org/10.1073/PNAS.90.23.10972

Zhang, Y., Lubberstedt, T., & Xu, M. (2013). The genetic and molecular basis of plant resistance to pathogens. Journal of Genetics and Genomics, 40(1), 23–35. https://doi.org/10.1016/j.jgg.2012.11.003

Zipfel, C. (2009). Early molecular events in PAMP-triggered immunity. Current Opinion in Plant Biology, 12(4), 414–420. https://doi.org/10.1016/j.pbi.2009.06.003

Zummo, N. (1984). Fusarium root and stalk disease complex. In L. K. Mughogho & G. Rosenberg (Eds.), Sorghum root and stalk rots, A Critical Review. Proceedings of the Consultative Group Discussion on Research Needs and Strategies for Control of Sorghum Root and Stalk Rot Diseases (pp. 25–29). ICRISAT.

CHAPTER 2 - MAPPING OF QUANTITATIVE TRAIT LOCI FOR RESISTANCE TO FUSARIUM STALK ROT (*Fusarium thapsinium*) IN SORGHUM (*Sorghum bicolor*) RECOMBINANT INBRED LINES

2.1 Abstract

Stalk rots are among the major constraints to sorghum production in the US and globally, with Fusarium stalk rot being the dominant in Kansas. Environment plays a significant role in Fusarium stalk rot (*Fusarium thapsinum*) infection and severity in sorghum. The use of resistant varieties is recommended to minimize the loss to the disease, but breeding for resistance is complex due to the difficulty of initiating uniform infection and disease scoring. Marker technology may be of value to accelerate the effort. This study aims to facilitate the development of marker tools through mapping QTL associated with resistance to the disease and dissecting the epistatic and environmental interactions. Two hundred and thirty-three recombinant inbred lines (RILs) from BTx3042 (susceptible) × SC599 (resistant) cross were evaluated for reaction to infection by *F. thapsinum* in summer of 2018, 2019, and 2020. The liquid inoculum of *F. thapsinum* was injected into basal stalks to initiate the disease. Disease development was rated as lesion length and number of diseased nodes. Flowering time, plant height, and lodging data were also recorded. SNP data were generated using genotyping-by-sequencing (GBS) on RILs and their parents. Phenotypic data showed significant differences and transgressive segregation among the RIL population for disease parameters. Heritability was lower for major lesion length (66%) and lodging (55.9%), and higher for plant height (92.2) and days to flowering (84.4%). Of the 299,685 SNPs generated from 192 individuals, 3297 SNPs for 126 RILs were used for linkage mapping and QTL analysis. The linkage map covered 3070.8 cM with an average distance of 1.8 cM between markers. Inclusive composite interval mapping detected four stable additive QTL by environment interactions on

chromosomes 1, 3, 5, and 9 for major lesion length. Sobic.005G216200 (O-methyltransferase) was a candidate gene in the QTL position on chromosome 5 located on the physical map between 70.2 and 70.3Mb and involved in quinone secondary metabolite biosynthetic reactions. This QTL was detected using interval mapping and inclusive composite interval mapping for major lesion length in all the years and the mean data explained 22% of the phenotypic variation. It was also detected on QTL by environment interaction. We discovered that a QTL for flowering time was consistent over environments on chromosome 6.

2.2 Introduction

Quantitative trait loci (QTL) mapping and marker-assisted selection (MAS) are two essential techniques in modern plant breeding that contributed to crop improvement (Collard et al., 2005; Collard & Mackill, 2008; Hasan et al., 2021). Sorghum is a vital cereal grown worldwide in arid and semi-arid regions (Rakshit et al., 2014). Developing disease-resistant sorghum varieties is essential for ensuring food security, and QTL mapping and MAS have played a significant role in the success of these endeavors (Ejeta & Knoll, 2007; Mengistu et al., 2021; Mores et al., 2021). Anthracnose is one of the major diseases affecting sorghum production. Several QTL associated with resistance to anthracnose have been identified and incorporated into MAS that paved the way for developing anthracnose-resistant sorghum varieties (Cuevas et al., 2019; Cruet-Burgos et al., 2020; Lee et al., 2022; Mewa et al., 2022). Grain mold is another disease that adversely affects sorghum production, particularly in warm and humid environments (Thakur et al., 2006). QTL associated with grain mold were identified using MAS (Nida et al., 2019). Similarly, *Striga*, a parasitic weed, poses a significant threat to sorghum production in sub-Saharan Africa (Ejeta, 2007). QTL mapping has led to identifying genomic regions associated with *Striga* resistance and employed in MAS to generate *Striga*-resistant sorghum varieties with increased yields for smallholder farmers (Haussmann et al., 2004; Kavuluko et al., 2021). Therefore, QTL mapping and MAS have significantly contributed to developing resistant sorghum varieties leading to improved crop yields and increased food security in regions where sorghum is a staple crop.

QTL mapping using recombinant inbred lines (RILs) is commonly employed in mapping studies for its controlled genetic background, reduced environmental influence, reproducibility, and stability in polygenic traits (Cavanagh et al., 2008). Since RILs are a finite population, they

can be assessed across multiple environments and growing seasons. This allows researchers to evaluate the consistency of QTL effects under different conditions for individual environments or QTL by environment interactions (QEI). Therefore, QEI analysis for multi-environmental trials is important; conducting QTL mapping for each environment is also helpful to ensure accuracy and combine the results obtained from all environments (Li et al., 2015). In addition, accessing QEI enhances the practical application of marker-assisted selection (MAS) in plant breeding while providing valuable insights into the genetic structure of significant quantitative traits and the interplay between genotypes and environmental factors (El-Soda et al., 2014). Several proposed QTL mapping methods and models like mixed linear model approaches (Wang et al., 1999), regression mapping approach (Hackett et al., 2001), composite interval mapping (Li et al., 2007), simple and composite interval mapping with mixed model combined (Boer et al., 2007), Bayesian model (Zhao & Xu, 2012) provide a biased estimation (Boer et al., 2007; Zhao & Xu, 2012; S. Li et al., 2015). However, inclusive composite interval mapping (ICIM), a two-step method for QTL mapping in biparental populations for additive, dominant, and epistatic effects, was proposed (Li et al., 2007, 2008; Wang, 2009). It involves stepwise regression for marker selection and adjusting phenotypic values for interval mapping. This technique improves genetic background control, estimation accuracy, and detection power, resulting in higher detection rates, lower false discoveries, and more precise QTL effect and position estimates (Li et al., 2015).

Stalk rot disease caused by fungal pathogens (*Macrophomina phaseolina* and *Fusarium thapsinum*) impacts sorghum production as it negatively impacts both yield and quality of the crop due to reduced grain filling and poor harvestability (Tesso et al., 2012; Adeyanju et al., 2016; Perumal et al., 2020). Because the environment highly influences the development and severity of the disease, genetic mapping studies have been inconsistent (Srinivasa Reddy et al., 2008;

Adeyanju et al., 2015 and 2016). Mapping approaches that involve applying QEI along with single environment QTL mapping could help get a reliable mapping output. Several factors besides the environmental effect pose challenges to stalk rot resistance breeding. These include the quantitative nature of host resistance, the diversity of the causal pathogens (species and strains), phenotyping difficulties, and competing breeding priorities. Despite these challenges, recent advances in genomics, marker-assisted selection, high-throughput phenotyping, and, most importantly, the availability of diverse genetic materials for resistance can help accelerate the breeding progress.

Previous genetic mapping studies on Fusarium stalk rot in sorghum lack integration of the epistatic and environmental interaction effects despite the significant role of the environment in affecting disease development (Srinivasa Reddy et al., 2008; Adeyanju et al., 2015, 2016). The present study proposed to dissect the additive, epistatic, and environmental QTL to discover stable QTL for Fusarium stalk rot. An $F_{2:8}$ RIL mapping population developed from a cross between BTx3042 (susceptible) and SC599 (resistant) was phenotyped in the field for three years (summer of 2018, 2019, and 2020) in Manhattan, Kansas. The RILs were also genotyped using the genotyping-by-sequencing method (GBS).

2.3 Materials and Methods

2.3.1 Plant materials and field experimental design

A mapping population of 233 $F_{2:8}$ recombinant inbred lines (RILs) was developed from a cross between BTx3042 and SC599. BTx4032 is an early maturing seed parent (B-line) used as a tester in a hybrid breeding effort. It is susceptible to *F. thapsinum* induced stalk rot disease (Tesso et al.,

2005). SC599 is an inbred R-line known for its resistance to most stalk rot causing pathogens (Tesso et al., 2005).

The RILs, along with their parent, were tested for three years in the summers of 2018, 2019, and 2020 at Ashland Bottoms, Kansas State University Agronomy research farm near Manhattan, Kansas. The experimental design was an alpha lattice with two replications. A 5 m long single-row plot was used for each line with the spacing between plots and blocks of 0.75 and 1.5 m, respectively. One hundred seeds of each RIL and parents were prepared and treated with a slurry mix of Maxim 4FS, Apron XL, Cruiser 5FS, Concept III, colorant, and water. The seeds were drilled into a 5m long single row using a cone planter. Fertilizer was applied at the rate of 34 kg P_2O_5 ha^{-1} and 90 kg N ha^{-1}. Pre-emergence herbicides were applied as recommended, and post-emergence weeds were controlled manually. In 2018 the experiment suffered from heavy armyworm infestation, and the 2019 and 2020 experiments suffered slightly from drought.

2.3.2 Laboratory inoculum preparation, field inoculation, and disease-scoring procedures

The potato dextrose agar (PDA) cultured pathogen inoculum of *F. thapsinum* was provided by the row crops pathology lab, Department of Plant Pathology, Kansas State University. Inoculum preparation and field inoculation followed the methods described by Tesso et al. (2009). Two small pieces (3-4 mm^2) of the pathogen culture were cut from the PDA culture stock and placed in a flask filled with 100 ml liquid potato dextrose broth (PDB-Difco) to initiate the inoculum suspension. The pathogen culture was incubated on a shaker for three days and strained using KenAG non-gauze milk filters to separate the mycelial mass from the conidia. Hemacytometer was used to count the number of conidia under a microscope to determine the concentration, and the inoculum concentration was adjusted to $5x10^4$ conidia ml^{-1} by diluting with a PBS (phosphate-

buffered saline) solution for inoculation. In each plot, six plants of uniform growth stage were randomly selected at 50% flowering and tagged with two distinct tapes. On day 14, after 50% flowering, three bearing one of the two tapes were inoculated with pathogen suspension, and the remaining three plants bearing the other tape were mock inoculated using PBS solution as a control. In other words, pathogen and mock-inoculated plants were tagged with distinct tapes to facilitate sorting during disease scoring. The inoculum and mock solutions were administered into the basal stalks approximately 10 cm above the ground. A modified syringe and needle were used to deliver approximately 1 ml of the suspension. On day 28 after inoculation, the inoculated plants (both pathogen and mock) were harvested by cutting them just above the ground and were stored at 4°c until disease scoring.

2.3.3 Phenotypic data collection and statistical analysis

The disease was scored by splitting the stalks longitudinally through the inoculation point, as Tesso et al. (2009) described. It was performed by measuring total lesion length (TLL), major lesion length (MLL) and by counting the number of diseased nodes (NDN). TLL (cm) was measured as the entire length of the visible lesion in the pith of the stalk, and MLL (cm) as the length of the uninterrupted wider and darker lesion measured around the inoculation site. Relative lesion length (RLL) was calculated by dividing the major lesion length by plant height. The NDN was determined by counting the number of nodes within the total lesion. In addition, plant height (PHT) and days to flowering (DTF) were recorded. Plant height was measured as the length of the plant from the ground level to the tip of the panicle, and days to flowering were the number of days from planting to when 50% of the plants in a plot reached 50% anthesis.

Analysis of variance on the phenotypic data was conducted using PROC GLM incomplete design procedure in SAS 9.4. All factors except genotypes, and their interactions, were considered random effects. Significant means for all traits were separated using Fischer's protected LSD. Heritability (broad sense) was computed for all characters as per the following formula adopted by Allard (1960).

$h^2 = \frac{\delta^2 G}{\delta^2 P}$, where h^2 is broad sense heritability, $\delta^2 G$ is the genotypic variance and $\delta^2 P$ is the phenotypic variance.

The character associations represented by the correlation coefficient between different pairs of characters at the genotypic and phenotypic levels (Falconer and Mackay, 1996) were estimated using the SAS. To estimate the genotypic correlation coefficient, covariance analysis between all pairs of characters was calculated as follows:

$$Cov_{g_{xy}} = {}^{(MSP_g - MSPe)}/_{r}$$

Where, Cov_{gxy} = genotypic covariance between traits *x* and *y*

MSP_g = Genotypic mean sum product of traits *x* and *y*

MSP_e = Environmental mean sum product of traits *x* and *y*

Genotypic correlation coefficients were calculated using the formula:

$$r_{g_{xy}} = (Cov_{g_{xy}}) / \sqrt{\sigma^2_{g_x} \sigma^2_{g_y}}$$

Where: r_{gxy} = genotypic correlation coefficient between character *x* and *y*

Cov_{gxy} = genotypic covariance between characters *x* and *y*

σ^2_{gx} = genotypic variance for character *x*

σ^2_{gy} = genotypic variance for character *y*

The coefficients of correlations at genotypic levels were tested for their significance using the formula described by Robertson (1959) as indicated below:

$$t = r_{gxy}/SEr_{gxy}$$

The calculated "*t*" value was compared with the tabulated "*t*" value at (*n-2*) degree of freedom at 5% level of significance. Where, *n* is number of genotypes.

$$SE_{gxy} = \sqrt{(1 - r^2 g_{xy})/(2h^2 x \,.\, h^2 y)}$$

Where, h^2_x = heritability of trait *x* and h^2_y = heritability of trait *y*.

2.3.4 High throughput DNA extraction and genotyping

A total of 190 RIL and their parents were planted in a greenhouse in the summer of 2020 for DNA extraction. Two weeks after planting, five-leaf pieces from young leaves were collected and freeze-dried at -51°C for 72 hours using a freeze dryer (ThermoSavant, Holbrook, NY). The tissues were ground, and DNA was extracted using a modified cetyltrimethylammonium ammonium bromide (CTAB) protocol (Saghai-Maroof et al., 1984). DNA extraction and GBS were performed in the USDA Central Small Grain Genotyping Lab, Kansas State University, Manhattan, Kansas. DNA

was quantified and normalized to a concentration of 25 ng/μL for constructing the GBS library using the *PstI* (recognition site: CTGCA—G) and *MspI* (recognition site: C—CGG) restriction enzymes (Fu et al., 2016; Boatwright et al., 2021).

In the following years, another set of tissue samples was collected from 186 RILs and the parents (three samples of each parent). The dried leaf samples were sent to the University of Wisconsin Bioinformatics Resource Center (UWBC) for DNA extraction, library preparation, and sequencing. Genotyping was performed at UWBC using *APeKI* restriction enzyme (recognition site: G-CWCG), commonly used for sorghum GBS (Elshire et al., 2011; Morris et al., 2013; Bouchet et al., 2017). The samples were sequenced by NovaSeq 6000 with a depth of 250 million reads per sample. GBS library was constructed using the protocol described in Elshire et al. (2011). After sequencing, quality control based on the Phred value and read trimming, using trimming software skewer (Jiang et al., 2014), processed on the raw FASTQ files to remove sequencing adapters and low-quality bases. The TASSEL GBS pipeline v2 (Glaubitz et al., 2014) was used for the single nucleotide polymorphism (SNP) variant calling. Reads were aligned to the sorghum reference genome, Sorghum bicolor v3.1.1 (McCormick et al., 2018), using Bowtie 2 alignment software to align the FASTQ data (Langmead & Salzberg, 2012). SNP variants detected were stored using Variant Call Format (VCF).

We discovered that the SNP GBS data from both sets of the run (*PstI/MspI* and *ApeKI* restriction enzyme genotyping) had similar trends on the markers in chromosomes 4, 6, and 7 in both, and results from GBS data with *APeKI* genotyping are discussed herein.

2.3.5 Data visualization, cleaning, filtering, and linkage map construction

The marker data structure and distribution were visualized using principal component analysis (PCA). We analyzed 192 individuals, all genotyped RILs of the biparental population and the two parents. GBS data was cleaned for more than 80% missing genotypes and 0.05 minor allele frequency using *vcftools* (Danecek et al., 2011) and imputed on *Beagle 5.4* (Browning et al., 2021) for the PCA plot. The GBS SNP data from the global sorghum association panel (SAP) containing 401 accessions (Hu et al., 2019) was used to visualize the RILs distribution on the PCA against the SAP. The bi-allelic SNP genotypes of SAP were cleaned for minor allele frequency at 0.05 and 80 percent missing using *vcftools* and imputed in *Beagle*. The SAP data was used as a training set for the PCA to determine the x- and y-axes of the PCA plot. These axes were used to predict the PCA eigenvalues for the RILs and their parents using *"prcomp"* and *"predict"* functions on the R program. The PCA was plotted using the merged SAP and the RIL data, and the SAP passport data was used to identify the parents of the RILs on the R program.

Apart from the cleaning for PCA, the RIL GBS data cleaning for linkage mapping was carried out on Beocat, the KSU remote computing facility. Raw sequence data were checked to keep only bi-allelic SNPs and filtered for minor allele frequency at 0.4 and 80 percent missing data using *vcftools* (Danecek et al., 2011). Out of 186 RILs genotyped, only 146 RILs with 19,180 total SNP markers were retained. Except for chromosomes 4, 6, and 7, the other chromosomes had more than 1000 markers (Table 2.1). Chromosome 3 has the highest number of markers (3946), while chromosome 4 with 76, chromosome 6 with 323, and chromosome 7 with 336 SNPs (Table 2.1). Then the cleaned data were imputed using *Beagle 5.4* (Browning et al., 2021). Each chromosome was imputed separately and merged using *Tassel 5* (Bradbury et al., 2007). The *vcf* file was

converted to *rqtl* format, saved in the *HapMap* file, and imported into R software for further cleaning using the *qtl* package.

The genotypes were plotted to check markers with larger missing data and individuals with low marker coverage using "*plotmissing"* and "*nmissing"* functions (Figure 2.1A and 2.1B). Names of the markers were identified and dropped the markers using "*drop.markers"* function. At this point, we had 134 RIL individuals with 19,144 markers retained (Table 2.1). Mismatched genotypes were removed using "*drop.markers*" function. Using *"findDupMarkers"* and *"comparegeno"* functions, we tried to identify duplicate markers and removed using "*drop.dupmarkers*" function. Only 3684 total markers and 126 individuals were retained after filtering (Table 2.1).

After filtering for their pairwise recombination frequency, segregation distortion, and the number of crossing over, 3297 markers were used for linkage mapping (Table 2.1; Figure 2.1C and 2.1D). First, the error linkage mapping was determined by plotting the error frequencies using the "*est.map"* function, and a 0.01 error probability was selected. Then, the linkage map was re-estimated using the new error p-value. However, the average and maximum spacing between markers on chromosomes 4, 6, and 7 were too high. Therefore, we tried to drop non-informative markers using "*dropmarker*" function on *qtl* package on R., but it was not improved. Finally, since ordering and rippling on *qtl* package of R takes too long and needs higher computation power, grouping, ordering, rippling, and linkage mapping on IciMapping software version 4.2 using MAP functionality (Meng et al., 2015) were performed.

On IciMapping software, using 3297 SNP markers for 126 individuals, a linkage map was constructed based on the Haldane mapping function. The grouping in the linkage mapping was

done using the threshold value of recombination frequency at 0.5, ordering using k-Optimality of nearest neighbor (2-OptMAP) for tour construction, and tour improvement by LOD, and the number of random nearest neighboring (NN) initials was 10. Rippling was done in a window size of seven by LOD value. The final output included LOD score, recombination frequency, pairwise distance (cM), and QTL mapping input files. The ordering was modified by changing marker positions to get a shorter distance between markers. In addition, distant markers were deleted to get even distribution of markers in each linkage group.

2.3.6 QTL analysis

QTL analysis was carried out using the IciMapping software version 4.2 (Meng et al., 2015). The mean trait value replaced missing phenotypes. The Haldane mapping function was used. Interval mapping for additive QTL (IM), inclusive composite interval mapping for additive QTL (ICIM), and ICIM for epistatic mapping (ICIM-EPI) were used to detect the QTL in their respective category using the BIP functionality. A step in scanning was represented by 1cM. The logarithm of odds (LOD) values greater than 3.0 for IM and ICIM additive QTL analysis was used to declare significant QTL. ICIM-EPI significance was declared LOD >4. The probability in stepwise regression of phenotype on marker variables (PIN) was set to 0.001.

In addition, QTL by environment interaction was analyzed using MET functionality on ICIM for ICIM for additive QTL (ICIM-ADD) only for the disease phenotypic trait MLL. ICIM first selects the optimal regression model, identifying markers and marker pairs accounting for additive and epistatic variations, and then applies interval mapping to the adjusted phenotypic values, determined by the chosen regression model, to locate QTL in marker intervals and estimate

their effects (Li et al., 2015; Meng et al., 2015). Adjusted phenotypic values help control the genetic background effect (Li et al., 2015).

We followed the commonly applied QTL nomenclature, where the name starts with q for QTL, followed by an organism (Sb for *Sorghum bicolor*), then two letters of the trait and chromosome number followed by trait number 1-4 (each trait has three-year data (2018, 2019 and 2020) and the mean). A letter was added when QTL is more than one in a chromosome and in a single year (McCouch, 1997). E.g., two QTL *(q)* for major lesion length *(ML)* identified on chromosome *5* in 2020 *(3)* and mean *(4)*: *qSbML5.3a* and *qSbML5.3b*, and *qSbML5.4a* and *qSbML5.4b* were used.

Table 2.1. APeKI GBS raw, and cleaned SNP genotypes of sorghum stalk rot RIL mapping population

Chromosomes	Raw data	Cleaned and filtered			
		PM & MAF	MIM	Dup	RF & CO
1	40,779	2076	2066	445	398
2	40,639	3546	3528	697	611
3	39,309	3946	3946	768	707
4	28,627	76	76	21	16
5	30,022	3051	3049	501	448
6	24,767	323	322	86	35
7	18,606	336	335	96	90
8	23,166	1798	1798	290	252
9	24,453	2847	2846	513	494
10	26,940	1181	1178	267	246
Whole genomes	299,685	19180	19,144	3684	3297
RILs	*192	146	134	126	126

PM = percent missing (>80%), MAF = minor alleles frequency (> 0.4); MIM = After a lower number of genotyped markers for each individual and lower number of genotyped individuals for each marker removed; Dup = After duplicates and mismatched markers removed; RF = after recombination frequency (<0.4) and CO = crossing over cleaned; *All individuals genotyped including parents

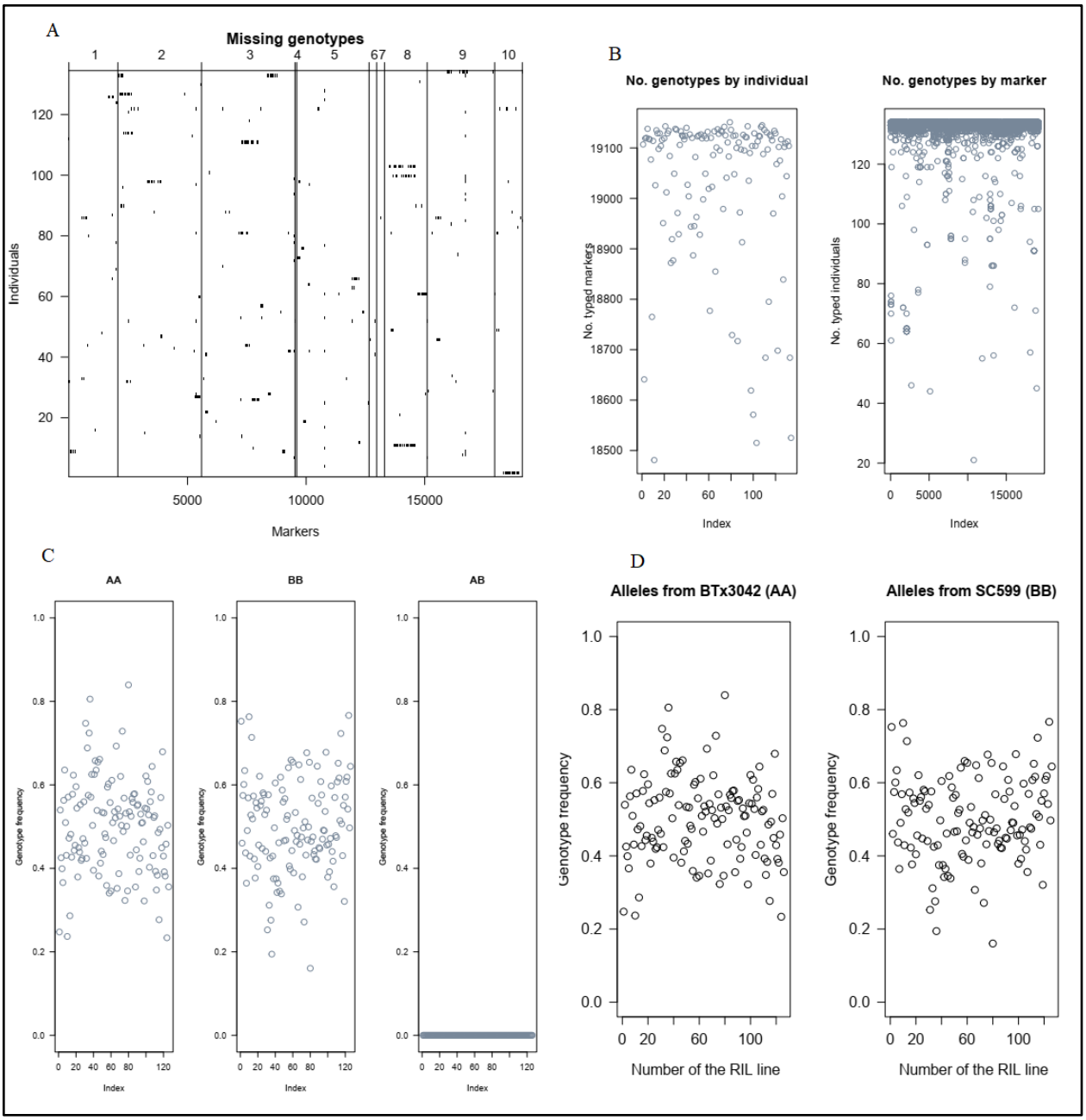

Figure 2-1. APeKI GBS SNPs data filtering and cleaning of sorghum stalk rot RIL mapping population.

A. After missing genotypes were cleaned. B. Plot of the number of genotyped markers for each individual (left) and number of genotyped individuals for each marker (right) after a low number of genotypes by an individual and markers were removed. C. AA, BB, and AB genotypes frequency distribution. D. Parental genotype distribution: AA alleles from BTx3042 and BB alleles from SC599.

2.4 Results

2.4.1 Variability, trait association, and heritability of the field phenotyping

The analysis of variance combined over the years shows significant variation among the RILs for all traits (Table 2.2). The mean major lesion length (MLL) among the RILs ranged from 1.5 to 12.3 cm. The MLL in the resistant parent, SC599, was 2.38 cm, and the susceptible parent, BTx3042, was 6.6 cm. Similarly, the total lesion length (TLL) ranged from 2.6 to 29.4 cm in the RILs. TLL for the resistant parent was 9 cm, and for the susceptible parent was 16.3 cm. Similar trends were observed for plant height and days to flowering. Several RILs were found to be more resistant, and others more susceptible than their corresponding resistant and susceptible parents. Likewise, there were novel segregants that were either shorter and/or taller, earlier maturing and/or later maturing than either of their founding parents. These indicate the presence of transgressive segregation among the RIL population.

Broad sense heritability for plant height (h^2 = 92.2%) and days to flowering (h^2 = 84.4%) were highest compared to that of lodging (h^2 = 55.9%), number of diseased nodes (NDN) (h^2 = 64%) and MLL had a (h^2 = 66%) (Table 2.3). The genotypic correlation between MLL and other traits except NDN was significant (Table 2.3). Lodging significantly and positively correlated with days to flowering. The genotypic correlation between days to flowering and other traits was small in magnitude.

Table 2.2. Combined analysis of variance for sorghum stalk rot mapping population (RILs) and their founding parents for agronomic and disease related traits evaluated at Manhattan, KS during 2018, 2019, and 2020 growing seasons.

Trait	Mean Squares				CV%	Parent			RILs Mean	Range
	Rep	Year	Geno	Error		P1	P2	Mean		
MLL	0.02NS	1004.6***	15.5***	5	44	2.4	5.7	4	5.1	1.5-12.3
RLL	10.9NS	457.9**	7.0**	3.6	41.9	2.1	5	3.5	4.6	1.4-8.9
TLL	6.7NS	2011.9***	66.4***	17.4	36.4	9.1	16.3	12.7	11.4	2.6-29.4
NDN	3.9NS	71.1***	1.8***	1	30.5	3.2	4	3.6	3.3	1.8-5.5
LDG	0.3NS	84.9**	1.9*	1.5	57.7	1.7	3	2.4	2.3	1-3.5
DTF	888.7***	1468.7***	89.0***	16.4	6.1	71	59.7	65.3	66.1	56-78
PHT	6793.6***	29116.5***	1549.8***	130.1	10.4	111.7	113.2	112.5	110.2	77-203

MLL = Major Lesion Length; RLL = Relative Major Lesion Length; TLL = Total Lesion Length; NDN = Number of diseased nodes; LDG = stalk lodging (1-5); DTF = Days to flowering, PHT = Plant height; Rep = Replication; Geno = individual genetic materials (genotypes); CV = coefficient of variation; P1 = SC599; P2 = BTx3042; RILs = Recombinant inbred lines; ^{NS} = nonsignificant; * = significant at 0.05; ** = significant at 0.01; *** = significant at 0.001.

Table 2.3. Genotypic correlation between the traits based on the three years mean and broad sense heritability (h^2).

Traits	MLL	RLL	TLL	NDN	LDG	DTF	PHT	h2 (%)
MLL	1							66.1
RLL	0.83**	1						66
TLL	0.89**	0.67**	1					79.2
NDN	0.023	0.21**	0.18**	1				64.3
LDG	0.61**	0.38**	0.58**	0.26**	1			55.9
DTF	0.12**	-0.00044	0.04**	0.03*	-0.12**	1		84.4
PHT	0.80**	0.34**	0.79**	-0.10**	0.75**	0.19**	1	92.3

Key: Refer to Table 2.2.

2.4.2 Genotypic data structure, visualization, and linkage map construction

PCA analysis was used to visualize the GBS SNPs structure and distribution compared to the 401 global sorghum association panel (SAP) ApeKI GBS data (Hu et al., 2019) (Figure 2.2). PCA1 and PCA 2 explained 14.3% of the total variability. The parents in the SAP (Black and purple dots) and our data (Red and green) were plotted at the same locations. The RILs were clustered between the two parents, while there were a few RILs that looked outliers.

A mapping population of 186 RILs and the two parents generated 299,685 raw GBS SNPs (Table 2.1). SNPs that were not polymorphic across the RILs, higher missing genotypes and individuals, heterozygotes, lower minor allele frequencies, and duplicate markers were filtered out, retaining 3297 SNPs in 126 individuals. These SNPs were maintained for linkage mapping and QTL analysis. The total length of the linkage map was 3070.8 cM, with an overall average genetic distance of 1.84 cM between adjacent markers (Table 2.4). The distribution of markers on chromosomes was uniform in most cases and covered the entire chromosome (Table 2.4; Figure 2.3). However, there were wider gaps on chromosomes 6 (94.02 cM) and 7 (83.70 cM) (Table 2.4;

Figure 2.3). The data cleaning and filtering step removed most duplicated markers from these chromosomes (retaining fewer markers). Marker density was highest on chromosome 3 (18.5%) with an average distance of 0.80 cM and lowest on chromosome 4 (0.4%) with an average distance of 0.79 cM.

2.4.3 QTL mapping for flowering time, plant height, and lodging identified previously mapped QTL

Several QTL were discovered for days to flowering both through IM (Table 2.5) and ICIM (Table 2.6) methods. On chromosome 6, QTL were detected consistently in all three years and their means using the ICIM. Those were *qSbDF6.1*, *qSbDF6.2*, *qSbDF6.3*, and *qSbDF6.4* (Table 2.6). The QTL identified on the mean data was *qSbDF6.4* and had a higher PVE. However, the IM detected significant QTL on chromosome 6 only for 2018 and on the mean data flanked by the same markers as the ICIM (S06_38162222 and S06_3223900) (Table 2.5). Additionally, QTL were detected on chromosomes 2 and 8 in both IM and ICIM methods and in years 2019 and 2020, as well as the mean data. There was no significant QTL in 2018 in both mapping methods for plant height. However, in 2019, 2020, and the mean, QTL were discovered consistently on chromosome 3 using both IM and ICIM. For those QTL, the PVE % ranged from 7.5 to 18.5. Additional two QTL were detected in 2019 on chromosome 5 with a PVE of 16% based on the ICIM analysis (Table 2.6). On chromosome 1, two QTL were detected for the 2020 and mean data using ICIM, while the IM only detected these QTL in the 2020 data. On stalk lodging, QTL were detected in 2019 in both mapping methods. ICIM detected significant QTL on chromosome 1 (5.6 PVE %) and 3 (9.6 PVE %). Likewise, IM identified two QTL on chromosome 3 (11.3 and 15.2 PVE %) (Table 2.5).

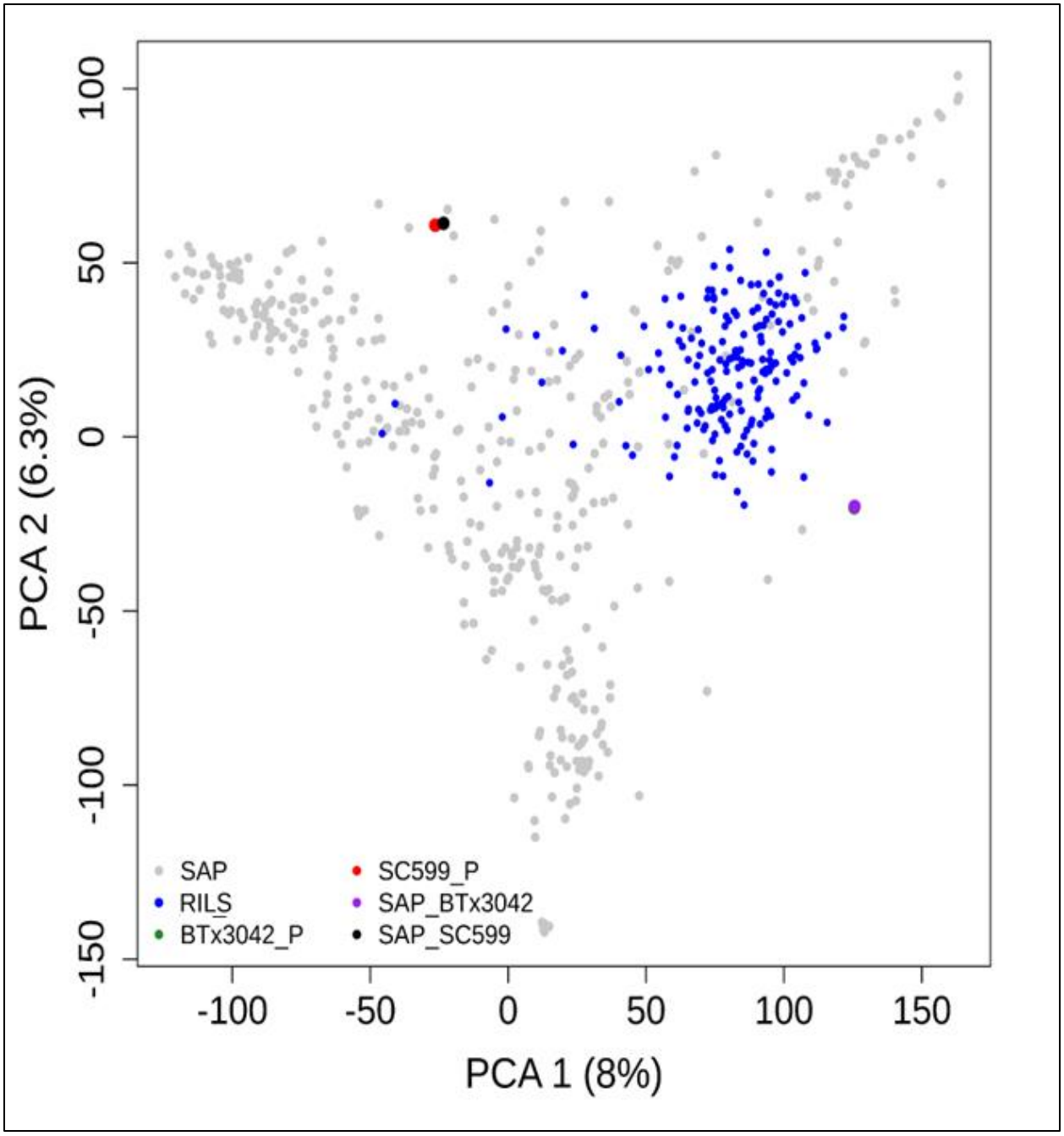

Figure 2-2. Principal component analysis (PCA) to visualize the distribution of GBS SNP of the RILs (186) compared to their parents plotted on PCA axes of 401 accessions of the global sorghum association panel (SAP).
The parents in the SAP (SAP_BTx3042 = purple and SAP_SC599=black dots) and in our GBS data (BTx3042_P=green and SC599_P= red dots)

Table 2.4. Summary of linkage map construction on sorghum stalk rot mapping population (RILs) for QTL mapping.

Chromosome	Number of SNP Markers	Average Distance	Maximum Distance	Chromosome Length (cM)
1	398	0.88	7.33	351.76
2	611	0.78	11.2	474.27
3	707	0.8	10.68	566.9
4	16	0.79	4.55	12.68
5	448	0.82	23.39	366.57
6	35	10.11	94.02	353.7
7	90	1.75	83.7	157.56
8	252	0.81	10.57	204.51
9	494	0.66	5.53	326.92
10	246	1.04	17.76	255.93
Whole genome	329	1.84	26.87	3070.81

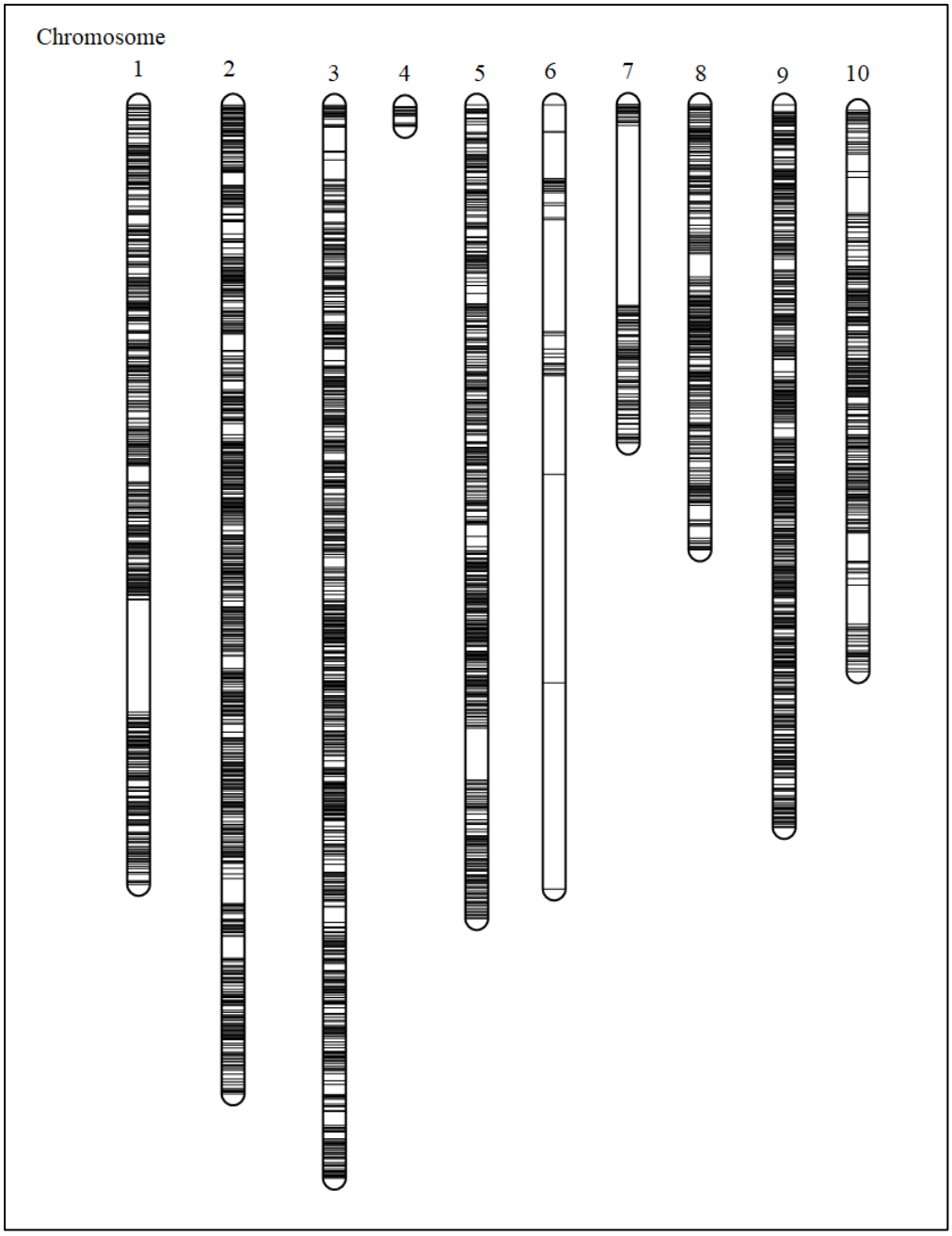

Figure 2-3. Linkage map constructed using 3297 SNP markers covering 3070.8 cM of the genome.

2.4.4 Additive QTL mapping for *Fusarium thapsinum*

The analysis was performed using IM (Table 2.5) and ICIM of additive QTL (Table 2.6). We measured disease severity based on lesion length to map the disease-related QTL. IM detected nine QTL for major lesion length (MLL) on chromosomes 1, 3, 5, and 9 (Table 2.5). On chromosome 1, two QTL, *qSbML1.1* and *qSbML1.3*, that explained 11.5 and 7.1% PVE, respectively, were detected for 2018 and 2020 (Table 2.6). For 2019, one QTL (*qSbML3.2*) with 11.7% PVE was discovered on chromosome 3. Similarly, on chromosome 5, *qSbML5.3a* and *qSbML5.3b* for 2020, and *qSbML5.4a* and *qSbML5.4b* for the mean were detected. The QTL identified in 2020 and on the mean were located in the same position, *qSbML5.3a* (2020) and *qSbML5.4a* (mean) at 12 cM, whereas *qSbML5.3b* (2020) and *qSbML5.4b* (mean) *at* 24 cM on the linkage map. In addition, two QTL were identified on chromosome 9 based on the mean data and not for the individual year data.

On the other hand, ICIM identified ten disease-related, significant QTL (Table 2.6). MLL had two QTL in 2018, one in 2019, and four in the mean data. In 2018 QTL *qSbML1.1* on chromosome 1 explained 12% of the total PVE, with a negative additive effect on the trait. *qSbML5.1* had a 9% PVE on the same year and chromosome but had a positive additive effect (Table 2.6). In 2019, a QTL on chromosome 3 explained 12% of the PVE with a positive additive effect. In 2020, no QTL was detected. On the mean data, we discovered QTL (*qSbML5.4*) with the largest PVE (33.9%), LOD (67.8), and additive effect (3.3) and IM also identified a QTL in 2020, and the mean data on the same location between markers S05_69288833 and S05_69704221 (Table 2.6). Additionally, on chromosome 9, two QTL were identified using IM (Table 2.5) and ICIM (Table 2.6).

The total lesion (TLL), the number of diseased nodes (NDN), and relative major lesion length (RLL), the other traits of disease severity, were analyzed for QTL mapping. A total of three QTL for TLL in chromosome 1, two in 2019, and one in the mean data were detected, explaining 10% on IM (Table 2.5) and 13% PVE on ICIM (Table 2.6). Neither IM nor ICIM detected any QTL for NDN and RLL.

Table 2.5. QTL detected on interval mapping of additive QTL (IM).

Trait	QTL	Ch	Pos.	Left Marker	Right Marker	LOD	PVE (%)	Add
MLL_2018	qSbML1.1	1	43	S01_72372621	S01_71998851	3.4	11.5	-0.4
MLL_2019	qSbML3.2	3	52	S03_68474855	S03_67903023	3.3	11.7	0.4
MLL_2020	qSbML1.3	1	108	S01_63359107	S01_63412222	3.3	7.1	1.0
MLL_2020	qSbML5.3a	5	12	S05_70250139	S05_70182285	3.3	7.2	1.0
MLL_2020	qSbML5.3b	5	24	S05_69288833	S05_69704221	3.2	7.0	1.0
MLL_Mean	qSbML5.4a	5	13	S05_70180835	S05_70180551	3.9	6.3	0.5
MLL_Mean	qSbML5.4b	5	24	S05_69288833	S05_69704221	4.2	6.7	0.5
MLL_Mean	qSbML9.4a	9	64	S09_51244364	S09_51243858	3.0	4.8	0.4
MLL_Mean	qSbML9.4b	9	75	S09_51521422	S09_51521893	4.0	6.4	0.5
TLL2019	qSbTL1.2a	1	26	S01_72086685	S01_72142848	4.2	8.7	-1.0
TLL2019	qSbTL1.2b	1	43	S01_72372621	S01_71998851	4.4	8.7	-1.0
TLLMean	qSbTL1.4	1	43	S01_72372621	S01_71998851	3.5	12.6	-0.9
DTF_18	qSbDF6.1	6	1	S06_38162222	S06_3223900	8.5	26.6	-2.5
DTF_19	qSbDF2.2a	2	354	S02_67574082	S02_67751888	3.3	4.0	-1.5
DTF_19	qSbDF2.2b	2	377	S02_69148759	S02_69498707	3.9	4.8	-1.7
DTF_19	qSbDF2.2c	2	398	S02_73692625	S02_73941818	3.4	4.2	-1.5
DTF_19	qSbDF2.2d	2	402	S02_73997081	S02_73997313	4.1	4.9	-1.6
DTF_20	qSbDF2.3	2	397	S02_73502950	S02_73692625	4.1	8.3	-1.2
DTF_20	qSbDF8.3a	8	92	S08_52074598	S08_49761866	3.1	6.4	-1.1
DTF_20	qSbDF8.3b	8	111	S08_7728324	S08_7105197	3.1	6.4	-1.1
DTF_Mean	qSbDF2.4a	2	382	S02_69498707	S02_72639799	3.5	11.2	-1.4
DTF_Mean	qSbDF2.4b	2	401	S02_73888898	S02_73942603	4.1	10.8	-1.3
DTF_Mean	qSbDF6.4	6	2	S06_38162222	S06_3223900	6.6	18.7	-1.8
PHT_19	qSbPH3.2a	3	15	S03_74155099	S03_72065287	4.5	12.7	6.1
PHT_19	qSbPH3.2b	3	67	S03_65364673	S03_65357487	4.0	8.9	5.1
PHT_20	qSbPH1.3	1	32	S01_72636869	S01_72678994	3.1	11.4	-5.9
PHT_20	qSbPH3.3	3	1	S03_73925045	S03_73935365	3.8	14.0	6.5
PHT_Mean	qSbPH3.4	3	1	S03_73925045	S03_73935365	3.5	12.2	5.0
Ldg_19	qSbLG3.2a	3	21	S03_72029588	S03_71421333	6.6	15.2	0.5
Ldg_19	qSbLG3.2b	3	36	S03_69630776	S03_69550952	4.8	11.4	0.5

Ch = chromosome number, Pos. = position on the linkage map in cM, LOD = logarithm of odds, PVE = percentage of variation explained, Add = additive effect of the QTL

Table 2.6. QTL detected on integrated composite interval mapping of additive QTL.

Trait	QTL	Ch	Pos.	Left Marker	Right Marker	LOD	PVE (%)	Add
MLL_2018	qSbML1.1	1	43	S01_72372621	S01_71998851	5.5	12.1	-0.5
MLL_2018	qSbML5.1	5	13	S05_70180835	S05_70180551	4.3	9.0	0.4
MLL_2019	qSbML3.2	3	53	S03_67673215	S03_67626559	3.3	12.2	0.4
MLL_2020	qSbML1.3	1	109	S01_63365364	S01_63364220	2.68	9.97	0.87
MLL_2020	qSbML5.3	5	13	S05_70180835	S05_70180551	2.90	10.88	0.92
MLL_Mean	qSbML1.4	1	114	S01_62950583	S01_62982132	3.0	0.4	0.3
MLL_Mean	qSbML5.4	5	24	S05_69288833	S05_69704221	67.8	33.9	3.3
MLL_Mean	qSbML9.4	9	9	S09_54669780	S09_54603795	4.9	0.6	-0.4
MLL_Mean	qSbML9.4	9	75	S09_51521422	S09_51521893	9.9	1.3	0.6
TLL2019	qSbTL1.2	1	23	S01_71839926	S01_71748685	16.7	9.2	2.1
TLL2019	qSbTL1.2	1	26	S01_72086685	S01_72142848	25.9	17.8	-2.9
TLLMean	qSbTL1.4	1	33	S01_72678994	S01_72841958	4.5	13.1	-1.0
DTF_18	qSbDF2.1	2	379	S02_69498707	S02_72639799	3.2	8.0	-1.4
DTF_18	qSbDF6.1	6	1	S06_38162222	S06_3223900	9.6	26.7	-2.5
DTF_19	qSbDF2.2	2	401	S02_73888898	S02_73942603	9.7	15.2	-2.0
DTF_19	qSbDF3.2	3	45	S03_68814998	S03_68605881	3.4	4.7	-1.1
DTF_19	qSbDF6.2	6	11	S06_38162222	S06_3223900	6.4	9.7	-1.7
DTF_19	qSbDF7.2	7	151	S07_54939251	S07_54707494	5.0	7.1	-1.4
DTF_19	qSbDF8.2	8	46	S08_59955339	S08_59879039	4.3	6.1	1.3
DTF_19	qSbDF8.2	8	161	S08_3111044	S08_2939983	5.6	8.0	-1.5
DTF_20	qSbDF2.3	2	398	S02_73692625	S02_73941818	6.8	15.8	-1.5
DTF_20	qSbDF6.3	6	8	S06_38162222	S06_3223900	4.1	10.7	-1.2
DTF_20	qSbDF8.3	8	159	S08_3177739	S08_3049256	3.4	7.2	-1.0
DTF_Mean	qSbDF2.4	2	379	S02_69498707	S02_72639799	4.3	10.8	-1.2
DTF_Mean	qSbDF6.4	6	1	S06_38162222	S06_3223900	8.8	23.3	-1.7
PHT_19	qSbPH3.2	3	52	S03_68474855	S03_67903023	6.3	0.6	5.7
PHT_19	qSbPH5.2	5	260	S05_8150667	S05_8225543	53.5	13.9	27.0
PHT_19	qSbPH5.2	5	264	S05_7698556	S05_8111449	59.9	18.6	-31.2
PHT_20	qSbPH1.3	1	33	S01_72678994	S01_72841958	4.9	1.3	-6.1
PHT_20	qSbPH3.3	3	1	S03_73925045	S03_73935365	36.8	18.5	23.6
PHT_20	qSbPH3.3	3	8	S03_73662786	S03_74207764	28.0	11.6	-18.6

Trait	QTL	Ch	Pos.	Left Marker	Right Marker	LOD	PVE (%)	Add
PHT_Mean	qSbPH1.4	1	28	S01_72206067	S01_72166118	5.1	13.5	-5.2
PHT_Mean	qSbPH3.4	3	4	S03_73831971	S03_73807474	3.0	7.5	3.9
PHT_Mean	qSbPH3.4	3	75	S03_64401496	S03_64378088	3.8	9.6	4.4
Ldg_19	qSbLG1.2	1	103	S01_63472763	S01_63380142	5.6	12.1	0.4
Ldg_19	qSbLG3.2	3	21	S03_72029588	S03_71421333	9.6	22.5	0.6
LDG_Mean	qSbLG1.4	1	103	S01_63472763	S01_63380142	3.3	11.3	0.2

Ch = chromosome number, Pos. = position on the linkage map in cM, LOD = logarithm of odds, PVE = percentage of variation explained, Add = additive effect of the QTL

2.4.5 Additive by additive epistatic and additive by environment QTL interaction for major lesion length

The QTL analysis for the interactions was analyzed by inclusive composite interval mapping for MLL. A total of thirty-two significant digenic epistatic QTL were identified for MLL; the significance of QTL interaction was determined at a LOD threshold of >4 (Figure 2.4; Table 2.7). No main effect additive QTL was identified in the significant epistatic QTL, but a few were located closely. The variation explained for the epistatic QTL ranged from 2.7 to 16.6 %, and the LOD ranged from 4.0 to 8.5. Most of the interacting QTL were opposite, negative versus positive effects, and the resulting additive-by-additive effect was negative in most cases. Epistatic interaction between chromosome 1 (*qSbML1.3*) and chromosome 6 (*qSbML6.3*) explained the highest phenotypic variance of 16.6%, in which QTL *qSbML1.3* had negative effect and *qSbML6.3* had positive effect, and their interaction resulted in higher negative effect (-1.4) (Table 2.7). In 2018, 11 epistatic QTL were obtained of which 10 of them were on the same chromosomes, but one epistatic interaction was between QTLs located on chromosomes 5 (*qSbML5.1*) and 6 (*qSbML6.1)*. Similarly, in 2019, 9 pairs of QTLs on chromosomes 1, 2, 3, 5, 6, and 9, and an interaction between QTL on chromosomes 2 and 7, 2 and 10, 3 and 7 were detected. However, in 2020 and the mean data, no interaction was observed within the same chromosome, rather QTL located in different chromosomes were epistatically interacting. QTL on chromosome 1 were associated with QTL on chromosomes 2, 6, and 10, whereas QTL on chromosome 3 were associated with QTL on chromosomes 7, 8, and 10.

The three years (2018, 2019 and 2020) were considered as environments (E1, E2 and E3) for MLL (Table 2.8) in the QTL by environment interactions (QEI). Ten QEI affecting MLL were

significant across the three environments. Significance was called for LOD > 4. The overall PVE ranged from 1.5 to 8.4%. The variation explained due to the additive effects were higher than the environmental effects. The additive (A) by E1 had a negative effect in all the QEI, whereas A × E3 had a mostly positive effect on the QEI. The average effects were positive for all the QEIs except *qeSbML1.1a*. QEI *qeSbML5.1* had the highest LOD = 6.19, LOD_A = 5.31, and LOD_{AE} = 0.89 and had the largest average and QEI effects. The QEIs were one each on chromosomes 3 and 5, three on chromosome 1, and five on chromosome 9. The chromosomes and locations corresponded with QTLs detected in the single environment analysis. Four QEIs were in the same position, with the single environment QTL located on chromosomes 1, 3, 5, and 9, respectively. They were *qSbML1.1* and *qeSbML1.1a* (S01_72372621: S01_71998851), *qSbML3.2* and *qeSbML3.1* (S03_67673215: S03_67626559), *qSbML5.3* and *qeSbML5.1* (S05_70180835:S05_70180551), and *qSbML9.4a* and *qeSbML9.1e* (S09_51521422: S09_51521893).

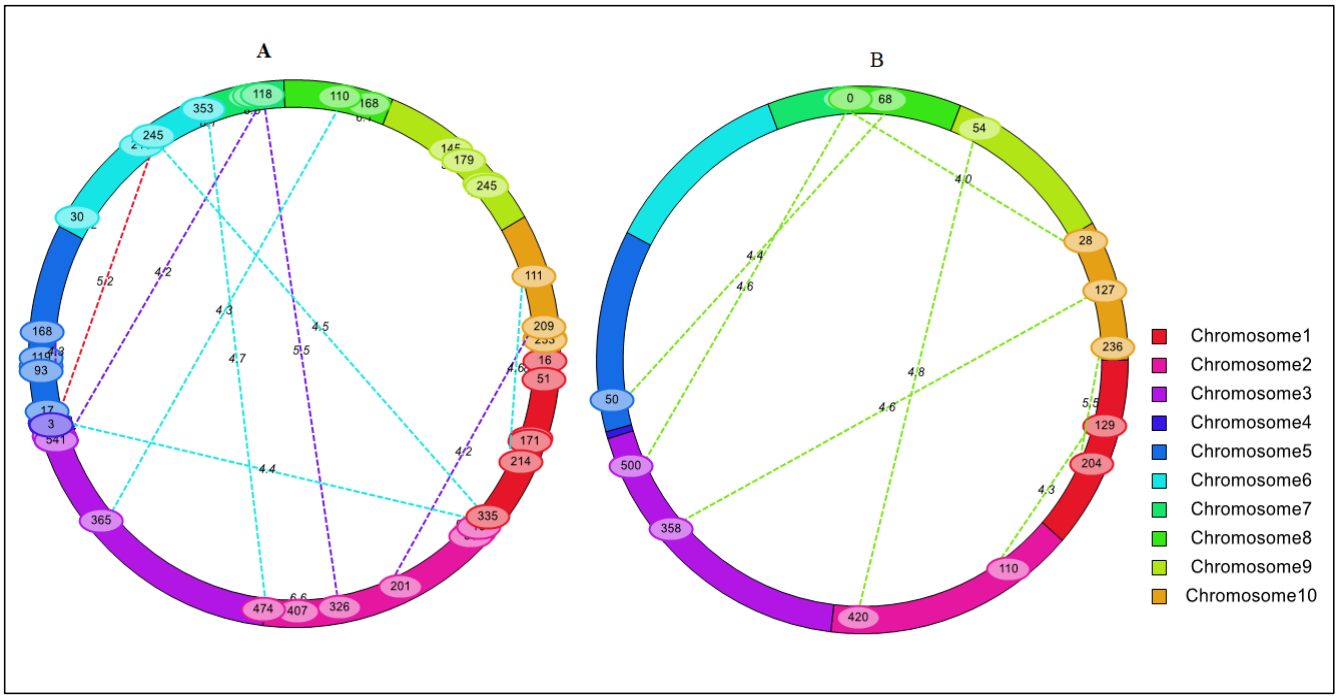

Figure 2-4. Digenic additive by additive epistatic QTL located in different chromosomes identified from inclusive composite interval mapping of epistatic QTL.
A = MLL_2018: the broken red line; MLL_2019: Purple broken line; MLL_2020: Light blue broken line. B = MLL_Mean epistatic QTL interaction. LOD: the numbers on the lines inside the big circle of chromosomes. Position on each chromosome: numbers in oval shapes on the big circle.

Table 2.7. Additive by additive interaction of digenic epistatic QTL identified from ICIM for MLL.

Trait	QTL1	Ch1	Pos1	LeftMarker1	RightMarker1	QTL2	Ch2	Pos2	LeftMarker2	RightMarker2	LOD	PVE	A1	A2	AA
MLL_2018	qSbML1.1a	1	16	S01_68328256	S01_70361928	qSbML1.1b	1	51	S01_71614848	S01_69193243	8.5	3.1	0.8	-0.8	-1
MLL_2018	qSbML2.1a	2	406	S02_74132115	S02_76435652	qSbML2.1b	2	407	S02_74132115	S02_76435652	6.6	3.1	-0.8	0.9	-1
MLL_2018	qSbML3.1a	3	541	S03_1486771	S03_2479998	qSbML3.1b	3	547	S03_2379499	S03_2047797	7.1	3	-0.9	0.9	-0.9
MLL_2018	qSbML4.1a	4	1	S04_1778425	S04_1577167	qSbML4.1b	4	8	S04_1663420	S04_2704215	4.2	2.8	-0.9	0.8	-1
MLL_2018	qSbML5.1a	5	104	S05_64206192	S05_64058694	qSbML5.1b	5	119	S05_64032102	S05_63808991	6.9	2.9	-0.9	0.9	-1
MLL_2018	qSbML5.1	5	17	S05_69717604	S05_69725760	qSbML6.1	6	215	S06_57076305	S06_14493351	5.2	3.5	0.7	-0.9	-0.9
MLL_2018	qSbML6.1a	6	349	S06_14493351	S06_46814845	qSbML6.1b	6	353	S06_14493351	S06_46814845	8.1	3.2	-0.9	0.8	-0.9
MLL_2018	qSbML7.1a	7	91	S07_614560	S07_7678356	qSbML7.1b	7	92	S07_614560	S07_7678356	8.5	3.7	-1.3	1.3	-0.5
MLL_2018	qSbML8.1a	8	166	S08_2683021	S08_2698461	qSbML8.1b	8	168	S08_2698461	S08_2752295	6.1	2.9	0.6	-0.6	-1.3
MLL_2018	qSbML9.1a	9	145	S09_46837959	S09_45671811	qSbML9.1b	9	179	S09_43147708	S09_42815569	5.3	2.7	1	-0.9	-1
MLL_2018	qSbML10.1a	10	230	S10_4603091	S10_2458883	qSbML10.1b	10	233	S10_4603091	S10_2458883	7.3	3.1	-1	1.1	-0.8
MLL_2019	qSbML1.2a	1	166	S01_62136125	S01_61439175	qSbML1.2b	1	171	S01_61596211	S01_61603779	4.5	6.7	-1	1.1	-1
MLL_2019	qSbML2.2a	2	25	S02_5085279	S02_5145804	qSbML2.2b	2	33	S02_5079841	S02_6206021	5.8	7	0.8	-1	-1.3
MLL_2019	qSbML2.2	2	201	S02_55048639	S02_55094464	qSbML10.2	10	209	S10_5218226	S10_5205127	4.2	3.6	-0.1	0.2	-0.4
MLL_2019	qSbML2.2	2	326	S02_64090262	S02_63408953	qSbML7.2	7	118	S07_7667403	S07_7667330	5.5	4.4	-0.2	0.2	-0.5
MLL_2019	qSbML3.2a	3	540	S03_1486771	S03_2479998	qSbML3.2b	3	549	S03_2379499	S03_2047797	5.5	7.1	-0.9	1	-1.1
MLL_2019	qSbML3.2	3	541	S03_1486771	S03_2479998	qSbML7.2	7	102	S07_6761329	S07_6751450	4.2	4.6	0.2	0.2	0.5
MLL_2019	qSbML5.2a	5	93	S05_64636380	S05_64424652	qSbML5.2b	5	168	S05_60740497	S05_60674563	4.3	3.8	-0.1	-0.2	-0.5
MLL_2019	qSbML6.2a	6	29	S06_3199659	S06_1787010	qSbML6.2b	6	30	S06_3199659	S06_1787010	5.2	9.7	-1.1	0.8	-0.8
MLL_2019	qSbML9.2a	9	237	S09_5871029	S09_5831491	qSbML9.2b	9	245	S09_5557535	S09_5519636	4.3	3.8	0.9	-0.8	-1.5
MLL_2020	qSbML1.3	1	214	S01_59709012	S01_59759825	qSbML10.3	10	111	S10_46184769	S10_46016750	4.6	7.4	0.1	-0.4	1.1
MLL_2020	qSbML1.3	1	335	S01_80588479	S01_80660308	qSbML6.3	6	245	S06_57076305	S06_14493351	4.5	16.6	-0.7	0.8	-1.4

Trait	QTL1	Ch1	Pos1	LeftMarker1	RightMarker1	QTL2	Ch2	Pos2	LeftMarker2	RightMarker2	LOD	PVE	A1	A2	AA
MLL_2020	qSbML2.3	2	10	S02_4257680	S02_4692258	qSbML4.3	4	3	S04_1570203	S04_1553927	4.4	7	0.1	0.4	-1
MLL_2020	qSbML2.3	2	474	S02_77450753	S02_77444207	qSbML6.3	6	353	S06_14493351	S06_46814845	4.7	7.1	0.2	-0.1	-1.1
MLL_2020	qSbML3.3	3	365	S03_12569711	S03_12505200	qSbML8.3	8	110	S08_9362245	S08_7728324	4.3	6.7	0	0.4	-1
MLL_Mean	qSbML1.4	1	204	S01_60517658	S01_60389603	qSbML10.4	10	236	S10_2451487	S10_2438939	5.5	7.7	0.1	0.1	0.4
MLL_Mean	qSbML1.4	1	129	S01_62806525	S01_62732270	qSbML2.4	2	110	S02_10199706	S02_10217682	4.3	6.8	-0.1	0.1	0.4
MLL_Mean	qSbML2.4	2	420	S02_76473062	S02_76472675	qSbML9.4	9	54	S09_51836756	S09_51935652	4.8	7.2	0.2	-0.1	-0.4
MLL_Mean	qSbML3.4	3	358	S03_12778076	S03_13174989	qSbML10.4	10	127	S10_15430461	S10_18068645	4.6	6.6	0.1	0	-0.4
MLL_Mean	qSbML3.4	3	500	S03_4218855	S03_4041855	qSbML7.4	7	146	S07_53852802	S07_53871006	4.6	6.4	-0.1	0.1	0.4
MLL_Mean	qSbML5.4	5	50	S05_67523571	S05_67518182	qSbML8.4	8	68	S08_56542105	S08_53852118	4.4	7	0.1	-0.1	-0.4
MLL_Mean	qSbML8.4	8	0	S08_61577351	S08_61581004	qSbML10.4	10	28	S10_56646749	S10_56646511	4	6.7	0	-0.2	-0.4

Ch1=Chromosome number of the interacting first QTL at the first position, Pos1=position of the first interacting QTL in cM, Ch2= Chromosome number of the other interacting QTL on the second position with the first QTL, Pos2= the position of the second interacting QTL in cM, LOD= LOD score caused by epistasis effects, PVE= percentage of phenotypic variation explained by epistatic QTL effects, A1=additive effect of the first QTL, A2=additive effect of the second interacting QTL, AA= additive by additive effect of QTL at the two positions.

Table 2.8. QTL by environment interaction (QEI) detected by inclusive composite interval mapping for MLL.

QEI	Chr	Pos	Left Marker	Right Marker	LOD	LOD (A)	LOD (AE)	PVE	PVE (A)	PVE (AE)	Average Effect	AE1	AE2	AE3
qeSbML1.1a	1	43	S01_72372621	S01_71998851	4.4	2.0	2.4	2.1	1.9	0.2	-0.3	-0.1	0.1	0.0
qeSbML1.1b	1	124	S01_62911170	S01_62865288	3.4	3.2	0.3	5.2	2.9	2.3	0.4	-0.3	-0.2	0.5
qeSbML1.1c	1	113	S01_63299887	S01_62943013	3.7	3.6	0.1	5.7	3.3	2.4	0.4	-0.3	-0.2	0.5
qeSbML3.1	3	53	S03_67673215	S03_67626559	4.1	1.9	2.1	2.1	1.9	0.2	0.3	-0.1	0.1	0.0
qeSbML5.1	5	13	S05_70180835	S05_70180551	6.2	5.3	0.9	8.4	5.3	3.1	0.5	-0.1	-0.4	0.5
qeSbML9.1a	9	307	S09_2688997	S09_2602994	3.1	1.5	1.6	1.5	1.5	0.0	0.3	0.0	0.0	0.0
qeSbML9.1b	9	52	S09_51911948	S09_51881455	3.8	1.9	1.9	1.9	1.8	0.0	0.3	0.0	0.0	0.0
qeSbML9.1c	9	91	S09_50360240	S09_50451584	3.0	2.3	0.7	2.6	2.2	0.4	0.3	-0.1	-0.1	0.2
qeSbML9.1d	9	64	S09_51244364	S09_51243858	4.0	3.2	0.9	3.5	3.0	0.4	0.4	-0.1	-0.1	0.2
qeSbML9.1e	9	75	S09_51521422	S09_51521893	5.2	4.2	1.0	4.6	4.0	0.6	0.4	-0.1	-0.1	0.2

Chr = chromosome, Pos = position in the linkage map, LOD = total logarithm of odds, LOD(A) = LOD for Additive effect, LOD(AE) = LOD for additive by environment effect, PVE = percentage of total variation, PVE(A) = percentage of variation due to additive effect, PVE(AE) = percentage of variation due to additive by environment interaction, AE1 = additive by environment 1 (2018) effect, AE2 = additive by environment 2 (2019) effect, AE3 = additive by environment 3 (2020) effect.

2.5 Discussion

Several fungal diseases of crop plants, including sorghum, are caused by the genus Fusarium (Leslie et al., 2005). *Fusarium thapsinum* is one of the causal pathogens of Fusarium stalk rot. Post-flowering drought and high-temperature stresses during grain filling and maturity favor Fusarium stalk rot as a secondary infection, resulting in severe economic damage due to reduced grain, sugar, and biomass yields (Tesso et al., 2012; Bandara et al., 2017; Perumal et al., 2020). This economic damage is caused by harvesting difficulty caused by lodging and poor grain filling due to the interference of the disease with the translocation of water and nutrients through the stem (Tesso et al., 2005; Claflin and Giorda, 2008).

QTL mapping is a powerful tool used to identify genomic regions contributing to the variation of complex traits, including disease resistance (Biruma et al., 2012; Adeyanju et al., 2015, 2016; Felderhoff et al., 2016; Patil et al., 2017; Cuevas et al., 2019). The significance of QTL mapping in marker-assisted selection (MAS) lies in identifying markers closely linked to the QTL responsible for disease resistance. This information can be used to develop diagnostic markers for selecting disease-resistance in breeding programs to select plants with desired traits at any stage of development. These diagnostic markers save time and resources and accelerate the traditional phenotypic selection process more accurately (Ramasamy et al., 2009; Patil et al., 2017; Kimball et al., 2019; Cruet-Burgos et al., 2020; Abreha et al., 2021). To assist the breeding effort on Fusarium stalk rot, we developed an $F_{2:8}$ RIL bi-parental mapping population from two contrasting parents (SC599, resistant) and BTx3042, susceptible) to stalk rot diseases. The main objective is to identify QTL associated with disease resistance and dissect digenic epistatic QTL and QTL by environmental interaction. A total of 233 $F_{2:8}$ RILs were field phenotyped for disease and

agronomic traits for three years in the summer of 2018, 2019, and 2020. Of the 233 RILs, 186 and their parents were GBS SNP genotyped for the linkage mapping and QTL analyses.

2.5.6 Phenotypic variability among the RILs and heritability of the traits

The analysis of variance resulted in higher genotypic variability among RILs for all traits under study (Table 2.2). The mean values of the traits in the RILs were intermediate between the parental lines. However, some of the RILs exhibited extreme phenotypes relative to their parents, showing that transgressive segregation was occurring for many of the traits under study (Table 2.2). Transgressive segregation can be caused by parental lines contributing favorable or unfavorable alleles of complementary additive genes or epistatic or overdominance for a particular trait, which is heritable and common in inbred populations that play a role in adaptation and speciation (Rieseberg et al., 1999, 2003; Koide et al., 2019). Earlier, transgressive segregation in the sorghum biparental RIL population has been reported by several authors (Gelli et al., 2016; Govindarajulu et al., 2020; de Souza et al., 2021; Ayalew et al., 2022).

Heritability for disease traits and lodging was low (Table 2.3) due to the larger environmental effect rather than the lack of variation. Reddy et al. (2008) reported lower heritability on the number of nodes crossed by the stalk rot and length of infection and higher heritability for lodging. Similarly, Kebede et al. (2001), Murray et al. (2008), and Wang et al. (2020) reported lower heritability for lodging in a diverse sorghum population. In the current study, the high heritability for plant height and days flowering indicate the low environmental influence on these traits. Marla et al. (2019) and Wang et al. (2020) for plant height and Zhang et al. (2015) for plant height and flowering time reported similar results.

2.5.7 QTL for flowering time, plant height, and lodging

The US sorghum conversion (SC) program targeted photoperiod-insensitivity, early maturity, and dwarfism to adapt the tropical germplasm to the temperate condition and to suit mechanized harvesting (Quinby, 1974; Thurber et al., 2013). The maturity loci (*Ma1-Ma6*) and dwarfing loci (*Dw1-Dw4*) were discovered a while ago. These traits are linked in several genomic regions and are mainly found in three chromosomes, chromosomes 6, 7, and 9, involving at least four major linked loci for both traits (Murphy et al., 2011; Hilley et al., 2016, 2017). Over the years, the extensive selection of these traits on the converted lines and their derivatives might have created a lack of variability in this region for flowering and plant height. The founding parents of our RIL population, SC599, is a converted line, and BTx3042 is a derivative of a converted line suited for the temperate environment. The SNP markers on chromosomes 4, 6, and 7 were almost duplicates and cleaned out during the SNP data cleaning step, retaining only a few markers (Table 2.1). This might show the lack of polymorphism on those chromosomes due to heavy selection pressure over the past decades. Therefore, we could not map QTL associated with those known dwarfing loci for plant height in chromosomes 6 and 7. However, we discovered consistent QTL on chromosome 3 using IM (Table 2.5) and ICIM (Table 2.6) methods for plant height. Additional QTL were detected on chromosome 1 and chromosome 5. Marla et al. (2019) reported QTL on chromosome 1.

However, a few QTL were discovered for days to flowering. This study identified a stable QTL, qSbDF6, between 32.2 Mb and 38.2 Mb on Sb-06 (Tables 2.5 and 2.6). One of the flowering time, the *Ma1* allele on *SBPRR37*, was mapped in Sb-06 (Murphy et al., 2011; Cuevas et al., 2016), which is closely located with the QTL identified in our study. Additionally, QTL on chromosomes

2 and 8 were shown to be stable over the years. This agrees with the earlier report that discovered flowering QTL on chromosome 2 in sorghum (Sukumaran et al., 2016). Similarly, Marla et al. (2019) reported flowering time QTL on chromosomes 2 and 8.

Stalk lodging is a quantitative and complex trait (Wang et al., 2020). A few authors reported QTL mapping studies on sorghum stalk lodging; in most cases, QTL reported were on different regions or chromosomes (Kebede et al., 2001; Murray et al., 2008; Srinivasa Reddy et al., 2008; Wang et al., 2020). In our study, we detected QTL in 2019 on chromosomes 1 and 3, which agreed with the earlier results by Wang et al. (2020).

2.5.8 Fusarium stalk rot associated QTL and their interactions

Stalk rot disease is a secondary infection dependent on the environment and overall plant physiological fitness (Perumal et al., 2020). The infection causes severe damage when the environment is favorable. Many significant QTLs associated with stalk rot disease incidence were detected in this and several previous studies. The number of QTL and the variation between environments and across populations speaks to the complexity of the disease. However, few QTLs stand out as significant and consistent across environments and populations, indicating that major effect QTL are cutting across and may be of priority interest for use in breeding programs. However, previous studies have paid little attention to epistasis effects on stalk rot disease resistance. Therefore, we studied additive and epistatic QTL interacting between pairs of additive QTL located on the same or separate chromosomes and their interaction with the environment. When QTL are identified consistently over environments with higher LOD using both mapping methods (IM and ICIM), we consider those as stable. Major effect QTL were determined by the percentage of phenotypic variation explained by the QTL (PVE). In this regard, we detected QTL

on chromosomes 1, 3, 5, and 9 using both mapping methods for each year and means of the three years phenotypic data (Table 2.4-2.5).

We consider the MLL QTL found on chromosome 5 between S05_70180835 and S05_70250139 (106.3Kb) as a stable and major QTL since they were consistently detected using IM in 2020 and the mean data and ICIM in 2018 and 2020 data. They explained 22% of the total phenotypic variation for MLL and had a positive additive effect. We searched on *Phytozome 13* for genes related to disease resistance in this region and found only 11 genes, most of them being plant proteins of unknown function. However, Sobic.005G216200 (O-methyltransferase) might be a candidate gene in that region. According to gene ontology annotation, it is involved in methyltransferase (GO:0008168) and protein dimerization (GO:0046983) activity in molecular function. In addition, in the PlantCyc pathway tool, the gene regulates an enzyme that catalyzes quinone, a secondary metabolite biosynthetic reaction in the sorgoleone biosynthesis pathway (PWY-5987). The reduced form of sorgoleone, dihydrosogoleone, faster oxidizing to the highly phytotoxic sorgoleone upon exudation into the soil, and quinones are secondary metabolites known in allelopathic and antimicrobial activities (Dayan et al., 2003; Pan et al., 2007; Cook et al., 2010). Additionally, O-methyltransferase in wheat contributed to resistance against sharp eyespot disease (*Rhizoctonia cerealis*) by involving in lignin biosynthesis, which increased stem strength (Wang et al., 2018).

On chromosome 5, another major QTL was discovered in two environments and, in both mapping methods (Tables 2.5 and 2.6), had the highest LOD (67.8), PVE (33.9 %), and additive effect (3.3) in the ICIM method (Table 2.6). Its physical location is between markers S05_69288833 and S05_69704221 (415.39 Kb). However, the region is wide, with more than 250

genes. In this region, disease resistance proteins (Leucine-rich repeat: CC-NBS-LRR, NB-ARC), stripe rust resistance protein Yr10, lysM, senescence-associated protein, disease resistance-responsive protein, and cytochrome P450 proteins were abundant. Furthermore, in sorghum, anthracnose resistance loci, *Cg1* at LG-05, was reported in this chromosomal region (Ramasamy et al., 2009). In addition, several QTL for anthracnose resistance (Patil et al., 2017; Cruet-Burgos et al., 2020; Abreha et al., 2021), leaf spot (Kimball et al., 2019) were reported on chromosome 5.

IM and ICIM methods identified a QTL in a position between S09_51521422 and S09_51521893 on the MLL mean, and it is only one gene (Sobic.009G157600) found on this region as the length is too short (398b). Nevertheless, the gene is a protein of unknown function (DUF740). Chromosome 9 in sorghum contains several disease-resistance loci (Biruma et al., 2012; Adeyanju et al., 2015, 2016; Felderhoff et al., 2016; Patil et al., 2017; Cuevas et al., 2019). Adeyanju et al. (2015) reported several SNPs and associated candidate genes in chromosome 9 for stalk rot disease resistance.

We have noticed in some chromosomal regions more frequent epistatic interaction with loci on the same or different chromosomes for MLL (Table 2.7). Chromosome 1 region on physical map S01_59759825 to S01_62806525 on intra-chromosomal (qSbML1.2a*qSbML1.2b) and three inter-chromosomal interactions with loci in chromosomes 2 (qSbML1.4*qSbML2.4) and 10 (qSbML1.3*qSbML10.3 and qSbML1.4*qSbML10.4) found (Table 2.7). Similarly, on chromosome 3, between S03_1486771 and S03_2479998, two intra-chromosomal interactions between QTL in this region interacted between themselves (qSbML3.1a*qSbML3.1b and qSbML3.2a*qSbML3.2b) and QTL on chromosome 7 (qSbML3.2*qSbML7.2).

When dealing with phenotypic data from multiple environments, the outcomes obtained from QTL by environment (QEI) mapping, which estimates the locations and effects of QTL, are more reliable than single-environment analysis because it uses multi-environments data (Jansen et al., 1995; Li et al., 2007; Li et al., 2015). Nevertheless, conducting a single-environment analysis will validate the reliability of the estimated locations and effects of QEI. Although the advantages of using QEI analysis for multi-environmental trials are undeniable, the QTL mapping for each environment cannot be avoided, and hence consolidating the mapping results across all environments would be better (Li et al., 2015). In our study, four QTL that were detected in more than one environment in the single environment analysis were also detected in QEI on chromosomes 1, 3, 5, and 9 (Table 2.6; Table 2.8). However, some QTL had not detected in a single environment QTL analysis but were identified in QEI. These were the ones with LOD slightly less than 3 in single environments. Therefore, we considered those QTL appearing both in single and QEI analysis as important QTL associated with stalk rot disease resistance. On the physical map, they were located at Sb-01 between 72.00 and 72.37Mb (0.5Kb), Sb-03 between 67.63 and 67.67Mb (0.43Kb), Sb-05 at 70.18Mb (0.28Kb) and Sb-09 at 51.52 (0.47Kb) (Table 2.8). The genes found in these regions were discussed above in the single environment analysis.

In addition to validating QEI using single environment analysis, assessing the QTL stability is also vital. It is important to have stable QTL across environments, but significant QTL detected for specific environments may also be of interest for use in those target environments. The QEI effects of QTL obtained through ICIM are estimated by evaluating the genotypic value of two QTL genotypes, AA and aa, in multiple environments through orthogonal decomposition (El-Soda et al., 2014; Li et al., 2015). The mapping results, including three LODs, three PVEs, major effects, and QEI effects, enable direct assessment of QTL stability and QEI level (Jansen et al., 1995; Li

et al., 2007; El-Soda et al., 2014; Li et al., 2015). Hence, if the major effect of a QTL has a significantly larger absolute value than its interactions, then it can be deemed stable. However, larger interactions suggest a higher environment interaction effect and less stability (Li et al., 2015). In this regard, those QTL detected in individual and QEI, *qeSbML1.1a* (S01_72372621: S01_71998851), *qeSbML3.1* (S03_67673215: S03_67626559), *qeSbML5.1* (S05_70180835:S05_70180551), and *qeSbML9.1e* (S09_51521422: S09_51521893) had higher average effect than the individual environments (Table 2.8). The sum of the absolute values of AE effects were less than the average (main) effects for *qeSbML1.1a* and *qeSbML3.1, and* this affirms their stability. On the other hand, we checked the stability of *qeSbML5.1* and *qeSbML9.1e.* using LOD_A and LOD_{AE}, where LOD_A was greater than LOD_{AE} for them so that they can be considered stable QTL.

2.6 Conclusion

QTL mapping for marker-assisted selection in resistance breeding is a powerful tool for developing crops with improved disease resistance. Breeders can select target traits more efficiently and effectively using markers as a proxy. However, the environment plays a critical role in the development and severity of stalk rot infections in sorghum. We studied the QTL associated with disease resistance in an individual environment and across environments, their epistatic interactions, and QTL by environment interactions. Using epistatic and QEI analyses, we observed that regions on chromosome 1, 3, 5, and 9 were important and harbor stable and significant QTL detected in both IM and ICIM methods across the environments. No significant main effect QTL in the individual environments were detected in the epistatic interaction. However, there were overlapping QTL positions in the main effects of individual environment analysis and QEI in the above chromosomes. QEI analysis in multi-environmental trials is beneficial, but QTL mapping should still be employed for each environment. In this study, four stable QEI for MLL (*qeSbML1.1a*, *qeSbML3.1*, *qeSbML5.1*, and *qeSbML9.1e*) were identified with higher LOD and PVE of main effects. However, the limitation is the lack of reproducibility revealed in the low marker density on chromosomes 4, 6, and 7, where important sorghum disease resistance QTL were reported in earlier studies. This study adds little information to the complex genetics of stalk rot resistance in sorghum.

References

Abreha, K. B., Ortiz, R., Carlsson, A. S., & Geleta, M. (2021). Understanding the sorghum *Colletotrichum sublineola* interactions for enhanced host resistance. Frontiers in Plant Science, 12. https://www.frontiersin.org/articles/10.3389/fpls.2021.641969

Adeyanju, A., Little, C., Yu, J., & Tesso, T. (2015). Genome-wide association study on resistance to stalk rot diseases in grain sorghum. G3: Genes, Genomes, Genetics, 5(6), 1165–1175. https://doi.org/10.1534/g3.114.016394

Adeyanju, A., Yu, J., Little, C., Rooney, W., Klein, P., Burke, J., & Tesso, T. (2016). Sorghum RILs segregating for stay-green QTL and leaf dhurrin content show differential reaction to stalk rot diseases. Crop Science, 56(6), 2895–2903. https://doi.org/10.2135/cropsci2015.10.0628

Ayalew, H., Peiris, S., Chiluwal, A., Kumar, R., Tiwari, M., Ostmeyer, T., Bean, S., & Jagadish, S. V. K. (2022). Stable sorghum grain quality QTL were identified using SC35 × RTx430 mapping population. The Plant Genome, 15(3), e20227. https://doi.org/10.1002/tpg2.20227

Bandara, Y. M. A. Y., Tesso, T. T., Bean, S. R., Dowell, F. E., & Little, C. R. (2017). Impacts of fungal stalk rot pathogens on physicochemical properties of sorghum grain. Plant Disease, 101(12), 2059–2065. https://doi.org/10.1094/PDIS-02-17-0238-RE

Biruma, M., Martin, T., Fridborg, I., Okori, P., & Dixelius, C. (2012). Two loci in sorghum with NB-LRR encoding genes confer resistance to *Colletotrichum sublineolum*. Theoretical and Applied Genetics, 124(6), 1005–1015. https://doi.org/10.1007/s00122-011-1764-8

Boatwright, J. L., Brenton, Z. W., Boyles, R. E., Sapkota, S., Myers, M. T., Jordan, K. E., Dale, S. M., Shakoor, N., Cooper, E. A., Morris, G. P., & Kresovich, S. (2021). Genetic characterization of a *Sorghum bicolor* multiparent mapping population emphasizing carbon-partitioning dynamics. G3: Genes, Genomes, Genetics, 11(4). https://doi.org/10.1093/g3journal/jkab060

Boer, M. P., Wright, D., Feng, L., Podlich, D. W., Luo, L., Cooper, M., & van Eeuwijk, F. A. (2007). A Mixed-model quantitative trait loci (QTL) analysis for multiple-environment trial data using environmental covariables for QTL-by-environment interactions, with an example in maize. Genetics, 177(3), 1801–1813. https://doi.org/10.1534/genetics.107.071068

Bouchet, S., Olatoye, M. O., Marla, S. R., Perumal, R., Tesso, T., Yu, J., Tuinstra, M., & Morris, G. P. (2017). Increased power to dissect adaptive traits in global sorghum diversity using a nested association mapping population. Genetics, 206(2), 573–585. https://doi.org/10.1534/genetics.116.198499

Bradbury, P. J., Zhang, Z., Kroon, D. E., Casstevens, T. M., Ramdoss, Y., & Buckler, E. S. (2007). TASSEL: Software for association mapping of complex traits in diverse samples. Bioinformatics, 23(19), 2633–2635. https://doi.org/10.1093/bioinformatics/btm308

Browning, B. L., Tian, X., Zhou, Y., & Browning, S. R. (2021). Fast two-stage phasing of large-scale sequence data. The American Journal of Human Genetics, 108(10), 1880–1890. https://doi.org/10.1016/j.ajhg.2021.08.005

Cavanagh, C., Morell, M., Mackay, I., & Powell, W. (2008). From mutations to MAGIC: Resources for gene discovery, validation and delivery in crop plants. Current Opinion in Plant Biology, 11(2), 215–221. https://doi.org/10.1016/j.pbi.2008.01.002

Claflin, L. E., & Giorda, L. M. (2008). Stalk rots of sorghum. Sorghum and Millets Diseases, 185–190. https://doi.org/10.1002/9780470384923.ch33

Collard, B. C. Y., Jahufer, M. Z. Z., Brouwer, J. B., & Pang, E. C. K. (2005). An introduction to markers, quantitative trait loci (QTL) mapping and marker-assisted selection for crop improvement: The basic concepts. Euphytica, 142(1–2), 169–196. https://doi.org/10.1007/s10681-005-1681-5

Collard, B. C. Y., & Mackill, D. J. (2008). Marker-assisted selection: An approach for precision plant breeding in the twenty-first century. Philosophical Transactions of the Royal Society B: Biological Sciences, 363(1491), 557–572. https://doi.org/10.1098/rstb.2007.2170

Cook, D., Rimando, A. M., Clemente, T. E., Schröder, J., Dayan, F. E., Nanayakkara, N. P. D., Pan, Z., Noonan, B. P., Fishbein, M., Abe, I., Duke, S. O., & Baerson, S. R. (2010). Alkylresorcinol synthases expressed in *Sorghum bicolor* root hairs play an essential role in the biosynthesis of the allelopathic benzoquinone sorgoleone. The Plant Cell, 22(3), 867–887. https://doi.org/10.1105/tpc.109.072397

Cruet-Burgos, C. M., Cuevas, H. E., Prom, L. K., Knoll, J. E., Stutts, L. R., & Vermerris, W. (2020). Genomic dissection of anthracnose (*Colletotrichum sublineolum*) resistance response in sorghum differential line SC112-14. G3: Genes, Genomes, Genetics, 10(4), 1403–1412. https://doi.org/10.1534/g3.120.401121

Cuevas, H. E., Prom, L. K., & Cruet-Burgos, C. M. (2019). Genome-wide association mapping of anthracnose (*Colletotrichum sublineolum*) resistance in NPGS Ethiopian sorghum germplasm. G3: Genes, Genomes, Genetics, 9(9), 2879–2885. https://doi.org/10.1534/g3.119.400350

Cuevas, H. E., Zhou, C., Tang, H., Khadke, P. P., Das, S., Lin, Y. R., Ge, Z., Clemente, T., Upadhyaya, H. D., Hash, C. T., & Paterson, A. H. (2016). The evolution of photoperiod-insensitive flowering in sorghum, A Genomic Model for Panicoid Grasses. Molecular Biology and Evolution, 33(9), 2417–2428. https://doi.org/10.1093/molbev/msw120

Danecek, P., Auton, A., Abecasis, G., Albers, C. A., Banks, E., DePristo, M. A., Handsaker, R. E., Lunter, G., Marth, G. T., Sherry, S. T., McVean, G., Durbin, R., & 1000 Genomes Project Analysis Group. (2011). The variant call format and VCFtools. Bioinformatics, 27(15), 2156–2158. https://doi.org/10.1093/bioinformatics/btr330

Dayan, F. E., Kagan, I. A., & Rimando, A. M. (2003). Elucidation of the biosynthetic pathway of the allelochemical sorgoleone using retrobiosynthetic NMR analysis. The Journal of Biological Chemistry, 278(31), 28607–28611. https://doi.org/10.1074/jbc.M304185200

de Souza, V. F., Pereira, G. da S., Pastina, M. M., Parrella, R. A. da C., Simeone, M. L. F., Barros, B. de A., Noda, R. W., da Costa e Silva, L., de Magalhães, J. V., Schaffert, R. E., Garcia, A. A. F., & Damasceno, C. M. B. (2021). QTL mapping for bioenergy traits in sweet

sorghum recombinant inbred lines. G3: Genes, Genomes, Genetics, 11(11), jkab314. https://doi.org/10.1093/g3journal/jkab314

deVicente, M. C., & Tanksley, S. D. (1993). QTL analysis of transgressive segregation in an interspecific tomato cross. Genetics, 134(2), 585–596.

Ejeta, G. (2007). Breeding for *Striga* Resistance in Sorghum: Exploitation of an Intricate Host–Parasite Biology. Crop Science, 47(S3), S-216-S-227. https://doi.org/10.2135/cropsci2007.04.0011IPBS

Ejeta, G., & Knoll, J. E. (2007). Marker-assisted selection in sorghum. In R. K. Varshney & R. Tuberosa (Eds.), Genomics-Assisted Crop Improvement: Vol 2: Genomics Applications in Crops (pp. 187–205). Springer. Netherlands. https://doi.org/10.1007/978-1-4020-6297-1_9

Elshire, R. J., Glaubitz, J. C., Sun, Q., Poland, J. A., Kawamoto, K., Buckler, E. S., & Mitchell, S. E. (2011). A robust, simple genotyping-by-sequencing (GBS) approach for high diversity species. PLoS ONE, 6(5), 1–10. https://doi.org/10.1371/journal.pone.0019379

El-Soda, M., Malosetti, M., Zwaan, B. J., Koornneef, M., & Aarts, M. G. (2014). Genotype× environment interaction QTL mapping in plants: Lessons from Arabidopsis. Trends in Plant Science, 19(6), 390–398.

Falconer, D. S. (1996). Introduction to quantitative genetics. Pearson Education India.

Felderhoff, T. J., McIntyre, L. M., Saballos, A., & Vermerris, W. (2016). Using genotyping by sequencing to map two novel anthracnose resistance loci in *Sorghum bicolor*. G3: Genes, Genomes, Genetics, 6(7), 1935–1946. https://doi.org/10.1534/g3.116.030510

Fu, Y.-B., Peterson, G. W., & Dong, Y. (2016). Increasing genome sampling and improving SNP genotyping for genotyping-by-sequencing with new combinations of restriction enzymes. G3: Genes, Genomes, Genetics, 6(4), 845–856. https://doi.org/10.1534/g3.115.025775

Gelli, M., Mitchell, S. E., Liu, K., Clemente, T. E., Weeks, D. P., Zhang, C., Holding, D. R., & Dweikat, I. M. (2016). Mapping QTL and association of differentially expressed gene transcripts for multiple agronomic traits under different nitrogen levels in sorghum. BMC Plant Biology, 16(1), 16. https://doi.org/10.1186/s12870-015-0696-x

Glaubitz, J. C., Casstevens, T. M., Lu, F., Harriman, J., Elshire, R. J., Sun, Q., & Buckler, E. S. (2014). TASSEL-GBS: a high capacity genotyping by sequencing analysis pipeline. PLoS ONE, 9(2), e90346.

Govindarajulu, R., Henderson, A. N., Xiao, Y., Chaluvadi, S. R., Mauro-Herrera, M., Siddoway, M. L., Whipple, C., Bennetzen, J. L., Devos, K. M., Doust, A. N., & Hawkins, J. S. (2020). Integration of high-density genetic mapping with transcriptome analysis uncovers numerous agronomic QTL and reveals candidate genes for the control of tillering in sorghum (p. 2020.07.06.189548). bioRxiv. https://doi.org/10.1101/2020.07.06.189548

Hackett, C. A., Meyer, R. C., & Thomas, W. T. B. (2001). Multi-trait QTL mapping in barley using multivariate regression. Genetics Research, 77(1), 95–106. https://doi.org/10.1017/S0016672300004869

Hasan, N., Choudhary, S., Naaz, N., Sharma, N., & Laskar, R. A. (2021). Recent advancements in molecular marker-assisted selection and applications in plant breeding programmes.

Journal of Genetic Engineering and Biotechnology, 19(1), 128. https://doi.org/10.1186/s43141-021-00231-1

Haussmann, B. I. G., Hess, D. E., Omanya, G. O., Folkertsma, R. T., Reddy, B. V. S., Kayentao, M., Welz, H. G., & Geiger, H. H. (2004). Genomic regions influencing resistance to the parasitic weed *Striga hermonthica* in two recombinant inbred populations of sorghum. TAG. Theoretical and Applied Genetics, 109(5), 1005–1016. https://doi.org/10.1007/s00122-004-1706-9

Hilley, J. L., Weers, B. D., Truong, S. K., McCormick, R. F., Mattison, A. J., McKinley, B. A., Morishige, D. T., & Mullet, J. E. (2017). Sorghum *Dw2* encodes a protein kinase regulator of stem internode length. Scientific Reports, 7(1), 1–13. https://doi.org/10.1038/s41598-017-04609-5

Hilley, J., Truong, S., Olson, S., Morishige, D., & Mullet, J. (2016). Identification of *Dw1*, a regulator of sorghum stem internode length. PLoS ONE, 11(3), 1–16. https://doi.org/10.1371/journal.pone.0151271

Hu, Z., Olatoye, M. O., Marla, S., & Morris, G. P. (2019). An integrated genotyping-by-sequencing polymorphism map for over 10,000 sorghum genotypes. The Plant Genome, 12(1). https://doi.org/10.3835/plantgenome2018.06.0044

Jansen, R., Van Ooijen, J., Stam, P., Lister, C., & Dean, C. (1995). Genotype-by-environment interaction in genetic mapping of multiple quantitative trait loci. Theoretical and Applied Genetics, 91, 33–37.

Jiang, H., Lei, R., Ding, S.-W., & Zhu, S. (2014). Skewer: A fast and accurate adapter trimmer for next-generation sequencing paired-end reads. BMC Bioinformatics, 15, 182. https://doi.org/10.1186/1471-2105-15-182

Kavuluko, J., Kibe, M., Sugut, I., Kibet, W., Masanga, J., Mutinda, S., Wamalwa, M., Magomere, T., Odeny, D., & Runo, S. (2021). GWAS provides biological insights into mechanisms of the parasitic plant (*Striga*) resistance in sorghum. BMC Plant Biology, 21(1), 392. https://doi.org/10.1186/s12870-021-03155-7

Kebede, H., Subudhi, P., Rosenow, D., & Nguyen, H. (2001). Quantitative trait loci influencing drought tolerance in grain sorghum (*Sorghum bicolor* L. Moench). Theoretical and Applied Genetics, 103, 266–276.

Kimball, J., Cui, Y., Chen, D., Brown, P., Rooney, W. L., Stacey, G., & Balint-Kurti, P. J. (2019). Identification of QTL for target leaf spot resistance in *Sorghum bicolor* and investigation of relationships between disease resistance and variation in the MAMP response. Scientific Reports, 9, 18285. https://doi.org/10.1038/s41598-019-54802-x

Koide, Y., Sakaguchi, S., Uchiyama, T., Ota, Y., Tezuka, A., Nagano, A. J., Ishiguro, S., Takamure, I., & Kishima, Y. (2019). Genetic properties responsible for the transgressive segregation of days to heading in rice. G3: Genes, Genome, |Genetics, 9(5), 1655–1662. https://doi.org/10.1534/g3.119.201011

Langmead, B., & Salzberg, S. L. (2012). Fast gapped-read alignment with Bowtie 2. Nature Methods, 9(4), Article 4. https://doi.org/10.1038/nmeth.1923

Lee, S., Fu, F., Liao, C.-J., Mewa, D. B., Adeyanju, A., Ejeta, G., Lisch, D., & Mengiste, T. (2022). Broad-spectrum fungal resistance in sorghum is conferred through the complex regulation of an immune receptor gene embedded in a natural antisense transcript. The Plant Cell, 1–25. https://doi.org/10.1093/plcell/koab305

Leslie, J. F., Zeller, K. A., Lamprecht, S. C., Rheeder, J. P., & Marasas, W. F. O. (2005). Toxicity, pathogenicity, and genetic differentiation of five species of Fusarium from sorghum and millet. Phytopathology, 95(3), 275–283. https://doi.org/10.1094/PHYTO-95-0275

Li, H., Ribaut, J.-M., Li, Z., & Wang, J. (2008). Inclusive composite interval mapping (ICIM) for digenic epistasis of quantitative traits in biparental populations. Theoretical and Applied Genetics, 116(2), 243–260. https://doi.org/10.1007/s00122-007-0663-5

Li, H., Ye, G., & Wang, J. (2007). A Modified algorithm for the improvement of composite interval mapping. Genetics, 175(1), 361–374. https://doi.org/10.1534/GENETICS.106.066811

Li, S., Wang, J., & Zhang, L. (2015). Inclusive composite interval mapping of QTL by environment interactions in biparental populations. PLoS ONE, 10(7), e0132414. https://doi.org/10.1371/journal.pone.0132414

Marla, S. R., Burow, G., Chopra, R., Hayes, C., Olatoye, M. O., Felderhoff, T., Hu, Z., Raymundo, R., Perumal, R., & Morris, G. P. (2019). Genetic architecture of chilling tolerance in sorghum dissected with a nested association mapping population. G3: Genes, Genomes, Genetics, 9(12), 4045–4057. https://doi.org/10.1534/g3.119.400353

McCormick, R. F., Truong, S. K., Sreedasyam, A., Jenkins, J., Shu, S., Sims, D., Kennedy, M., Amirebrahimi, M., Weers, B. D., McKinley, B., Mattison, A., Morishige, D. T., Grimwood, J., Schmutz, J., & Mullet, J. E. (2018). The *Sorghum bicolor* reference genome: Improved assembly, gene annotations, a transcriptome atlas, and signatures of genome organization. Plant Journal, 93(2), 338–354. https://doi.org/10.1111/tpj.13781

McCouch, S. R. (1997). Report on QTL nomenclature. Rice Genetics Newsletter, 14, 11–13.

Meng, L., Li, H., Zhang, L., & Wang, J. (2015). QTL IciMapping: Integrated software for genetic linkage map construction and quantitative trait locus mapping in biparental populations. The Crop Journal, 3(3), 269–283. https://doi.org/10.1016/J.CJ.2015.01.001

Mengistu, G., Shimelis, H., Assefa, E., & Lule, D. (2021). Genome-wide association analysis of anthracnose resistance in sorghum [*Sorghum bicolor* (L.) Moench]. PLoS ONE, 16(12), e0261461. https://doi.org/10.1371/journal.pone.0261461

Mewa, D. B., Lee, S., Liao, C.-J., Souza, A. M., Adeyanju, A., Helm, M., Lisch, D., & Mengiste, T. (2022). Anthracnose resistance *GENE2* confers fungal resistance in sorghum. BioRxiv, 497546. https://doi.org/10.1101/2022.06.24.497546

Miao, C., & Schnable, J. (2019). Genotype dataset for sorghum association panel (SAP). https://doi.org/10.6084

Mores, A., Borrelli, G. M., Laidò, G., Petruzzino, G., Pecchioni, N., Amoroso, L. G. M., Desiderio, F., Mazzucotelli, E., Mastrangelo, A. M., & Marone, D. (2021). Genomic approaches to identify molecular bases of crop resistance to diseases and to develop future breeding

strategies. International Journal of Molecular Sciences, 22(11), 5423. https://doi.org/10.3390/ijms22115423

Morris, G. P., Ramu, P., Deshpande, S. P., Hash, C. T., Shah, T., Upadhyaya, H. D., Riera-Lizarazu, O., Brown, P. J., Acharya, C. B., & Mitchell, S. E. (2013). Population genomic and genome-wide association studies of agroclimatic traits in sorghum. Proceedings of the National Academy of Sciences, 110(2), 453–458.

Murphy, R. L., Klein, R. R., Morishige, D. T., Brady, J. A., Rooney, W. L., Miller, F. R., Dugas, D. V., Klein, P. E., & Mullet, J. E. (2011). Coincident light and clock regulation of pseudoresponse regulator protein 37 (*PRR37*) controls photoperiodic flowering in sorghum. Proceedings of the National Academy of Sciences of the United States of America, 108(39), 16469–16474. https://doi.org/10.1073/pnas.1106212108

Murray, S., Rooney, W., Mitchell, S., Sharma, A., Klein, P., Mullet, J., & Kresovich, S. (2008). Genetic improvement of sorghum as a biofuel feedstock: II. QTL for stem and leaf structural carbohydrates. Crop Science, 48. https://doi.org/10.2135/cropsci2008.01.0068

Nida, H., Girma, G., Mekonen, M., Lee, S., Seyoum, A., Dessalegn, K., Tadesse, T., Ayana, G., Senbetay, T., Tesso, T., Ejeta, G., & Mengiste, T. (2019). Identification of sorghum grain mold resistance loci through genome wide association mapping. Journal of Cereal Science, 85, 295–304. https://doi.org/10.1016/j.jcs.2018.12.016

Pan, Z., Rimando, A. M., Baerson, S. R., Fishbein, M., & Duke, S. O. (2007). Functional characterization of desaturases involved in the formation of the terminal double bond of an unusual 16:3$\Delta^{9,12,15}$ fatty acid isolated from *Sorghum bicolor* root hairs. The Journal of Biological Chemistry, 282(7), 4326–4335. https://doi.org/10.1074/jbc.M606343200

Patil, N. Y., Klein, R. R., Williams, C. L., Collins, S. D., Knoll, J. E., Burrell, A. M., Anderson, W. F., Rooney, W. L., & Klein, P. E. (2017). Quantitative trait loci associated with anthracnose resistance in sorghum. Crop Science, 57(2), 877–890. https://doi.org/10.2135/cropsci2016.09.0793

Perumal, R., Tomar, S. S., Bandara, A., Maduraimuthu, D., Tesso, T. T., Prasad, P. V. V., Upadhyaya, H. D., & Little, C. R. (2020). Variation in stalk rot resistance and physiological traits of sorghum genotypes in the field under high temperature. Journal of General Plant Pathology, 86(5), 350–359. https://doi.org/10.1007/s10327-020-00940-4

Quinby, J. R. (1974). Sorghum improvement and the genetics of growth. Texas agricultural experiment station.

Rakshit, S., Hariprasanna, K., Gomashe, S., Ganapathy, K. N., Das, I. K., Ramana, O. V., Dhandapani, A., & Patil, J. V. (2014). Changes in area, yield gains, and yield stability of sorghum in major sorghum-producing countries, 1970 to 2009. Crop Science, 54(4), 1571–1584. https://doi.org/10.2135/cropsci2012.12.0697

Ramasamy, P., Menz, M. A., Mehta, P. J., Katilé, S., Gutierrez-Rojas, L. A., Klein, R. R., Klein, P. E., Prom, L. K., Schlueter, J. A., Rooney, W. L., & Magill, C. W. (2009). Molecular mapping of *Cg1*, a gene for resistance to anthracnose (*Colletotrichum sublineolum*) in sorghum. Euphytica, 165(3), 597–606. https://doi.org/10.1007/s10681-008-9791-5

Rieseberg, L. H., Archer, M. A., & Wayne, R. K. (1999). Transgressive segregation, adaptation and speciation. Heredity, 83(4). https://doi.org/10.1038/sj.hdy.6886170

Rieseberg, L. H., Widmer, A., Arntz, A. M., & Burke, B. (2003). The genetic architecture necessary for transgressive segregation is common in both natural and domesticated populations. Philosophical Transactions of the Royal Society of London. Series B: Biological Sciences, 358(1434), 1141–1147. https://doi.org/10.1098/rstb.2003.1283

Srinivasa Reddy, P., Fakrudin, B., Rajkumar, Punnuri, S. M., Arun, S. S., Kuruvinashetti, M. S., Das, I. K., & Seetharama, N. (2008). Molecular mapping of genomic regions harboring QTL for stalk rot resistance in sorghum. Euphytica, 159(1–2), 191–198. https://doi.org/10.1007/s10681-007-9472-9

Sukumaran, S., Li, X., Li, X., Zhu, C., Bai, G., Perumal, R., Tuinstra, M. R., Prasad, P. V. V., Mitchell, S. E., Tesso, T. T., & Yu, J. (2016). QTL mapping for grain yield, flowering time, and stay-green traits in sorghum with genotyping-by-sequencing markers. Crop Science, 56(4), 1429–1442. https://doi.org/10.2135/cropsci2015.02.0097

Tesso, T. T., Claflin, L. E., & Tuinstra, M. R. (2005). Analysis of stalk rot resistance and genetic diversity among drought tolerant sorghum genotypes. Crop Science, 45(2), 645–652. https://doi.org/10.2135/cropsci2005.0645

Tesso, T. T., Perumal, R., Little, C. R., Adeyanju, A., Radwan, G. L., Prom, L. K., & Magill, C. W. (2012). Sorghum Pathology and Biotechnology—A Fungal Disease Perspective: Part II. Anthracnose, Stalk Rot, and Downy Mildew. The European Journal of Plant Science and Biotechnology, 6, 31–44.

Thakur, R. P., Reddy, B. V. S., Indira, S., Rao, V. P., Navi, S. S., Yang, X. B., & Ramesh, S. (2006). Sorghum Grain Mold Information Bulletin No. 72 [Monograph]. International Crops Research Institute for the Semi-Arid Tropics. http://oar.icrisat.org/4942/

Thurber, C. S., Ma, J. M., Higgins, R. H., & Brown, P. J. (2013). Retrospective genomic analysis of sorghum adaptation to temperate-zone grain production. Genome Biology, 14(6), R68. https://doi.org/10.1186/gb-2013-14-6-r68

Wang, D. L., Zhu, J., Li, Z. K. L., & Paterson, A. H. (1999). Mapping QTL with epistatic effects and QTL×environment interactions by mixed linear model approaches. Theoretical and Applied Genetics, 99(7), 1255–1264. https://doi.org/10.1007/s001220051331

Wang, J. (2009). Inclusive composite interval mapping of quantitative trait genes. Acta Agronomica Sinica, 35(2), 239–245.

Wang, M., Zhu, X., Wang, K., Lu, C., Luo, M., Shan, T., & Zhang, Z. (2018). A wheat caffeic acid 3-O-methyltransferase TaCOMT-3D positively contributes to both resistance to sharp eyespot disease and stem mechanical strength. Scientific Reports, 8(1). https://doi.org/10.1038/s41598-018-24884-0

Wang, X., Mace, E., Tao, Y., Cruickshank, A., Hunt, C., Hammer, G., & Jordan, D. (2020). Large-scale genome-wide association study reveals that drought-induced lodging in grain sorghum is associated with plant height and traits linked to carbon remobilisation. Theoretical and Applied Genetics, 133(11), 3201–3215. https://doi.org/10.1007/s00122-020-03665-2

Zhang, D., Kong, W., Robertson, J., Goff, V. H., Epps, E., Kerr, A., Mills, G., Cromwell, J., Lugin, Y., Phillips, C., & Paterson, A. H. (2015). Genetic analysis of inflorescence and plant

height components in sorghum (*Panicoidae*) and comparative genetics with rice (*Oryzoidae*). BMC Plant Biology, 15(1), 107. https://doi.org/10.1186/s12870-015-0477-6

Zhao, F., & Xu, S. (2012). Genotype by environment interaction of quantitative traits: A case study in barley. G3 Genes, Genomes, Genetics, 2(7), 779–788. https://doi.org/10.1534/g3.112.002980

CHAPTER 3 - DEFENSE TRANSCRIPTOME RESPONSE TO *Fusarium thapsinum* INDUCED STALK ROT INFECTION IN SORGHUM [S*orghum bicolor* (L.) MOENCH] USING RNA-SEQ ANALYSIS

3.1 Abstract

Fusarium spp. are hemi-biotrophic pathogens infecting sorghum, maize, and soybean, causing stalk and root rots, seedling blight, grain mold, and wilting. In sorghum, *Fusarium thapsinum* causes Fusarium stalk rot. Understanding the molecular mechanism of host resistance and responses to pathogen infection is vital for resistance breeding. Sorghum inbreds, SC599 (resistant) and BTx3042 (susceptible), were used for the transcriptome analysis to investigate genes regulating disease resistance and identify the molecular basis of host resistance. Early activation of the defense response was observed in the resistant line at 24 hours post-inoculation (hpi). Differentially expressed genes (DEGs) such as nucleotide-binding site leucine-rich repeat (NBS-LRR, SbRWRKY1, SbLRx4, and Sobic.005G226400), pathogenesis-related (PR10, Sobic.001G401200), disease resistance-response (DIR, Sobic.009G021300), wall-associated kinase (Sobic.008G170800 and Sobic.002G249600), peroxidase (*SbPrx34* and *SbPrx30)*, chalcone synthase (*SbCHS1* and *SbCHS5*), and flavonoid synthases (*SbDFR3*) genes were upregulated in the resistant and downregulated in the susceptible genotype at 24 hpi. Gene ontology terms and Kyoto Encyclopedia of Genes and Genomes pathway analyses showed that genes involved in defense response, flavonoid biosynthesis, and signal transduction were significantly enriched at 24 hpi. The resistance genotype displayed a time-regulated transcriptome response, early upregulated DEGs related to hypersensitive response, believed to be effective against biotrophic pathogens. Later, upregulated DEGs like PR10, flavonoids, and CHS were assumed to be effective against necrotrophs, showing that defense regulation might be related to

the pathogen's hemi-biotrophic nature. The research result provides a foundation for future studies to understand genes and pathways involved in the molecular mechanisms of Fusarium stalk rot resistance in sorghum.

3.2 Introduction

Plant innate immunity is a complex and multifaceted system protecting plants from pathogens. Plant immunity involves two layers of defense. The first layer involves the recognition of conserved microbial molecules called microbe or pathogen-associated molecular patterns (MAMPs or PAMPs) by surface-localized pattern recognition receptors (PRRs), which trigger a cascade of physiological changes in the plant cells called PAMP-triggered immunity (PTI) (Boller & Felix, 2009). PTI is sufficient to halt the ingress of most microbes, but some pathogens secrete effector proteins to evade or suppress PTI (Nicaise et al., 2009). To defend against these adapted pathogens, plants are provided with a second layer of immunity mediated by NBS-LRR receptors (R-genes), which recognize the effector proteins and trigger robust defense programs, including localized cell death (Dodds & Rathjen, 2010). These mechanisms are effective against biotrophic pathogens but may not be sufficient to protect against necrotrophic pathogens, which depend on dead tissues. R-gene-mediated cell death through the hypersensitive reaction may increase susceptibility to necrotrophs (Niks et al., 2015). Understanding the molecular basis of host plant resistance, conferred by a single gene in the case of qualitative resistance or involving multiple genes, as in quantitative resistance, is essential to improve host resistance using modern breeding tools.

The growing climate adversity increased the effect of biotic and abiotic stresses on field crops. Sorghum is a heat and drought-tolerant crop grown worldwide as a staple food, biofuel

feedstock, and animal feed (Smith & Frederiksen, 2000). However, sorghum is vulnerable to several fungal stalk rot pathogens that cause lodging, particularly under drought conditions (Leslie, 1990). *Fusarium thapsinum* and *Macrophomina phaseolina* are among the dominant fungal pathogens causing sorghum Fusarium stalk and charcoal rot, respectively (Bramel-Cox & Claflin, 1989; Leslie et al., 2005). Fusarium is a hemi-biotrophic pathogen, containing an initial biotrophic phase and converting to a necrotrophic phase as the infection progresses. It causes various crop diseases, including stalk and root rots, seedling blight, grain mold, leaf spots, ear and kernel rot, and Fusarium wilt (Leslie, 1990). *F. thapsinum* is among the predominant and virulent species of stalk rots (Tesso et al., 2010). It affects sorghum production by interfering with grain filling, causing lodging and thus resulting in reduced grain yield and quality, with losses reaching up to 100% under heavy infestation (Rajewski & Francis, 1991). In addition, it affects biomass yields and quality in sweet sorghum and forage sorghum (Das et al., 2008; Bandara et al., 2017). In Kansas, the grain loss due to the disease goes up to ~50% in higher disease seasons and ~4% loss annually across the state (Jardine & Leslie, 1992; Claflin & Giorda, 2008).

Despite significant progress in sorghum breeding in the US (Pfeiffer et al., 2019), yield losses due to stalk rot diseases persist because of a combination of factors, namely poor stalk strength and climate change-induced post-flowering drought stress (Jardine & Leslie, 1992; Tesso et al., 2004; Yahaya & Shimelis, 2022). In the sorghum Fusarium pathosystem, the complex mechanisms of resistance and host-pathogen interactions are not yet understood as artificial inoculation, and disease-scoring methods are slow and labor-intensive. Additionally, the influence of environmental stress and the opportunistic nature of Fusarium pathogens can further slow progress in breeding for resistance to the disease. Despite these challenges, different genetic sources of resistance were identified (Adeyanju et al., 2015). Next-generation sequencing (NGS)

technologies offer the potential to identify the genetic architecture of host resistance and understand its molecular basis (Gelli et al., 2016, 2017; Kebede et al., 2018). Transcriptome analysis, which compares transcript expression between samples, can provide insights into the underlying molecular mechanisms of Fusarium resistance in sorghum (de Sá et al., 2018; Garg, 2021). Overall, using NGS technologies can provide valuable insights into the resistance mechanisms to Fusarium stalk rot, improve understanding of this complex disease, and help identify strategies for breeding resistant varieties.

RNA-seq has been used to study the molecular responses of sorghum to various abiotic stresses, including nitrogen stress, drought stress, and chilling stress (Gelli et al., 2014; Fracasso et al., 2016; Gelli et al., 2016, 2017; Marla et al., 2017), and biotic stresses like disease and insect (Fu et al., 2020; Adhikari et al., 2021; Cui et al., 2021; Natarajan et al., 2021; Nida et al., 2021; Serba et al., 2021). However, only a few such studies were made to investigate the molecular mechanisms of sorghum to stalk rot diseases, including charcoal and Fusarium stalk rot (Sharma et al., 2014; Bandara et al., 2018; Funnell-Harris et al., 2019). These studies identified genes and pathways in response to the diseases and provided insights into disease resistance mechanisms. For instance, Sharma et al. (2014) used RNA-seq to study the role of defense genes, including chitinase and stilbene synthase, in sorghum subjected to infection by *M. phaseolina*. They found that chitinase and stilbene synthase expression was higher in the resistant genotype than the susceptible genotype, suggesting that these genes play roles in disease response. Bandara et al. (2018) conducted RNA-seq analysis in sorghum infected by *M. phaseolina* and found that the infection had a more significant effect on cell-wall-degrading enzyme-encoding genes. Funnell-Harris et al. (2019) studied RNA-seq in *bmr* (brown midrib) and its wild-type sister line and reported increased expression of monolignol biosynthesis genes in response to infection by stalk

rot pathogens, *F. thapsinum* and *M. phaseolina,* in *bmr* lines than that of its corresponding wild-type. Overall, these studies have contributed to our understanding of the molecular mechanisms underlying disease resistance in sorghum and have identified potential targets for breeding to improve resistance to stalk rot diseases.

RNA-seq study to analyze differentially expressed genes due to infection has prime importance in the search for genes or loci responsible for the resistance or susceptibility and would facilitate the ongoing breeding effort. Therefore, we explored the transcriptome profiles in two sorghum genotypes to investigate the resistance mechanisms to Fusarium stalk rot. The objectives of the study were (i) to identify genes differentially expressed between stalk rot-resistant (SC599) and susceptible (BTx3042) sorghum genotypes (ii) to elucidate the major pathways in biological processes and molecular functions involved in the role of susceptibility and resistance, and (iii) to investigate the significance of temporal variation between the genotypes in overall infection responses based on the samples collected at two different time points.

3.3 Materials and Methods

3.3.1 RNA-Seq experimental design and greenhouse experiment

Sorghum lines, a resistant (SC599) and susceptible (BTx3042) to Fusarium stalk rot, were selected for transcriptome analysis based on previous reports by Tesso et al. (2004; 2005; 2010) and Bandara et al. (2018). These two lines were grown in the greenhouse using a Sun Gro nursery potting mix (Sun Gro Bellevue, WA, U.S.A) in a 19 L pot during the fall of 2021. Each genotype was grown in 12 pots of 30 cm top diameter and 35 cm height. The experimental design contained three biological replications for two sampling times, 24 and 48 hpi, for both genotypes. This study

was conducted with 24 samples comprising two genotypes, two-time points (24 and 48 hpi), and two treatments (pathogen and control inoculated) in three replications. The first 12 samples (3 replications × 2 treatments ×2 time points) were BTx3042 samples, and the remaining 13 to 24 were SC599 samples (Appendix A. Table A.1).

The pure *F. thapsinum* culture was obtained from the Row Crops Pathology Laboratory, Department of Plant Pathology, Kansas State University. It was grown in a liquid potato dextrose broth (PDB-Difco) to initiate the inoculum suspension, incubated on a shaker for three days, and strained using KenAG non-gauze milk filters to retain the conidia. The number of conidia was counted under a microscope using a hemocytometer to estimate the concentration and adjusted to 5×10^4 conidia ml^{-1} by diluting with a PBS (phosphate-buffered saline) solution for inoculation. At 50% flowering, each plant was inoculated on the stalk with *F. thapsinum* or PBS solution for control treatments. The inoculation point was approximately 10 cm above the soil surface, and plants were subjected to mild water stress to induce infection.

3.3.2 RNA extraction, cDNA library construction, and sequencing

Tissue samples were collected from inoculated plants by cutting the stalk at 3 cm above and below the inoculation point. Tissue samples were collected at 24 and 48 hpi, using 2 ml tubes with two metal beads, snap-freezed in liquid nitrogen, and stored at -80°C for RNA extraction. A schematic representation of the experimental design is included in Appendix A. Figure A.1. All 24 samples were ground using Tissue Lyser II. Approximately 100 mg of each ground sample was used for RNA extraction. Using the RNeasy Plant Mini Kit (QIAGEN, Germantown, MD, USA), RNA was extracted and diluted in 50 µl nuclease-free water. Nanodrop 2000 (Thermo Scientific, Waltham, MA, USA) and Agilent 2100 Bioanalyzer (Agilent Technologies Genomics, USA)

measurements were taken to check the quantity and quality of RNA before RNA sequencing. The cDNA libraries were constructed at the Integrated Genomic Facility at Kansas State University using the Illumina TruSeq stranded mRNA protocol (Illumina Inc., USA). The samples were enriched in two rounds for poly-A mRNAs using oligodT attached magnetic beads. The cDNA from each library was separately barcoded with adapter indexes (Appendix A. Table A.1) and pooled. NextSeq500 platform (Illumina Inc., USA) sequenced the samples at the Genome Sequencing Facility of Kansas University Medical Center. Single-end reads of 75 bp were obtained from a NextSeq500 run.

3.3.3 Quality control, read alignment, and visualization

The first 12 RNA-Seq libraries of BTx3042 generated one billion reads out of 1.42 billion total reads (Appendix A. Table A.3). However, two libraries out of the 12, namely "BC24.1" with 405 million reads and "BC24.2" with 209 million reads, shared 60% of the total BTx3042 reads generated (Appendix A. Table A.3). On the other hand, SC599 of the remaining 12 libraries generated 417 million reads distributed proportionally across the twelve libraries (Appendix A. Table A.3). Raw reads were evaluated for sequence quality, GC content, adapter sequence, over-represented k-mers, and duplicated reads using FastQC v.0.11.9 (Andrews, 2015). All samples passed the FastQC quality parameters except per base sequence content and sequence duplication levels (Appendix A. Table A.2; Appendix A. Figure A.2). All twenty-four single-end sequencing libraries were 100% good quality sequences based on the mean quality scores, and no significantly overrepresented adapter sequences were detected (Appendix A. Table A.2; Appendix A. Figure A.2).

Trimmomatic v.0.39, a flexible read-trimming tool for Illumina NGS data, was used to remove low-quality reads, remnant adapter sequences, and poor-quality bases (Bolger et al., 2014). TruSeq3 for the single end was used for adapter trimming. Fixed parameters were per base sequence content and sequence duplication levels. Trimmomatic retained 97% of the raw reads on average (Appendix A. Table A.3). Sequence length after trimming was 60-75 bases for all samples, with an average length of 74 bases. Quality was rechecked with FastQC before alignment. The Trimmomatic improved the GC content and overrepresented sequences of a few samples. However, per base sequence quality and sequence duplication were not improved. A total of 1.38 billion quality filtered raw reads were obtained.

NCBI Sorghum bicolor v3.1.1 reference genome and annotation file v3.53 (McCormick et al., 2018) were used for the reference genome indexing and alignment of the reads into the reference genome using splice-aware aligner, STAR v 2.7.10a (Dobin et al., 2013). The quality-filtered total reads of the 24 samples were mapped to the *Sorghum bicolor* reference genome, BTx623 v3.1.1. On average, 88% of reads were uniquely mapped to the reference genome (Appendix A. Table A.4). FeatureCounts quantified read counts per gene from the results of STAR alignment BAM files (Liao et al., 2014). The featureCounts assigned 65% of the reads, removing unassigned ones due to ambiguity and no feature (Appendix A. Table A.4). The two outliers still had higher unassigned reads than others.

MultiQC (Ewels et al., 2016) was run in the directory where all FastQC, Trimmomatic, and STAR outputs were located to get the combined summary report. MultiQC calculated the percentage of mapped reads to indicate the overall quality and sequencing accuracy. In addition, multi-mapping was estimated on MultiQC. Generally, the raw and trimmed mean read counts of

BTx3042, excluding the two outliers, are higher than SC599. Details of the raw read FastQC report summarized by MultiQC are provided in the supplementary files (Appendix A. Table A.2; Appendix A. Figure A.2).

Principal component analysis (PCA) was performed to determine how the biological replicates and genotypes were grouped based on their categories. PCA using the normalized and logarithm base two transformed count data was carried out on the *ggplot2 V3.3.0* R package. The read count data were converted into fragments per kilobase of transcript per million mapped reads (FPKM). FPKM values ranked for the genes within different genotypes and treatments to identify which genes are most highly expressed in specific conditions. The data was presented with a heat map where each cell's color (red and black) represents the FPKM value for that gene in that genotype or treatment. Heatmap using *ggplot2 V3.3.0* R package and the *heatmap3* function in R using the transformed and averaged FPKM values of three replicates for each genotype and treatment is used for plotting.

3.3.4 Differential expression analysis

The *DESeq*' R package was used for differential gene expression analyses using the *Wald* pairwise comparisons method (Love et al., 2014). Prior to the *DESeq2* run, reads were filtered, leaving minimum mean counts across samples greater than or equal to two. The significance of the *DESeq2 Wald* test was based on the Benjamini-Hochberg multiple test correction (false discovery rate, FDR), in which p-values less than 0.05 were declared significant, and the base two logarithmic fold change (LFC).

3.3.5 Gene ontology and KEGG enrichment analyses for DEGs

Functional annotation and KEGG pathway analysis using the web-based graphical tool ShinyGo v0.61 (Ge et al., 2020) categorized up or downregulated genes in each pairwise comparison from *DESeq2* results into their functional groups. If they were significantly enriched, GO enrichment analysis set these genes into biological processes, molecular function, and cellular components. All the GO was downloaded from http://amigo.geneontology.org/amigo using *AmiGo 2* (Carbon et al., 2009). The KEGG enrichment analysis provided significant metabolic pathways enriched in each comparison. KEGG were analyzed using ShinyGO 0.61 (Ge et al., 2020) and downloaded from https://www.genome.jp (Kanehisa et al., 2021) and KEGG diagrams from *pathview* (Luo & Brouwer, 2013). Only significant DEGs with the FDR > |2| were used for the GO and KEGG analysis.

3.4 Results

3.4.1 Clustering pattern of differential gene expression in response to *F. thapsinum* infection

To identify differentially expressed genes in response to infection by *F. thapsinum*, 24 single-end sequencing libraries from the susceptible BTx3042 and the resistant SC599 lines were used for RNA-Seq analysis. Filtering for genes with at least two mean counts across samples retained 22,220 genes for DEGs analysis with *DESeq2*. DEGs comparisons were conducted between the two genotypes, BTx3042 and SC599, control and pathogen (*F. thapsnium*) inoculations, and time of sample collection post-inoculation (24 or 48 hours). In this regard, eight pairwise comparisons were conducted; they were assigned a short comparison code and sequence number (Table 3.1). A principal component analysis (PCA) plot of BTx3042 and SC599 transcriptomes to identify the

clustering pattern of different treatments explained 80% of the variability (PC1 and PC2) (Figure 3.1). Replicated samples from each treatment were mostly clustered together, with few exceptions, indicating the reproducibility and validity of the biological samples. Genotypes were distinctly separated into two groups, BTx3042 clustered on the right and SC599 on the left. The pathogen, control-treated, and the two sampling times were grouped in clusters. (Figure 3.1). However, there were two outliers plotted in between the two genotypes, which were control-treated BTx3042 samples sampled at 24 hpi. They had exceptionally higher read numbers (sequencing depth) than the other samples discussed in the material and methods section above (Appendix A. Table A.2; Appendix A. Figure A.2).

The summary heatmap plot (Figure 3.2) using a random 22% of the total DEGs was plotted to observe the overall expression trend in the data. The expression profile was discrete and showed clear differences. The DEGs were clustered into five broader groups. In the first, fourth, and fifth clusters, the controlled treatments showed relatively higher expression over the pathogen in both genotypes. In clusters 2 and 3, the pathogen-treated resistant genotype (SC599) showed higher expression.

3.4.2 Comparative transcriptomic analysis revealed the presence of DEGs among samples

Transcriptomes of the resistant and susceptible sorghum lines inoculated with the pathogen were compared with their respective control treatments at 24 and 48 hpi to identify the expressed genes during Fusarium infection. In BTx3042, out of 360 significant DEGs, 73 were up-, and the remaining 287 were down-regulated at 24 hpi; the LFC ranged between 0.5 and 4.3 for upregulated genes, the smallest among the comparisons (Table 3.1). Genes involved in host defense responses based on Phytozome v3 (https://phytozome-next.jgi.doe.gov/) sorghum (BTx623) annotation

(McCormick et al., 2018), such as pathogenesis-related proteins (PR), cytochrome P450, Leucine-rich repeat, chalcone and stilbene synthase family protein, and other related gene families, contained higher negative fold changes in BTx3042 at 24 hpi (Figure 3.3). In the susceptible genotype, a large number of significant DEGs were observed at 48 hpi (BC48-vs-BP48) compared to 24 hpi (BC24-vs-BP24) (Table 3.1; Figure 3.3). At 48 hpi, out of the 5006 DEGs, 2593 were up, and 2413 were downregulated (Table 3.1; Figure 3.4).

In the resistant genotype, many DEGs were observed at 24 hpi (SC24-vs-SP24) compared to the susceptible at 24 hpi and itself at 48 hpi (SC48-vs-SP48). Cytochrome P450, secondary metabolite synthases, PR5, LRR, NB-ARC, disease resistance-responsive (dirigent-like protein) family proteins, chalcone and stilbene synthase, wall-associated kinases and peroxidase superfamily were highly upregulated (Figure 3.4; Figure 3.8; Figure 3.9). There were also upregulated genes mostly related to cellular carbohydrate metabolism and fluid and solute transport that can contribute to the host defense mechanism by reducing growth and maintaining plant cell carbon and water balance (Figure 3.4). At 48 hpi, SC599 (SC48-vs-SP48) had more downregulated DEGs than the upregulated (Table 3.1; Figure 3.4).

Co-expressed genes could regulate biological or metabolic processes in normal physiological activities or commonly expressed conserved resistance genes in response to pathogen infection signals. Both up and downregulated DEGs were co-expressed due to infection between the genotypes (Figure 3.3). Samples collected from both genotypes at 24 hpi (BC24-vs-BP24 and SC24-vs-SP24) shared nine upregulated DEGs (Figure 3.3A). The remaining 3056 DEGs in SC599 and 64 in BTx3042 were uniquely upregulated (Figure 3.3A). In contrast, 2273 DEGs in BTx3042 and only 292 in SC599 were exclusively upregulated in samples collected at 48 hpi

(BC48-vs-BP48 and SC48-vs-SP48) (Figure 3.3B). Similarly, in the downregulated DEGs, 51 were shared at 24 hpi between comparison BC24-vs-BP24 and SC24-vs-SP24 (Figure 3.3C), whereas 397 were shared at 48 hpi between BC48-vs-BP48 and BC48-vs-BP48 (Figure 3.3D).

DEGs were due to inherent genotypic similarity and variation between the two genotypes, possibly due to reaction towards pathogen stimuli or other normal cellular or molecular activities. When the two genotypes infected with the pathogen were compared both at 24 hpi (BP24-vs-SP24) and 48 hpi (BP48-vs-SP48), a higher number of genes were downregulated or less expressed in the resistant genotype at 48 hpi. In other words, genes with negative LFC in the resistant were highly expressed in the susceptible genotype. However, compared to the two genotypes at 24 hpi (BP24-vs-SP24), a larger number of R-gene families (NB-ARC, CC-NBS-LRR, LRR), and cytochrome P450 families were upregulated compared to the downregulated ones. In contrast, at 48 hpi (BP48-vs-SP48), those gene families were more expressed in the susceptible genotype. In Figure 3.3E – 3.3F, upregulated DEGs of control and pathogen treated shared 1.9% at 24 hpi and 31% at 48 hpi. In the down-regulated DEGs, 16% at 24 hpi and 29% at 48 hpi were shared and commonly expressed due to inherent similarity between the genotypes or conserved disease resistance genes among the genotypes. The DEGs between the control treatments in either of the times could be due to the inherent genotypic difference.

3.4.3 Essential defense genes were enriched in gene ontology and KEGG pathway analysis

Gene ontology (GO) analysis categorizes the DEGs into the biological process (BP), cellular components (CC), and molecular function (MF) (Thomas, 2017). GO and Kyoto Encyclopedia of Genes and Genomes (KEGG) pathway enrichment analyses were carried out on four of the eight comparisons, as shown in Table 3.1, using the DEGs comparisons due to infection only but not

the comparison due to genotypic difference, since our interest is differential expression due to infection on both genotypes. Additionally, DEGs with LFC between 2 and -2 were removed from the list to get those genes with strong effects. In this regard, the filtered DEGs highlighted in Table 3.1 were used for downstream analysis. The total number of genes obtained from *DESeq2* in each comparison was used as a background in the analysis. In the GO and KEGG analyses, most comparisons showed significant enrichment, presented in Figures 3.4-3.5, Appendix A Figure A3-A4. However, there were few non-significant enrichments. In BTx3042 (BC24-vs-BP24), upregulated DEGs at 24 hpi were non-significant for all GO terms and KEGG as the number of DEGs were only 9, too small for enrichment (Table 3.1). GO:CC was not significantly enriched in BTx3042 for downregulated DEG at 24 hpi (BC24-vs-BP24) and upregulated DEGs at 48 hpi (BC48-vs-BP48). On the other hand, in the resistant genotype (SC599), GO:CC was not significant for upregulated DEGs at 24 hpi (SC24-vs-SP24) and downregulated DEGs at 48 hpi (SC48-vs-SP48).

In a susceptible genotype (BC24 vs BP24) at 24 hpi, down-regulated genes were enriched for BP pathways, including flavonoid biosynthesis and metabolic processes, response to biotic stimulus, defense response, and regulation of phosphoprotein phosphatase activity (Figure 3.4; Appendix A Figure A.3A; Table S8a). Enriched MF terms included naringenin-chalcone synthase activity, abscisic acid binding, and protein phosphatase inhibitor activity. Additionally, flavonoid and secondary metabolite biosynthesis were significant pathways in the KEGG analysis in down-regulated DEGs of BTx3042 at 24 hpi. Cellular response to reactive nitrogen species, photosynthesis, light harvesting, secondary metabolic processes, cellular response to stress, and cell wall organization or biogenesis were enriched in BTx3042 at 48 hai the downregulated DEGs in GO:BP, which could be related to stress (Figure 3.4; Appendix A Figure A.3B). Similarly, in

the same comparison, the GO:MF was significantly enriched for tetrapyrrole binding, chlorophyll-binding, heme binding, kinase activity, and DNA-related terms (Figure 3.6B). Photosynthesis, flavonoid biosynthesis, phenylpropanoid biosynthesis, and biosynthesis of secondary metabolites were also enriched in the KEGG pathways of downregulated BTx3042 at 48 hai. However, in the upregulated DEG of BTx3042 at 48 hpi, carbohydrate metabolic processes, trehalose metabolism in response to stress, and chitin catabolic process in GO:BP enriched (Figure 3.4; Appendix A Figure A.4C). In the GO:MF defense-related response to the fungal infection, like signaling receptor, secondary metabolite processes, kinase activities, and chitinase activity, were also enriched, although it was delayed response after 48 hpi (Figure 3.6C).

In a resistant plant genotype (SC24 vs. SP24) at 24 hpi, upregulated DEG enriched GO:BP pathways related to defense against early pathogen infection, such as trehalose metabolism and biosynthesis, hydrogen peroxide catabolic/ROS metabolic processes, immune response/defense response, carbohydrate metabolism, and fluid/water transport (Figure 3.5; Appendix A Figure A.4B). The downregulated DEGs in the same genotype at 24 hpi GO:BP were enriched for plant-type secondary cell wall biogenesis, plant-type cell wall biogenesis, cellular polysaccharide biosynthetic process, polysaccharide biosynthetic process, and carbohydrate metabolic process (Figure 3.5; Appendix A Figure A4A). The study also found significant GO:MF pathways enriched for upregulated DEGs at 24 hpi, such as oxidoreductase activity, calcium ion binding, heme binding, tetrapyrrole binding, hydrolase activity, protein serine/threonine kinase activity, protein kinase activity, and transmembrane transporter activity (Figure 3.7B). In the KEGG pathways, starch and sucrose metabolism, phenylpropanoid biosynthesis, metabolic pathways, and biosynthesis of secondary metabolites were enriched for upregulated DEGs at 24 hpi. In the KEGG pathways, photosynthesis, phenylalanine, flavonoid biosynthesis, carbon metabolism,

biosynthesis of secondary metabolites, and metabolic pathways were enriched in the downregulated DEGs at 24 hpi. At 48 hpi, the downregulated DEGs in the resistant genotype (SC599) GO:BP were enriched for lignin biosynthetic process, xenobiotic transmembrane transport, phenylpropanoid biosynthetic process, and transmembrane transport (Figure 3.5; Appendix A Figure A.4C), while the upregulated DEG were not significant for all the GO terms except for KEGG carbon metabolism.

3.4.4 Defense, perception, and signaling in the upstream cell wall and membrane-bound DEGs

During infection to enter the host cell, pathogens produce enzymes to disrupt cell wall components that provide a physical barrier (Höfte & Voxeur, 2017). Several diseases resistance-responsive (dirigent-like protein) proteins (DIR) contained differential expression in response to *F. thapsinum* infection, which are involved in lignan and lignin biosynthesis that helps inhibit pathogen enzymes used for cell wall degradation (Halls et al., 2004; Paniagua et al., 2017). They were downregulated in the resistant genotype at 24 hpi and in the susceptible genotype at 48 hpi. However, Sobic.009G021300 was exceptionally upregulated at 24 (LFC=20.8) and 48 hpi (LFC= 7.2) in the resistant (Figure 3.8) but down-regulated in the susceptible genotype at 24 hpi. Several WAKs (Sobic.008G170800, Sobic.002G249600) were upregulated in the resistant genotype (Figure 3.8). The role of DIR protein family in the cell wall is manifested in the GO: BP, plant-type secondary cell wall biogenesis (GO:0009834), and plant-type cell wall biogenesis (GO:0009832) (Appendix A Figure A.4A). GO: MF cellulose synthase activity (GO:0016760) (Figure 3.7A) were significantly enriched in the resistant genotype at 24 hpi.

In this study, several peroxidase superfamily proteins (*SbPrx)* showed differential expression in both hosts with different expression levels over time, which plays an essential role in the accumulation of ROS and hence HR. Genes in the peroxidase hotspot on chromosome 2 were differentially expressed, which was reported to be an essential region against disease in sorghum (Scully et al., 2016). Sobic.002G391900 (*SbPrx4.1)* is an ortholog with arabidopsis *AtPrx4* (AT1G14540) class III peroxidase cell wall-targeted protein (Jemmat et al., 2020), appeared to be a highly downregulated (LFC>|-20|) in the susceptible genotype at 24 hpi (Figure 3.8) and the resistant genotype at 48 hpi (Figure 3.8). Sobic.002G357000 (*SbPrx34*) was upregulated in SC599 at 24 hpi and BTx3042 at 48 hpi (Figure 3.8). Sobic.002G416600 (*SbPrx46*) was downregulated in BTx3042 at 24 hpi (Figure 3.8); also an ortholog with rice gene OS07G0677100 *(Pox8.1*) that was differentially induced during infection by *Xanthomonas oryzae* (Chittoor et al., 1997). Sobic.002G010700 (*SbPrx30*) orthologous with the arabidopsis *AtPrx51* (At4g37530) gene (Valério et al., 2004) and the rice *Prx98 (*Os07g0115300) gene (Matić et al., 2021) was upregulated at 48 hpi in the susceptible genotype (Figure 3.8) and at 24 hpi in resistant genotype (Figure 3.8). The Prx differential expression was similarly manifested on peroxidase pathways in GO: BP, such as hydrogen peroxide catabolic processes (GO:0042744) and ROS metabolic process (GO:0072593) (Figure 3.5), and GO:MF, like heme binding (GO:0020037) and peroxidase activity (GO:0004601) in upregulated DEGs of resistant genotype at 24 hpi (Figure 3.7B). Contrarily, the polyketide metabolic/biosynthetic process (GO:0030638/GO:0030639) in GO:BP (Figure S3A) and heme binding (GO:0020037) pathways significantly enriched the downregulated DEG of susceptible genotype at 24 hpi (Figure 3.6A).

EF-hand calcium-binding protein family (Sobic.009G083600, Sobic.002G199500) and calmodulin-like 42 (Sobic.001G383700) were downregulated in the susceptible genotype (Figure

3.8). In the resistant genotype, Calcium-dependent lipid-binding (CaLB domain) family protein (Sobic.002G411900), EF-hand calcium-binding protein family (Sobic.009G242700) and others (Figure 3.8) were upregulated and might contribute to the early accumulation of ROS. In sorghum, early ROS accumulation is related to resistance; late accumulation contributes to pathogenesis by adding stress to the plant for anthracnose infection (Basavaraju et al., 2009) and aphid resistance (Scully et al., 2016; Pant & Huang, 2021). In the functional analysis of GO:MF, Calcium ion binding (GO:0005509) was significantly enriched in the resistant genotype at 24 hpi (Figure 3.6B).

3.4.5 Increased early expression of Nucleotide-binding leucine-rich repeat proteins

Nucleotide-binding domain leucine-rich repeat (NBS-LRR) genes are the largest among the disease-resistance genes found in clusters in the genome involved in the recognition of pathogen effectors, HR, and signal transduction after pathogen infection (Mchale et al., 2006; Mace et al., 2014). A large number of the NBS-LRR DEGs were observed in this study. In the susceptible genotype, they were downregulated in the early infection stage at 24 hpi (Figure 3.4). The downregulated NBS-LRR gene families in the susceptible genotype (BTx3042) at 24 hpi included Sobic.005G047800, Sobic.005G128000, Sobic.005G150700, Sobic.008G184900, and Sobic.008G174100 with LFC of -26.5, -11.6, -4.7, -8.2, and -5.2, respectively (Figure 3.4; Figure 3.9). Sobic.005G047800 *(RPM1)* homologs reported in arabidopsis, controlling the onset of early signs of hypersensitive reaction (HR), and it gets degraded when the cell controls HR lesion length in the resistant lines (Boyes et al., 1998). In rice, overexpression of *RPM1* confers broad-spectrum disease resistance (Li et al., 2019). Similarly, Sobic.005G150700 is an NB-ARC domain-containing disease resistance protein homologous to the ribonuclease inhibitor of maize (Zm00008a010181) and rice (Os11g0551700) gene. In addition, Sobic.005G128000 is similar to

stripe rust resistance protein *Yr10* in rice, wheat, and corn (Chalupska et al., 2008; W. Liu et al., 2014). However, NBS-LRR DEGs were up and downregulated later at 48 hpi in the susceptible genotype (Figure 3.6). Sobic.008G117600 and Sobic.009G204300 were the top NB-LRR DEGs with positive higher fold change in BTx3042 (susceptible) at 48 hpi in comparison #2 (BC48-vs-BP48) (Figure 3.9).

In the resistant genotype (SC599), a total of 35 NBS-LRR DEGs at 24 hpi and 8 at 48 hpi were upregulated. Interestingly, Sobic.002G104400 (*SbRWRKY1*), Sobic.002G050900 (*SbLRx4),* and Sobic.005G226400 were upregulated both at 24 hpi (SC24-vs-SP24) and 48 hpi (SC48-vs-SP48) (Figure 3.9). *SbRWRKY1,* a resistance (R) protein and WRKY transcription factor, an arabidopsis *ortholog, LRRAC1 (*AT3G14460) showed increased susceptibility to *Golovinomyces orontii* and *Pseudomonas syringae* in the knock-out mutants and increased expression in the resistant cultivar (Rinerson et al., 2015; X. Yang & Wang, 2016; Bianchet et al., 2019). Sobic.002G226000, an ortholog to arabidopsis gene *LLR4* (AT3G19230) encoding malecin-like domain (MLD)-and leucine-rich repeat (LRR) (Sultana et al., 2020), was upregulated at 24 and 48 hpi in the resistant genotype, and at 48 hpi in the susceptible genotype (Figure 3.9). Two closely located NB-ARC genes, Sobic.002G062800 and Sobic.002G062900 on chromosome two were upregulated at 24 hpi in the resistant and 48 hpi in the susceptible line. The significantly enriched GO:BP early immune (GO:0006955) and defense responses (GO:0006952) pathways in the upregulated DEGs on the resistant genotype at 24 hpi also revealed this (Figure 3.5; Appendix A Figure A.4B. In these pathways, Sobic.002G062800 and Sobic.005G226400 were involved.

3.4.6 Differential regulation and functional analysis of pathogenesis-related protein in the downstream defense cascade

So far, 17 families of PR proteins (PR-1 to PR-17) have been reported based on their sequence similarity or other functions (Sinha et al., 2014). In our result, a group of closely located PR family protein (PR10)/*Bet_v_1 Pyr (pyrabactin resistance) 1-like-6* gene members (Sobic.001G400700, Sobic.001G400800, Sobic.001G400900, and Sobic.001G401300) in a range between 79Kb distance on chromosome 1 were downregulated together in the susceptible genotype at 24 hpi (Figure 3.6). These genes were involved in the regulation of protein serine/threonine phosphatase activity (GO:0080163), negative regulation of phosphoprotein phosphatase activity (GO:0032515), abscisic acid-activated signaling pathway (GO:0009738), and response to biotic stimulus (GO:0009607) in the GO:BP enriched pathways in the downregulated DEGs of susceptible genotype at 24 hpi (Figure 3.4; Appendix A, Figure A.3A). The genes involved in these pathways were down-regulated in BTx3042 at 24 hpi, which means their respective processes were not acting against external infection stimuli. Hence, the defense mechanism was negatively affected and might contribute to the susceptibility of the genotype to the infection and early pathogenesis.

In the resistant genotype, Sobic.001G400900 and Sobic.001G400700 were also downregulated at 24 and 48 hpi, respectively. On the other hand, Sobic.001G401200 was consistently upregulated in the resistant genotype at 24 and 48 hpi (Figure 3.9). It was involved in several pathways like hormone-mediated signaling pathway (GO:0009755), response to endogenous stimulus (GO:0009719), defense response (GO:0006952), and signal transduction (GO:0007165) in the GO analysis (Figure 3.5; Figure 3.4B). Similarly, Cui et al. (2021) reported

upregulation of Sobic.001G401200 in the resistant line; however, they also reported the increased expression of Sobic.001G400800 and Sobic.001G401300 in the resistant line. Those were downregulated in our study.

The other vital PR families observed in this study were PR-5, thaumatin superfamily proteins (*Tyr*), or thaumatin-like proteins (*TLP*), which are involved in plant defense against pathogen infection (J. J. Liu et al., 2010; de Jesús-Pires et al., 2020). Two closely located PR5-like receptor kinase *(Pkinase_Tyr)* genes (Sobic.003G097200 and Sobic.003G097000) were upregulated in the resistant genotype at 24 and susceptible at 48 hpi (Figure 3.9). They were part of the phosphorylation (GO:0016310) pathway in the GO:BP (Figure 3.5) and protein kinase activity (GO:0004672) in the GO:MF pathways (Figure 3.4B). The other PR5-like receptor kinase, *LysM* (Sobic.009G019100) was downregulated in the susceptible genotype at 24 hpi. Similarly, Nida et al. (2021) reported differential expression of the *LysM* gene in response to grain mold infection in sorghum.

3.4.7 Chalcone and Stilbene Synthase Roles in Defense Against *Fusarium thapsinum* Infection

Most of the chalcones (CHS) and stilbene synthase (STS) family proteins were cloned *(SbCHS1 to SbCHS8)* and characterized in sorghum for their function in defense against pathogen infection (Lo et al., 1999; Lo et al., 2002; Yu et al., 2005; Dao et al., 2011; Sharma et al., 2014; Bhavsar et al., 2019). Several CHS and STS family proteins were differentially expressed between genotypes in this study (Figure 3.9). Lo et al. (2002) reported a cluster of CHS closely linked, highly conserved genes, all having a single intron and sharing 97.5% amino acid sequence identity in chromosome 5, closely related to maize C2 and *WHP* genes. In our study, this cluster of chalcone

and stilbene synthase family proteins in chromosome 5 (within a region of 127.9Kb according to Phytozome v13) were downregulated during early infection in the susceptible genotype (BTx3042) (Figure 3.9). They were Sobic.005G136200 *(SbCHS5; Chr05; 58859094..58862916)*, Sobic.005G136300 *(SbCHS4; Chr05:58879891..58882287)*, Sobic.005G137000 *(SbCHS1; Chr05: 58925898..58927778)*, and Sobic.005G137200 *(SbCHS7; Chr05: 58985306..58986992)*. In contrast, Sobic.005G137000 *(SbCHS1)*, similar to *WHP1*, upregulated in SC599 at 24 hpi (Figure 3.9), was one of the downregulated in the susceptible genotype. *SbCHS5* and *SbCHS1* were also highly expressed in the resistant line when the two pathogen-infected genotypes were compared at 24 hpi.

Our results further indicated the importance of CHS and STS by the significant GO pathways in the DEGs of susceptible and resistant genotypes due to infection. Interestingly, the KEGG, CHS, and STS genes regulating flavonoid biosynthesis (sbi00941) and biosynthesis of secondary metabolites (sbi01110) pathways were enriched in the downregulated DEGs of both genotypes (result not shown). The significant pathway in the resistant downregulated should not be a surprise; the KEGG pathway for the biosynthesis of secondary metabolites (sbi01110) was also significantly enriched but with different DEGs. The flavonoid or secondary metabolites are regularly produced in the plant system for normal metabolism. However, we were interested in the genes involved in the biosynthesis of an essential class of flavonoids: CHS and STS (Naringenin), whose biosynthesis is directly regulated by biotic stress. In the GO:MF, this specifically important pathway, naringenin-chalcone synthase activity (GO:0016210), was significantly enriched (Figure 3.6A).

The other interesting result related to CHS in flavonoid synthesis was the differential expression of Sobic.004G050200, *SbDFR3* (bifunctional dihydroflavonol 4-reductase/ dihydroflavonol 4-reductase). It was down-regulated at 24 hpi and upregulated at 48 hpi in the susceptible genotype (Figure 3.9). *SbDFR3* was also upregulated in the resistant genotype at 24 and 48 hpi (Figure 3.9). In addition, it was involved in oxidoreductase activity (GO:0016491) in GO:MF and biosynthesis of secondary metabolites (sbi01110) of the KEGG pathway in both genotypes. *SbDFR3* is an enzyme induced during 3-deoxyanthocyanidin accumulation due to fungal infection, which is unique to sorghum, where it synthesizes it into anthocyanidins (Liu et al., 2010).

3.5 Discussion

RNA-seq has been used to study the molecular responses of sorghum to various abiotic and biotic stresses such as nitrogen stress (Gelli et al., 2014, 2016, 2017), drought stress (Fracasso et al., 2016), chilling stress (Marla et al., 2017), anthracnose infection (Fu et al., 2020; Cui et al., 2021; Natarajan et al., 2021), *Exserohilum turcicum* infection (Adhikari et al., 2021), grain mold infection (Nida et al., 2021), and sugarcane aphid resistance (Serba et al., 2021). Unraveling the molecular and genetic bases of the DEGs involved in defense-related roles against stalk rot infection using the RNA-Seq method has been practiced in sorghum (Sharma et al., 2014; Bandara et al., 2018). In this sense, our transcriptome study aimed to identify differential gene expression and assess temporal regulation against *F. thapsinum* infection and their biological and molecular functions. Two inbred sorghum genotypes previously characterized as resistant and susceptible to *F. thapsinum* infection (Tesso et al., 2010) were inoculated with the pathogen 15 days after 50 % flowering. Stalk tissues were collected 24 and 48 hours after inoculation (hpi) for RNA extraction.

Our transcriptome and functional analysis provide basic information on the potential genes and molecular pathways activated in response to *F. thapsinum* infection, identify possible metabolic processes involved in the defense response, and hypothesize disease resistance mechanisms against the pathogen.

3.5.1 The temporal regulation of genes in defense against hemibiotrophic Fusarium stalk rot

F. thapsinum is a hemibiotrophic pathogen with a biotroph nature during the initial stages of infection and changes into necrotrophy in the later stages of infection (Lyons et al., 2015; Robles-Barrios et al., 2022). The defense mechanism in the resistance genotype was turned on early with cell wall-related signaling and defense, the accumulation of ROS, flavonoids, and other antifungal proteins, in which the HR and disease defense responses were seen early at 24 hpi (Figure 3.5, 3.7, and 3.8). However, in the susceptible genotype (BTx3042), only 73 genes were upregulated. In comparison, 287 genes were downregulated at 24 hpi. The overall expression level was low compared to other comparisons (Table 3.1), suggesting that this lower early expression may have contributed to its susceptibility to the pathogen in addition to the delayed upregulation of the cell wall-associated DEGs. Delayed response, including ROS, and HR, led to further disease progression as the pathogen in the later stages depends on the dead tissues as it turns to necrotrophy. That means the programmed cell death by the plant defense system added an opportunity for the pathogen to depend on it. The pathogen kills additional tissues, leading to an increased lesion length, affecting the overall plant system as it affects the plant fluid and nutrient transport through the stem/stalk, pushing the plant's susceptibility (Glazebrook, 2005). The necrotrophic pathogens are opportunists utilizing the plant's HR responses, hence effective pathogenesis that makes the host susceptible(Govrin & Levine, 2000; Bandara et al., 2018).

Plant cell walls are essential for growth and development, providing structural support and protection against biotic and abiotic stresses (Engelsdorf et al., 2018). They comprise several components, including cellulose, hemicellulose, lignin, and pectin. Pathogens produce enzymes that can break down cell walls, allowing them to initiate infections. In our study, we found that certain genes, such as Sobic.009G021300 (DIR) and peroxidases (*SbPrx34* and *SbPrx30),* were upregulated in the resistant genotype but not in the susceptible genotype at 24 hpi (Figure 3.8). These genes are involved in lignan and lignin biosynthesis, which can inhibit pathogen enzymes such as cellulases, polygalacturonases, glucosidases, and laccases, responsible for cell wall degradation (Paniagua et al., 2017). Lignin also serves as a barrier against pathogens, limiting the spread of toxins and enzymes and providing stability to the plant's vascular system (Miedes et al., 2014). Pathogen-induced cell wall damage releases fragments of cell wall components like oligogalacturonides (OG), which are recognized by wall-associated-kinase-like-5 (WAKs) proteins, initiating an immune response (Ferrari et al., 2013; Wolf, 2017). We observed that WAKs (Sobic.008G170800 and Sobic.002G249600) were upregulated in the resistant genotype (Figure 3.8). In addition, the accumulation of ROS like hydrogen peroxide through activating the peroxidase superfamily protein (SbPrx) also helps regulate cell wall strength and the hypersensitive reaction (Gechev & Hille, 2005; Shetty et al., 2008; Basavaraju et al., 2009). Ultimately, the programmed cell death or HR triggered by the resistant host limits the pathogen's access to water and nutrients (Glazebrook, 2005). The coordinated effect of DIR, Prx, and WAKs likely helped to limit pathogen colonization in the early stages of biotrophic infection in the resistant genotype, in the time the pathogen depends on living cells.

Efficient defense against a plant pathogen involves early detection and signaling mechanisms that precede the activation of defense responses. The NBS-LRRs like

Sobic.002G104400 (*SbRWRKY*1), Sobic.002G050900 (*SbLRx4*), and Sobic.005G226400 are essential components of the secondary innate immune system (ETI) that plays a critical role in resistance against a pathogen. These genes were upregulated in the resistance genotype but downregulated in the susceptible at 24 hpi (Figure 3.9). NBS-LRRs recognize virulence effectors that activate receptor proteins like Sobic.003G097200 and Sobic.003G097000 (Figure 3.9) to accumulate pathogenesis-related (PR) proteins to prevent infection via programmed cell death or HR (Mace et al., 2014; Zhang et al., 2018). Despite the pathogen compromising this upstream defense, this leads to activating downstream defense mechanisms, such as PR proteins, defensins, and secondary metabolite enzymes (Corwin & Kliebenstein, 2017). The PR-10 (Sobic.001G401200) gene was highly expressed in the resistant line, whereas several PR-10 genes were downregulated in the susceptible genotype at both times (Figure 3.9). This PR-10 protein belongs to the PR-10 family. It is also known as betallergen, which acts as an abscisic acid receptor and plays an essential role in plant resistance to biotic and abiotic stresses (Nishimura et al., 2009; Radauer et al., 2008; Santiago, Dupeux, et al., 2009; Santiago, Rodrigues, et al., 2009). Studies in sorghum have shown that PR-10 expression is critical in the defense response to different fungal pathogens (Lo et al., 2007; Katilé et al., 2010; Cui et al., 2021; Nida et al., 2021). In our study, PR-10 was expressed more than others, indicating its importance in the defense mechanism against the pathogen.

The antifungal proteins and secondary metabolites like 3-deoxyanthocyanidin flavonoids kill both the plant cell under fungal attack and the pathogen limiting the pathogen's further colonization (Snyder & Nicholson, 1990). Chalcones (CHS) and stilbene synthase (STS), such as Sobic.005G137000 *(SbCHS1)* and Sobic.005G136200 (*SbCHS5*) known for their defense function against pathogen infection in sorghum (Lo et al., 2002; Yu et al., 2005; Dao et al., 2011) were

upregulated in the resistance and downregulated in the susceptible genotype (Figure 3.9). *SbCHS1* gene, expressed differently in both genotypes at 24 hpi, catalyzes 3-deoxyanthocyanidins, a major phytoalexin in defense response towards fungal infection (Lo et al., 1999; Yu et al., 2005; Liu et al., 2010). They are only induced by pathogen infection, except *SbCHS5,* which is activated by a light signal in addition to fungal infection signals (Liu et al., 2010). Early accumulation of 3-deoxyanthocyanidins and induction of genes encoding CHS synthase in resistant cultivars were reported to be the main resistance mechanism in sorghum against *Colletotrichum sublineolum* (Lo et al., 2002). Sharma et al. (2014) reported delayed expression of chitinase *(SbChit)* and stilbene *(SbSTS1)* synthase genes in the susceptible sorghum cultivar against stalk rot fungal pathogen, *M. phaseolina*. Similarly, Adeyanju et al. (2015) reported the chalcone and stilbene synthase protein family gene in chromosome 9 as one of the candidate genes in their genome-wide association study on resistance to *M. phaseolina* and *F. thapsinum* stalk rot in sorghum.

CHS and STS are members of the polyketide synthase superfamily (PKS III) in plants that play a role in metabolizing antimicrobial compounds called phytoalexins. These compounds are essential in defending the plant against pathogens and are synthesized through flavonoid and isoflavonoid biosynthesis (Springob et al., 2003; Yu et al., 2005; Dao et al., 2011). Sobic.004G050200 (*SbDFR3*) is a gene that encodes an enzyme involved in flavonoid biosynthesis and was found to be highly upregulated in resistant plants but downregulated in susceptible plants at 24 hpi (Figure 3.9). However, at 48 hpi, *SbDFR3* was upregulated in both genotypes. Flavonoids produced by *SbDFR3* are involved not only in the early defense response but also in the later stages of the plant-pathogen interaction (Agati et al., 2012; Mierziak et al., 2014; Treutter, 2005). They have antioxidant activities that help to scavenge reactive oxygen species (ROS) produced due to the infection, reducing further damage to the host (Agati et al., 2012; Mierziak et al., 2014;

Treutter, 2005). In addition, flavonoids play a role in regulating auxin activity, which helps to tighten plant tissues and overall structure (Beckman, 2000; Mierziak et al., 2014; Treutter, 2005).

It can be seen from this that a combination of multiple differentially regulated genes in the resistant genotype in the earliest infection response contributed to resistance to the disease. It is not a single gene that brought much effect, so it is more of quantitative resistance, with multiple genes involved. The defense mechanism seen was temporal; it varies over time along with the pathogen's hemibiotrophic nature. The temporal cellular regulation of carbohydrate metabolism, water, nutrient, and photosynthetic processes was also vital (Figure 3.4 and 3.5). As the pathogen colonization progresses, it affects the plant solute and water translocation when the vascular tissues are damaged (Tesso et al., 2012; Tesso et al., 2010). These processes were significantly enriched in the upregulated and downregulated DEGs of the resistant and the susceptible genotypes, respectively (Figure 3.4 and 3.5). They help maintain the plant's overall functioning and balance carbon spent for disease defense and growth.

DEGs were enriched in various gene ontology (GO) and Kyoto Encyclopedia of Genes and Genomes (KEGG) pathways in both genotypes. In the susceptible genotype, the down-regulated genes were enriched in BP pathways related to flavonoid and secondary metabolite biosynthesis, response to biotic stimulus, and regulation of phosphoprotein phosphatase activity. In contrast, upregulated DEGs at 48 hpi were enriched in trehalose metabolism in response to stress and chitin catabolic processes (Figure 3.4). Nida et al. (2021) reported similar GO:BP in downregulated DEGs of the susceptible genotype. In the early infection stage, the downregulation of DEGs involved in those defense-related pathways might have contributed to susceptibility to the pathogen. On the other hand, in the resistant genotype, the upregulated DEGs were enriched in

pathways related to defense against early pathogen infection, such as trehalose metabolism, hydrogen peroxide catabolic/ROS metabolic processes, immune response/defense response, carbohydrate metabolism, and fluid/water transport (Figure 3.5). Cui et al. (2021) reported significant enrichment of immune response/defense response in resistant sorghum genotypes compared to the susceptible ones. In the resistant genotype (SC599), 48 hpi, the downregulated DEG were enriched for lignin biosynthetic process, xenobiotic transmembrane transport, phenylpropanoid biosynthetic process, and transmembrane transport, while the upregulated DEG were not significant for all the GO terms except for KEGG carbon metabolism.

3.5.2 Possible hypothetical QDR mechanism against Fusarium stalk rot disease in sorghum

Quantitative disease resistance (QDR) is a durable disease resistance mechanism that reduces host susceptibility but does not bring a complete absence of disease symptoms phenotypically (Poland et al., 2009; St. Clair, 2010). In QDR, the host shows the continuous distribution of the trait from susceptibility to resistance (Poland et al., 2009; St. Clair, 2010; Niks et al., 2015). The genetic inheritance of the underlining genes or loci may or may not necessarily be quantitative (St. Clair, 2010), and multiple genes are involved in QDR (Zhang et al., 2013). However, disease resistance controlled by polygenic or quantitative traits is an important part of the molecular architecture of QDR's integrated response pathways (Roux et al., 2014). QDR has reportedly been effective against necrotrophic and hemibiotrophic pathogens and provides broader resistance (Wang et al., 2019; Ding et al., 2021; Yang et al., 2022). In sorghum, 36% of the genome was reportedly involved in QDR against fungal pathogens (Mace et al., 2014). Sorghum Fusarium stalk rot is polygenically controlled (Adeyanju et al., 2015) and has a hemibiotrophic life cycle (Robles-Barrios et al., 2022). Therefore, we hypothesize sorghum resistance mechanism against Fusarium

stalk rot follows the QDR mechanism, where multiple elevated expressions of QDR-related genes in the resistance genotype control molecular mechanism in response to infection. The broader categories in QDR are the upstream perception, signaling, and defense, and the downstream signaling and signal transduction and defense response (Corwin & Kliebenstein, 2017). We followed this category in the hypothetical model (Figure 3.7). Early detection and signaling to activate a multilayered network of QDR defense responses based on the nature of the pathogen have prime importance for resistance.

It begins with the upstream perception of the pathogen (or microbe)-associated molecular patterns (P/MAMPs) or damage-associated molecular patterns (DAMPs) by plant-cell-surface pattern recognition receptors in the cell wall (PRRs) or intracellular recognition of pathogen effectors and signaling by R-genes and receptor kinases (Jones & Dangl, 2006). In our experiment, upregulation of DIR (SORBI_3009G021300), WAKs (Sobic.008G170800, Sobic.002G249600), PR5-like receptor kinase (Sobic.003G097000, Sobic.003G097200), protein kinase superfamily (Sobic.003G096400, Sobic.003G097100), and calcium-binding/ dependent lipid-binding protein family (Sobic.002G376800, Sobic.002G376900, Sobic.002G377000, Sobic.002G411900) at 24 hpi could be early pathogen perception response to initiate QDR in the resistant genotype (Figure 3.7). DIR has been reported for their QDR against wheat stripe rust (Singh et al., 2022). WAKs are also known for their involvement in QDR through signal transduction against fungal pathogens (Zuo et al., 2015; Q. Yang et al., 2017; Wang et al., 2019; Adhikari et al., 2021; Nida et al., 2021). Weak R-genes (NBS-LRR/ARC) and ROS are involved in signaling and defense through programmed cell death or HR and also link perception to defense responses like kinases in QDR (He et al., 2004; Boller & Felix, 2009; Marone et al., 2013; Corwin & Kliebenstein, 2017). Closely

found NB-ARC genes, Sobic.002G062800 and Sobic.002G062900, were upregulated in our study and might be involved in QDR.

The binding of PAMPs or DAMPs to PRRs triggers a response known as PAMP-triggered immunity (PTI) (Monaghan & Zipfel, 2012). PTI involves many physiological changes in the plant cell, including the release of calcium and reactive oxygen species (ROS), as well as the activation of mitogen-associated and calcium-dependent protein kinases (MAPKs and CDPKs) (Nicaise et al., 2009; Tena et al., 2011). These changes lead to transcriptional reprogramming, which involves the activation of several defense-related genes that help the plant mount a response to the pathogen or damage (Nicaise et al., 2009). The main defense network after signal transduction in the downstream defense cascade included pathogenesis-related (PR) proteins like PR-10 (Sobic.001G401200), flavonoid and secondary metabolites biosynthesis proteins like *SbCHS1* (Sobic.005G137000), and *SbDFR3* (Sobic.004G050200). They might have been involved in QDR as they were consistently upregulated in the resistant genotype at 24 and 48 hpi (Figure 3.6). Rice genotypes with QDR recessive gene (*pi21)* showed higher expression of PR genes and increased resistance against rice blast (Fukuoka & Okuno, 2001). In addition, the cytochrome P450 family (Sobic.007G071800) regulates allene oxide synthase (AOS) that biosynthesizes jasmonic acid (JA) and is involved in JA signaling pathways (Itoh et al., 2002; Pandian et al., 2020). JA biosynthesis is induced during infection against necrotrophic and hemibiotrophic pathogens (Pieterse et al., 2012; Yang et al., 2019; Gupta et al., 2020). Flavonoid structural genes (CHS and DFR) were upregulated against *C. heterostrophus* infection in sorghum and induced methyl jasmonate biosynthesis (Liu et al., 2010).

3.6 Conclusion

Fusarium stalk rot caused by *F. thapsinum* is reported to be the most virulent occurring in the post-flowering stage when the environmental condition permit, specifically dry and humid conditions. In this study, we report that a single or few major genes did not seem to control the resistance mechanism in the resistant cultivar. Instead, it was more likely to be QDR, in which perception in the cell wall and signaling by receptors and kinases coordinated activation of antifungal proteins, resistance genes, peroxides that regulate programmed cell death, phytoalexins, and others. It was also regulated temporarily. The defense mechanism was turned on early, and later carbon metabolism, water and nutrient transport, secondary metabolites, and photosynthetic processes were highly expressed in the resistant cultivar suggesting that the resistance mechanism evolved well with the hemibiotrophic nature of the pathogen. Quantitative genetic mapping studies can further support DEGs involved in the defense mechanism for Fusarium stalk rot resistance for marker-assisted selection to support resistance breeding efforts. This preliminary discovery of molecular and genetic regulators activated in the early stages of infection would add new knowledge and contribute to future molecular and genetic studies to locate genes or loci responsible for activating the QDR, and eventually assist the crop improvement effort against stalk rot disease resistance.

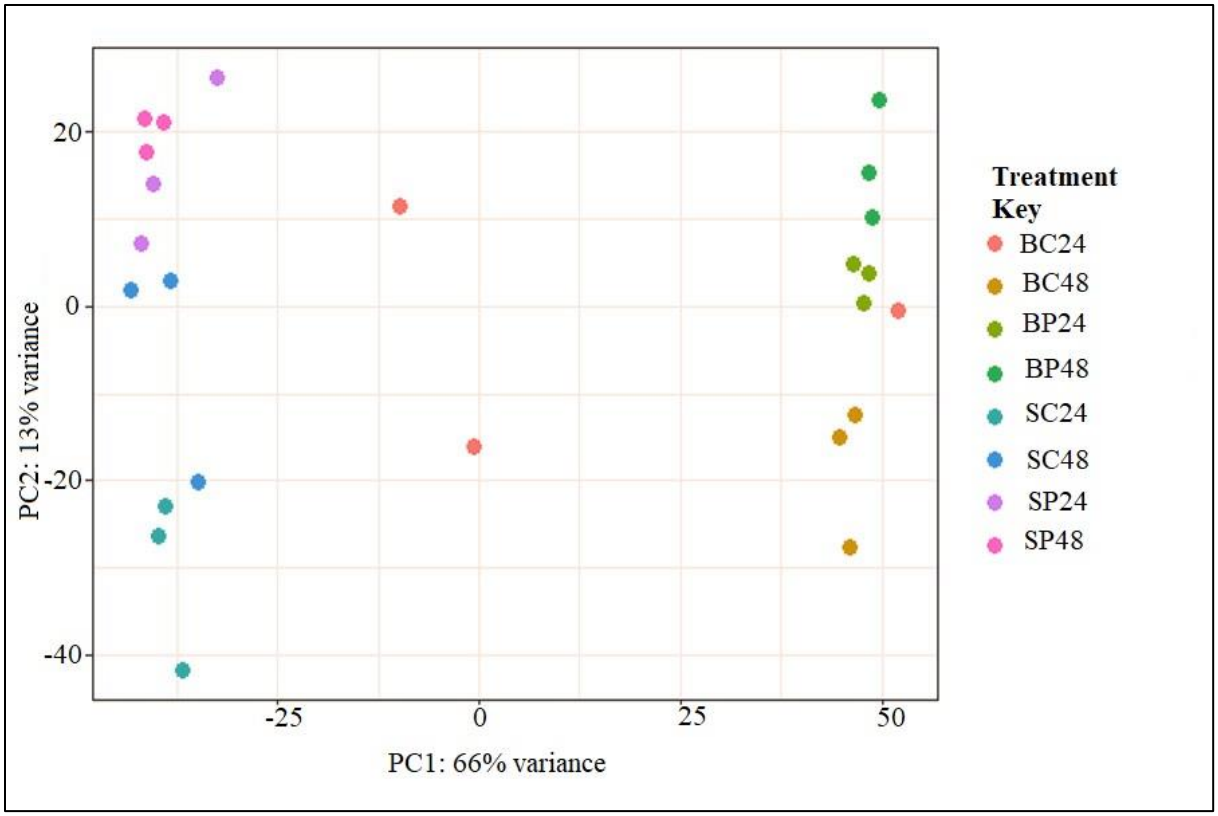

Figure 3-1. PCA plot of regularized log (rlog) transformed RNA-Seq count data of BTx3042 (B) and SC599 (S), control (C) and pathogen inoculated (P), sampled at 24 and 48 hours after inoculation in three replications. e.g., BC24: stands for BTx3042 control treatment 24 hpi.

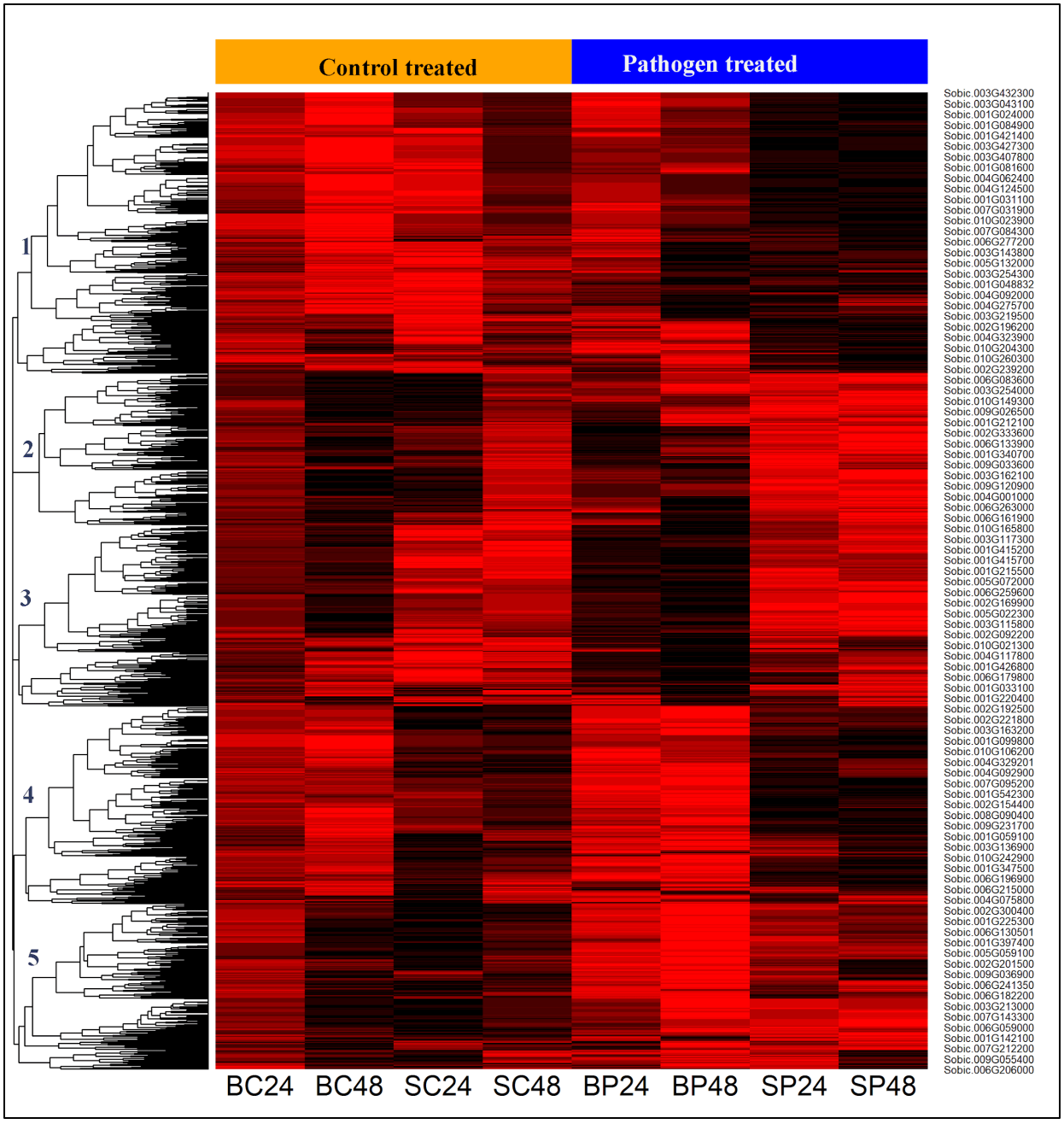

Figure 3-2. Summary heat map of 22% (4786) of the total 22,220 DEGs displaying the overall gene expression in BTx3042 and SC599 under control treatment (orange color bar on the heat map) and *F. thapsinum* (blue color bar on the heat map).
Red color represents a high expression rank, while black represents the low expression rank of a transcript. *Sample Abbreviations*: *Genotypes*: BT, BTx3042; SC, SC599; *Treatments*: C, control; P, pathogen (*F. thapsinum*) treated; *Time*: 24 & 48, 24 & 48 hpi. BT.C24, BTx3042 control treated sampled at 24 hpi; Average of the three replications in fragments per kilobase of exon per million reads mapped (FPKM) values for each sample are included as text in the heat maps.

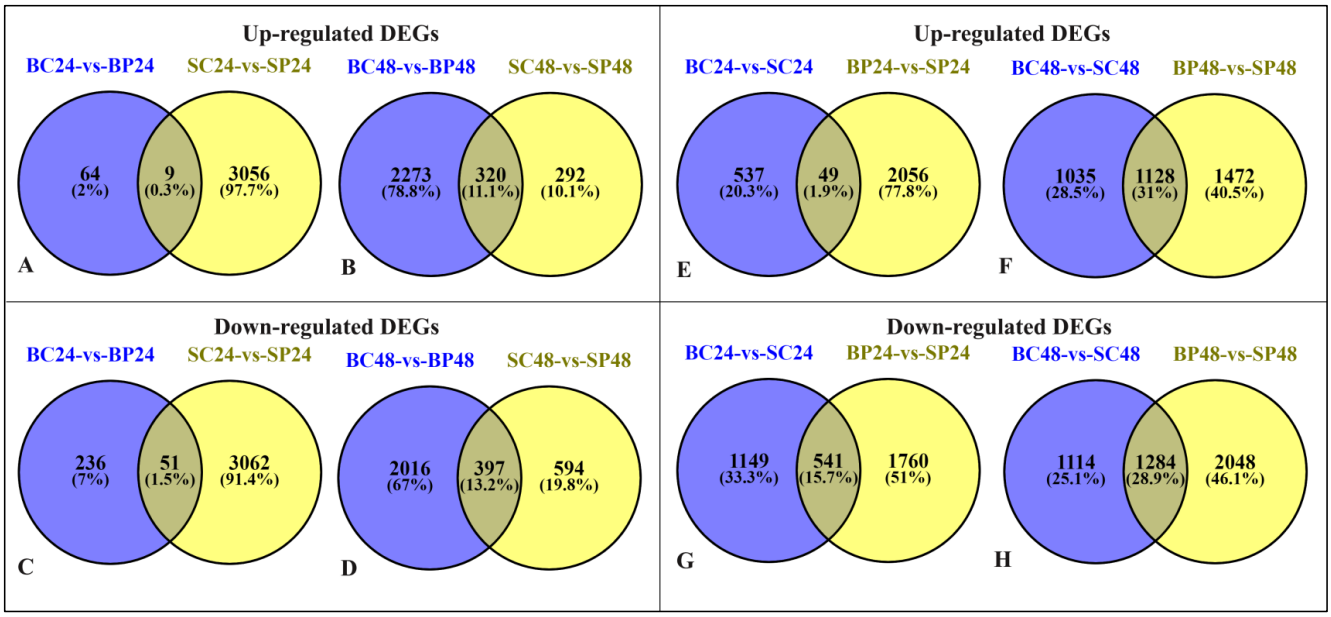

Figure 3-3. Venn diagram showing up, down-regulated, and common DEGs between BTx3042 and SC599 harvested at 24 and 48 hours after inoculation (hpi) of pathogen (*F.thapsinum*) and control inoculation.

(A) Upregulated and common DEGs due to infection for BTx3042 and SC599 at 24 hpi (BC24-vs-BP24 and SC24-vs-SP24). (B) Up-regulated and common DEGs due to infection for BTx3042 and SC599 at 48 hpi (BC48-vs-BP48 and SC48-vs-SP48). (C) Down-regulated and common DEGs due to infection for BTx3042 and SC599 at 24 hpi (BC24-vs-BP24 and SC24-vs-SP24). (D) Down-regulated and shared DEGs due to infection for BTx3042 and SC599 at 48 hpi (BC48-vs-BP48 and SC48-vs-SP48). (E) Up-regulated and common DEGs due to infection between control genotypes and pathogen inoculated at 24 hpi (BC24-vs-SC24 verses BP24-vs-SP24). (F) Up-regulated and common DEGs due to infection between genotypes of control and pathogen inoculated at 48 hpi (BC48-vs-SC48 verses BP48-vs-SP48). (G) Down-regulated and common DEGs due to infection between control genotypes and pathogen inoculated at 24 hpi (BC24-vs-SC24 verses BP24-vs-SP24). (H) Down-regulated and common DEGs due to infection between control genotypes and pathogen inoculated at 48 hpi (BC48-vs-SC48 verses BP48-vs-SP48).

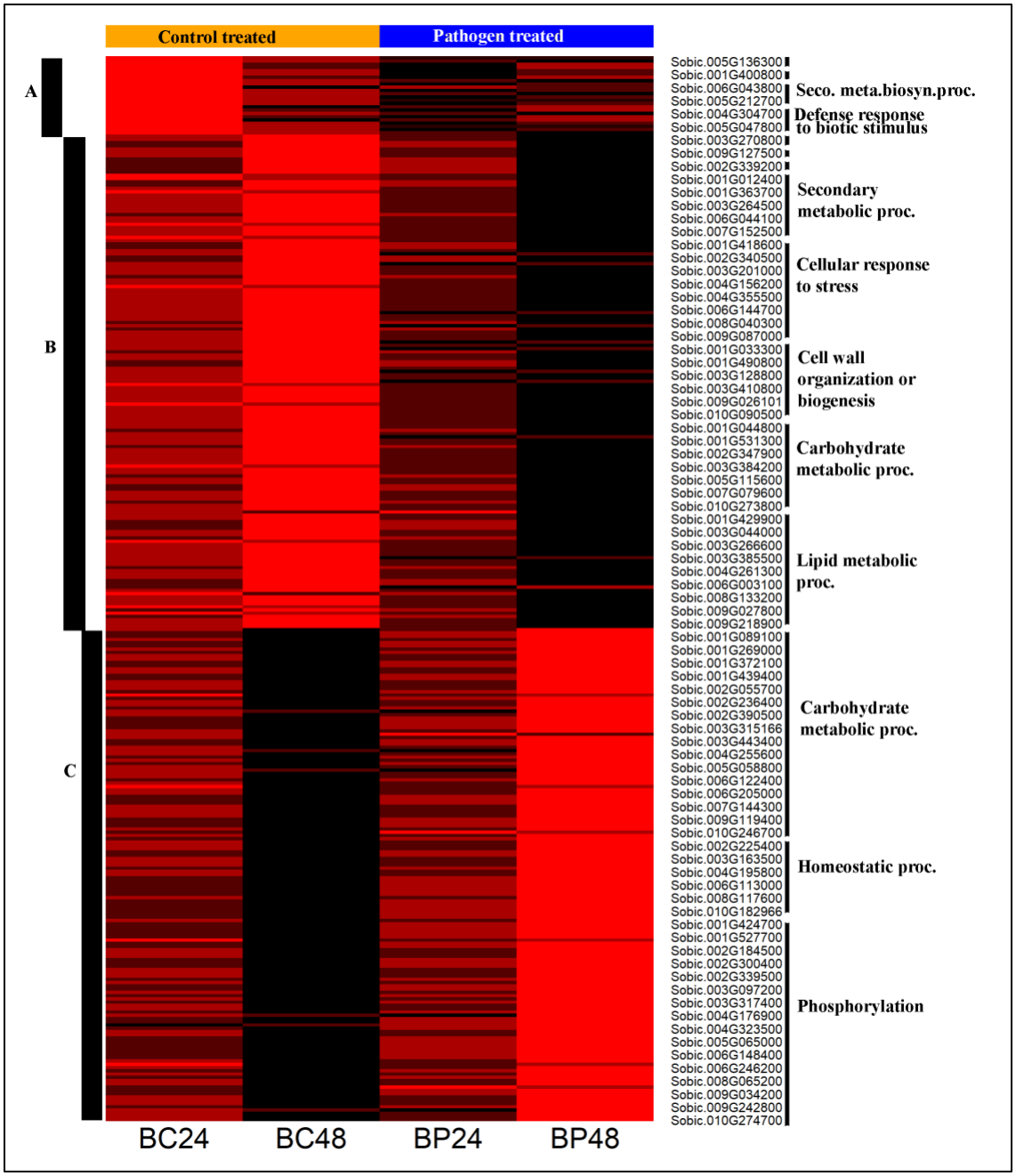

Figure 3-4. GO enriched 327 significant DEGs categorized based on Biological process in BTx3042 (Susceptible) under control treatment (orange color bar on the heat map) and *F. thapsinum* (blue color bar on the heat map).
Red color represents a high expression rank, while black represents the low expression rank of a transcript. Sample Abbreviations: Genotypes: B, BTx3042; treatments: C, control; P, pathogen (*F. thapsinum*) treated; Time: 24 & 48, 24 & 48 hpi. BC24, BTx3042 control treated sampled at 24 hpi; Average of the three replications in fragments per kilobase of exon per million reads mapped (FPKM) values for each sample are included as text in the heat maps. A. Down-regulated DEGs in BC24 vs. BP24; B. Down-regulated DEGs in BC48 vs. BP48; C. Down-regulated DEGs in BC48 vs. BP48.

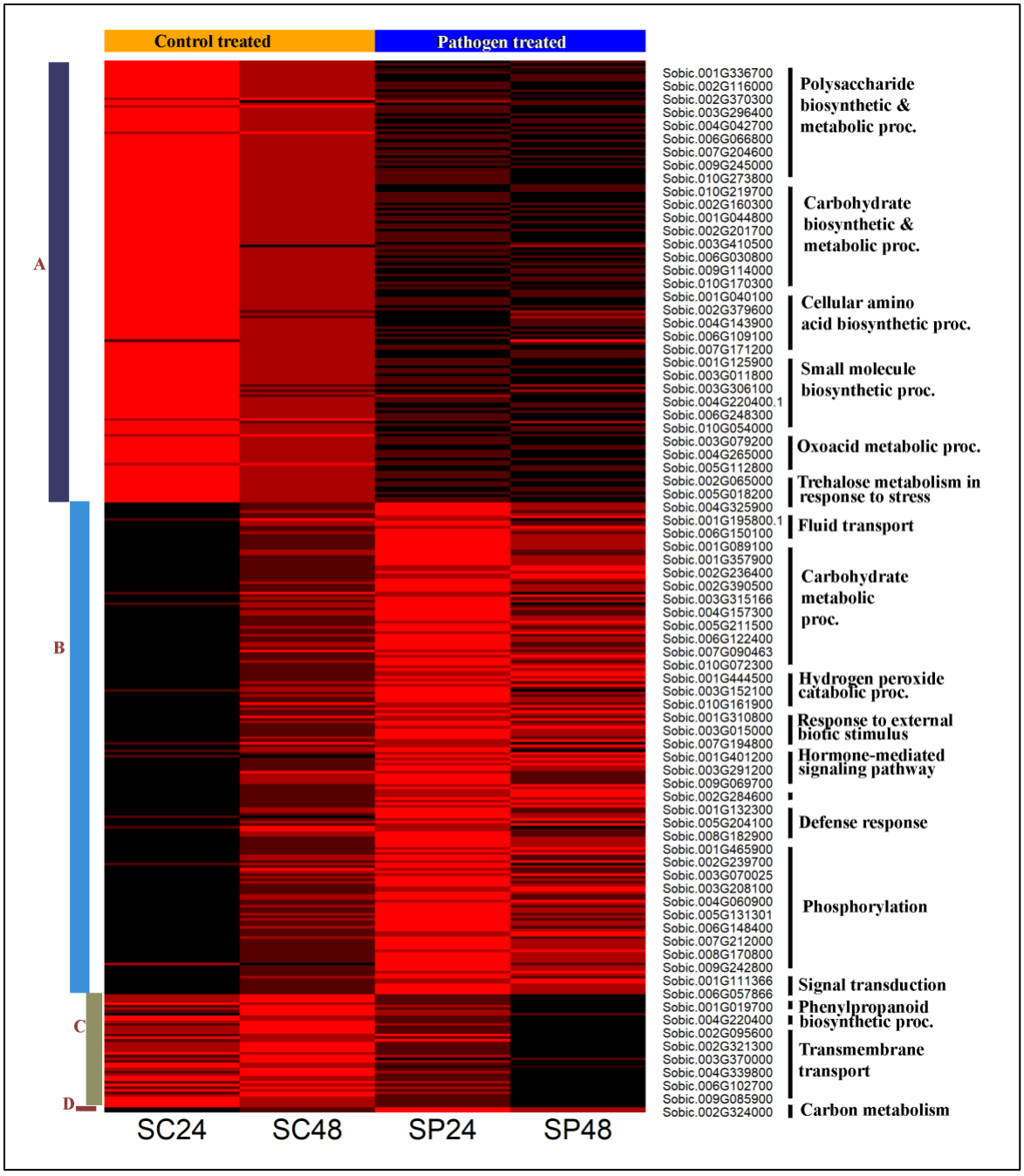

Figure 3-5. GO enriched 401 significant DEGs categorized based on Biological process in SC599 (resistant) under control treatment (orange color bar on the heat map) and *F. thapsinum* (blue color bar on the heat map).

Red color represents a high expression rank, while black represents the low expression rank of a transcript. Sample Abbreviations: Genotypes: S, SC599; treatments: C, control; P, pathogen (*F. thapsinum*) treated; Time: 24 & 48, 24 & 48 hpi. SC24, SC599 control treated sampled at 24 hpi; Average of the three replications in fragments per kilobase of exon per million reads mapped (FPKM) values for each sample are included as text in the heat map. A. Down-regulated DEGs in SC24 vs. SP24; B. Up-regulated DEGs in SC24 vs. SP24; C.Down-regulated DEGs in SC48 vs. SP48; D. Up-regulated DEGs in SC48 vs. SP48.

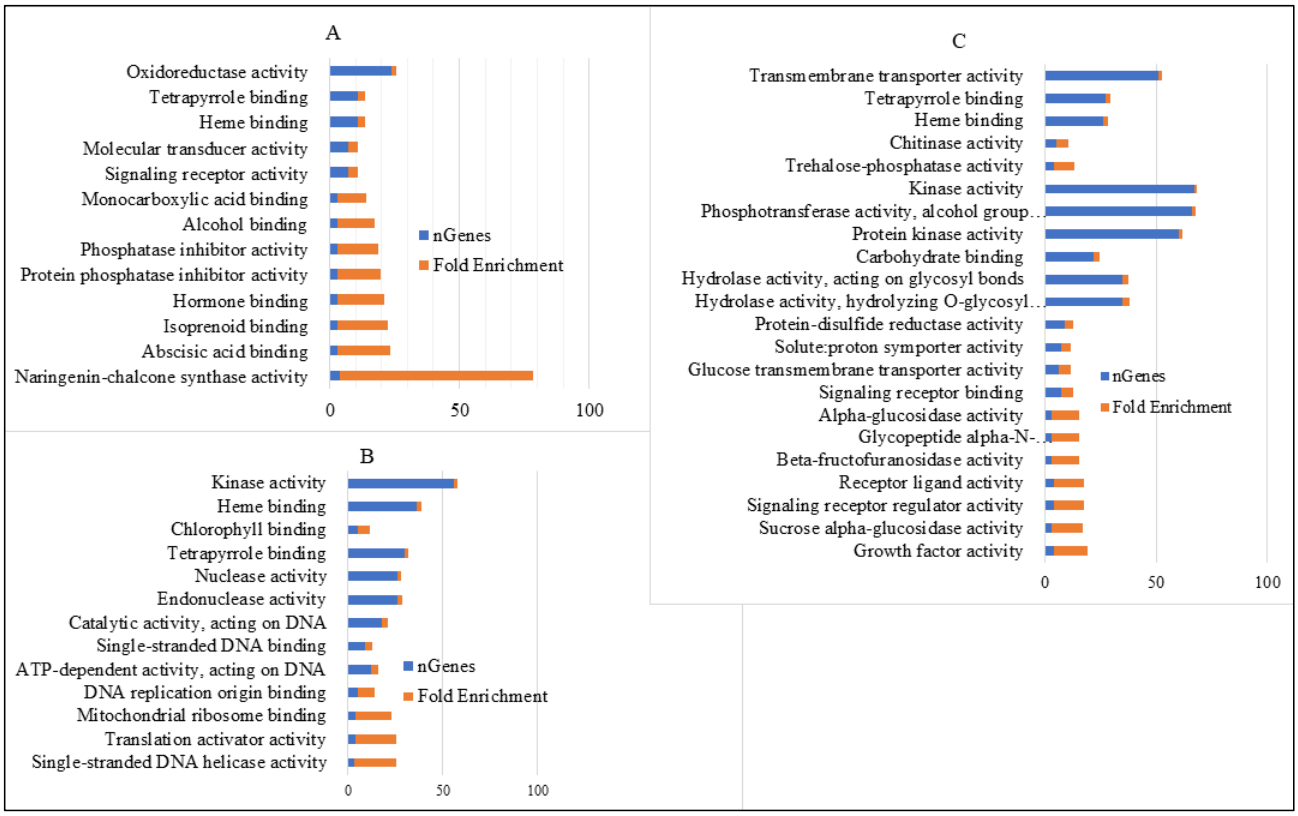

Figure 3-6. Significant GO:MF terms of DEGs between control and pathogen-treated BTx3042 (susceptible) at 24 and 48 hpi.

(A) Downregulated DEG at 24 hpi; (B) downregulated DEG at 48 hpi; and (C) upregulated DEGs at 48 hpi Y-axis = GO pathways, X-axis = Number of genes (blue) and fold enrichment (orange).

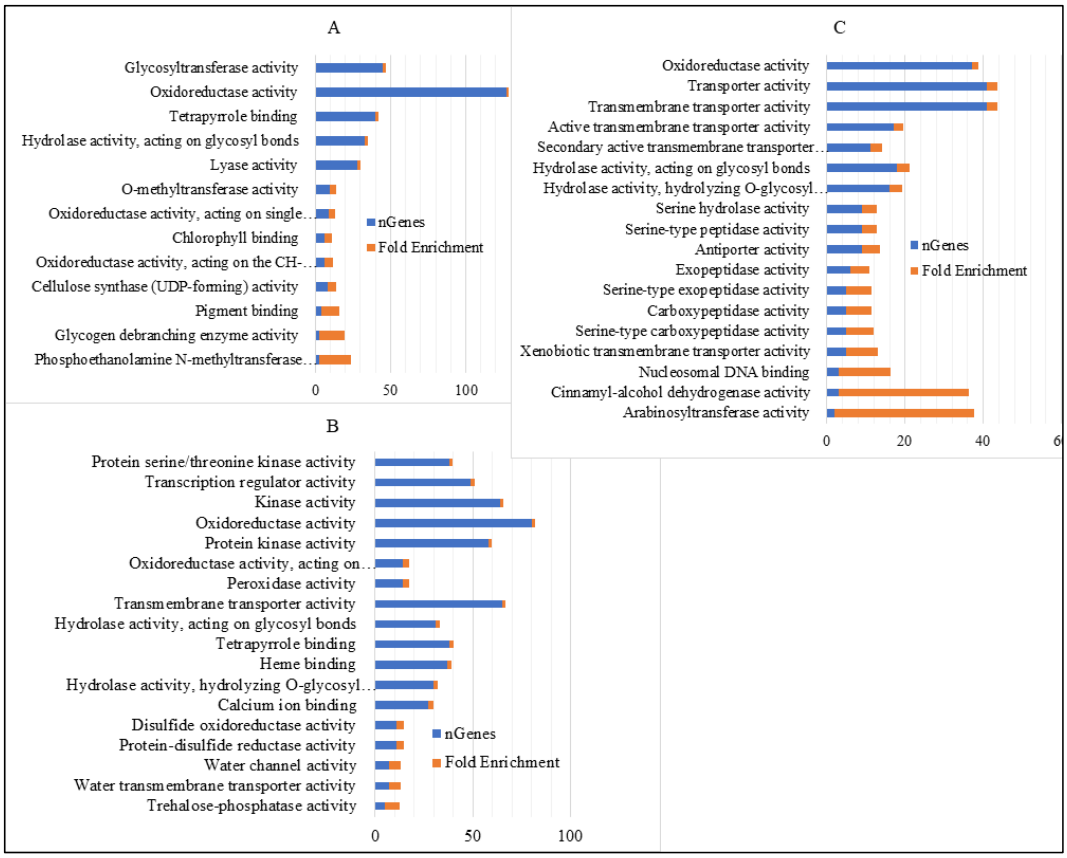

Figure 3-7. Significant GO:MF terms of DEGs between control and pathogen-treated SC599 (resistant) at 24 and 48.

(A) Downregulated DEGs at 24 hpi; (B) Upregulated DEGs at 24 hpi; (C) Downregulated DEGs at 48 hpi. Y-axis = GO pathways, X-axis = Number of genes (Blue) and fold enrichment (orange).

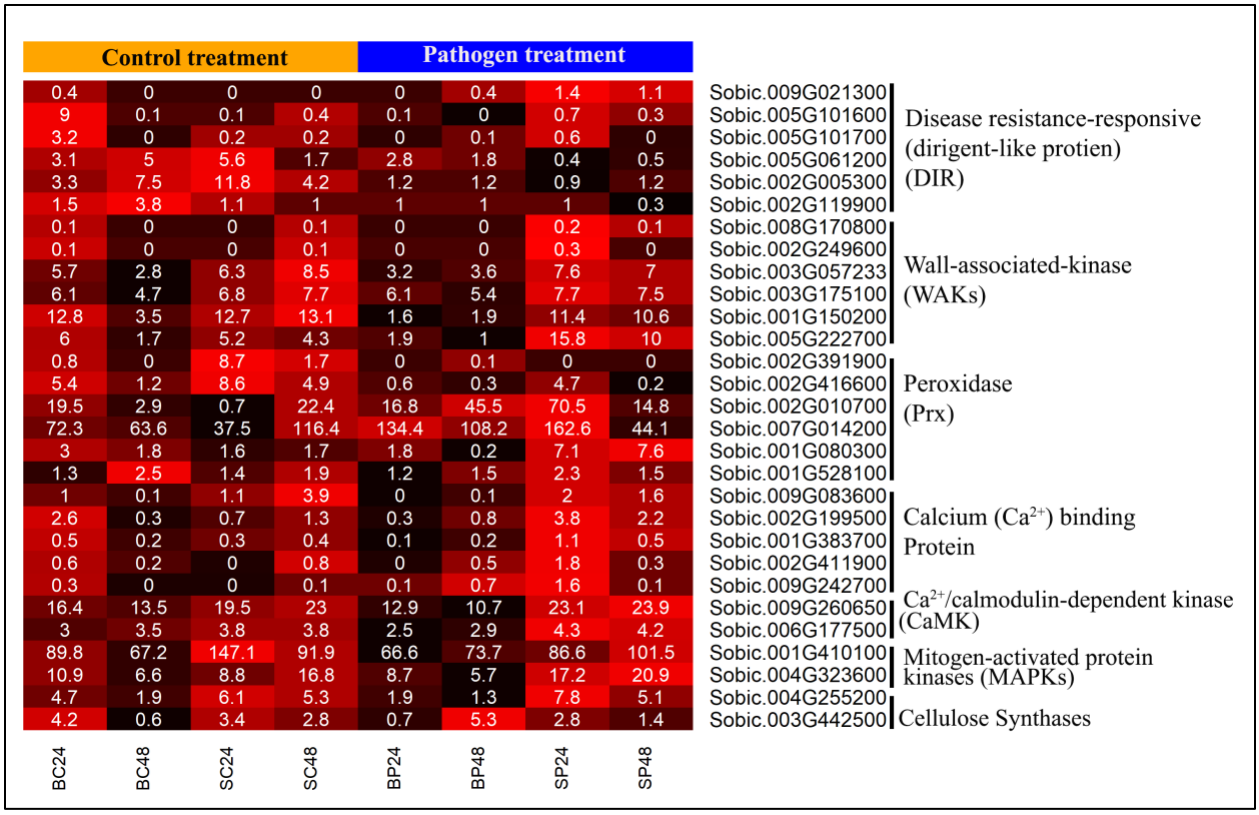

Figure 3-8. DEGs involved in the upstream cell wall and membrane perception signaling and defense.

Disease resistance-responsive (dirigent-like protein) protein (DIR), peroxidases, wall-associated-kinase-like-5 (WAKs), calcium-binding and calmodulin-like, calcium/calmodulin-dependent protein kinases (CaMK), cellulose synthase, and mitogen-activated protein kinase (MAPK) gene expression in BTx3042 and SC599 under control treatment (orange color bar on the heat map) and *F. thapsinum* (blue color bar on the heat map). Red color represents a high expression rank, while black represents the low expression rank of a transcript. *Sample Abbreviations*: *Genotypes*: B, BTx3042; S, SC599; *Treatments*: C, control; P, pathogen (*F. thapsinum*) treated; *Time*: 24 & 48, 24 & 48 hpi. BC24, BTx3042 control treated sampled at 24 hpi; Average of the three replications in fragments per kilobase of exon per million reads mapped (FPKM) values for each sample are included as text in the heat maps.

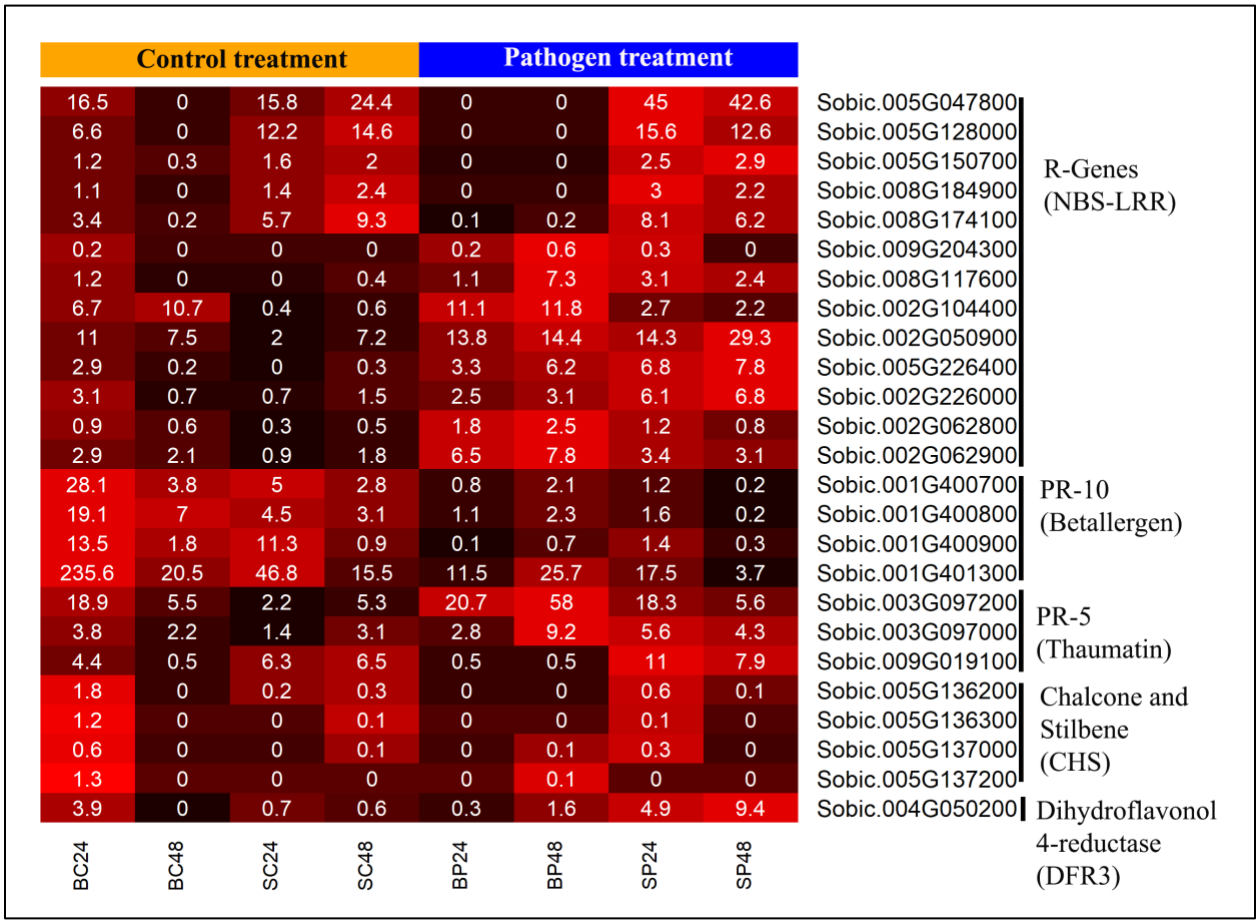

Figure 3-9. Differential expression of genes involved in the downstream signaling and defense.

R-genes (NBS-LRR), PR-10, PR5, chalcone, and stilbene (CHS) gene expression in BTx3042 and SC599 under control treatment (orange color bar on the heat map) and *F. thapsinum* (blue color bar on the heat map). Red color represents a high expression rank, while black represents the low expression rank of a transcript. *Sample Abbreviations*: *Genotypes*: B, BTx3042; S, SC599; *Treatments*: C, control; P, pathogen (*F. thapsinum*) treated; *Time*: 24 & 48, 24 & 48 hpi. BC24, BTx3042 control treated sampled at 24 hpi; Average of the three replications in fragments per kilobase of exon per million reads mapped (FPKM) values for each sample are included as text in the heat maps.

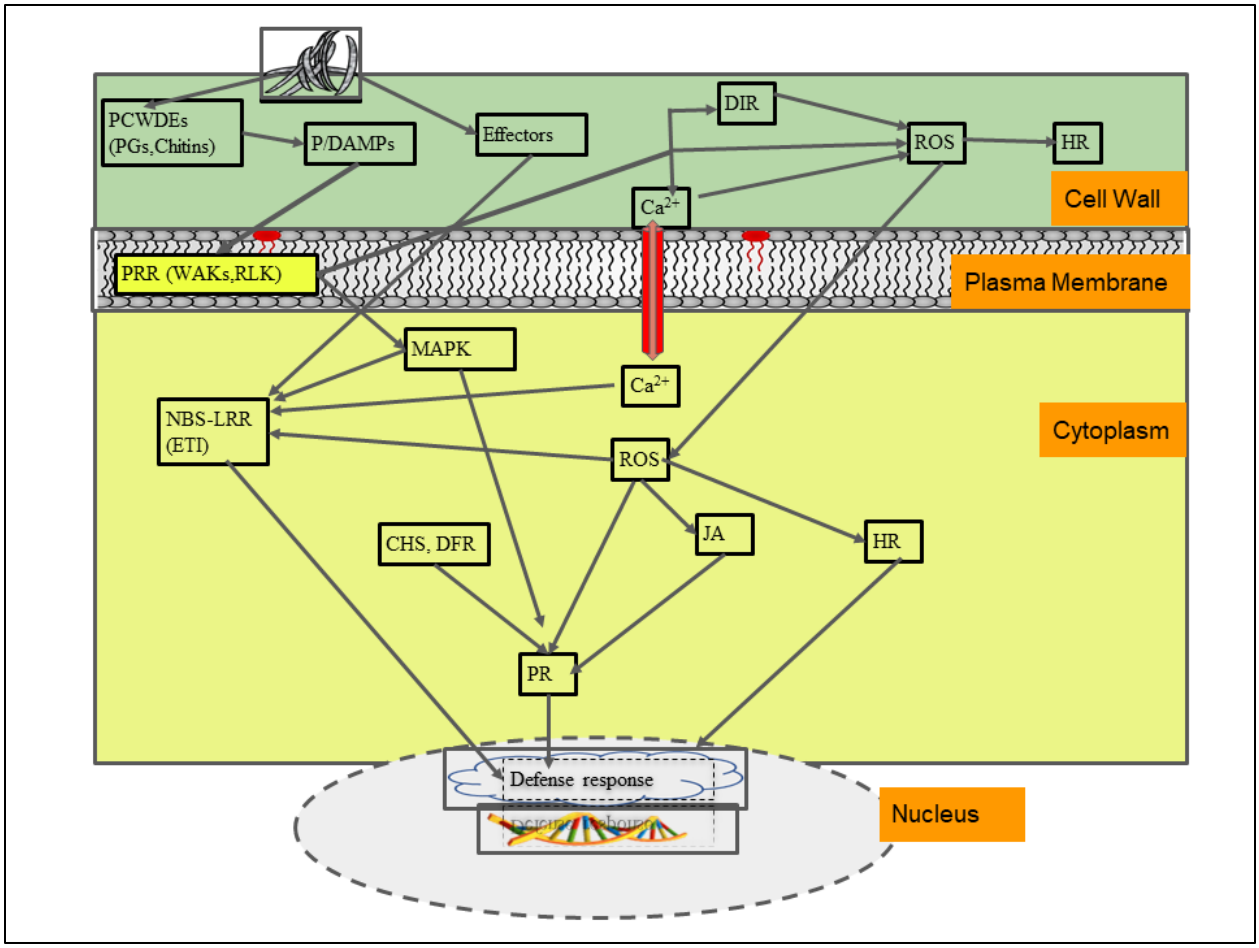

Figure 3-10. Hypothetical model of how sorghum plants defense mechanism against infection by the fungus *F. thapsinum*.

The model is split into three parts: perception, signaling, and defense response (Corwin & Kliebenstein, 2017). In the upstream perception step, the plant recognizes pathogen-associated molecular patterns (PAMPs) and damage-associated molecular patterns (DAMPs) through pattern recognition receptors (PRRs) like WAKs, and RLK in the cell wall and plasma membrane. The signaling step is performed by the mitogen-activated protein kinase (MAPK) cascade or the calcium signaling pathway. Finally, the downstream defense response step is directed by transcription factors and protein kinases, which activate specific defense responses such as pathogenesis-related proteins (PR), ROS production, detoxification, oxidative protection, and secondary metabolites like flavonoids, CHS, and DFR3.

Table 3.1. Summary of Significant DEGs between different treatments and comparison.

No	Comparison Code	Genotype	Constant Treatments (hpi)	Compared Treatments	Significant Genes	Up regulated	Down regulated	Filtered*	
								up	down
1	BC24-vs-BP24	BTx3042	24	Control vs. Pathogen	360	73	287	9	241
2	BC48-vs-BP48	BTx3042	48	Control vs. Pathogen	5006	2593	2413	932	930
3	SC24-vs-SP24	SC599	24	Control vs. Pathogen	6178	3065	3113	970	1008
4	SC48-vs-SP48	SC599	48	Control vs. Pathogen	1603	612	991	145	473
5	BP24-vs-SP24	Both	24, Pathogen	BTx3042 vs. SC599	4406	2105	2301	-	
6	BC24-vs-SC24	Both	24, Control	BTx3042 vs. SC599	2276	586	1690		
7	BP48-vs-SP48	Both	48, Pathogen	BTx3042 vs. SC599	5932	2600	3332		
8	BC48-vs-SC48	Both	48, Control	BTx3042 vs. SC599	4561	2163	2398		

* Filtered = Exclusive DEGs with LFC > |2| used for Gene ontology (GO) and Kyoto Encyclopedia of Genes and Genomes (KEGG) analysis; Code Key: B = BTx3042, S = SC599, C = control, P = *Fusarium thapsnium* hpi = 24 or 48 hours hpi. e.g., in BC24: B stands for BTx3042, C stands for control treatment, and 24 stands for 24 hpi, BC24 indicates control treated BTx3042 sampled at 24 hpi, BP24 indicates BTx3042 pathogen (*F.thapsinum*) treated, sampled at 24 hpi. SC24-vs-SP24 indicates control treated SC99 (S) at 24 hpi compared with SC599 pathogen treated at 24 hpi.

References

Adeyanju, A., Little, C., Yu, J., & Tesso, T. (2015). Genome-wide association study on resistance to stalk rot diseases in grain sorghum. G3: Genes, Genomes, Genetics, 5(6), 1165–1175. https://doi.org/10.1534/g3.114.016394

Adhikari, P., Mideros, S. X., & Jamann, T. M. (2021). Differential regulation of maize and sorghum orthologs in response to the fungal pathogen *Exserohilum turcicum*. Frontiers in Plant Science, 12. https://doi.org/10.3389/fpls.2021.675208

Agati, G., Azzarello, E., Pollastri, S., & Tattini, M. (2012). Flavonoids as antioxidants in plants: Location and functional significance. Plant Science: An International Journal of Experimental Plant Biology, 196, 67–76. https://doi.org/10.1016/J.PLANTSCI.2012.07.014

Bandara, Y. M. A. Y., Weerasooriya, D. K., Liu, S., & Little, C. R. (2018). The necrotrophic fungus *Macrophomina phaseolina* promotes charcoal rot susceptibility in grain sorghum through induced host cell-wall-degrading enzymes. Phytopathology, 108(8), 948–956. https://doi.org/10.1094/PHYTO-12-17-0404-R

Bandara, Y. M. A. Y., Weerasooriya, D. K., Tesso, T. T., & Little, C. R. (2017). Stalk rot diseases impact sweet sorghum biofuel traits. Bioenergy Research, 10(1), 26–35. https://doi.org/10.1007/S12155-016-9775-6/FIGURES/2

Basavaraju, P., Shetty, N. P., Shetty, S. H., De Neergaard, E., & Jørgensen, H. J. L. (2009). Infection biology and defense responses in sorghum against *Colletotrichum sublineolum*. Journal of Applied Microbiology, 107(2), 404–415. https://doi.org/10.1111/J.1365-2672.2009.04234.X

Beckman, C. H. (2000). Phenolic-storing cells: Keys to programmed cell death and periderm formation in wilt disease resistance and in general defense responses in plants. Physiological and Molecular Plant Pathology, 57(3), 101–110. https://doi.org/10.1006/PMPP.2000.0287

Bhavsar, B., Patel, M. I., & Kalaria, R. K. (2019). Molecular and in silico identification of chalcone synthase gene-2 (CHS-2) in sorghum (*Sorghum bicolor* L.) against anthracnose. International Journal of Chemical Studies, 7(4), 839–844.

Bianchet, C., Wong, A., Quaglia, M., Alqurashi, M., Gehring, C., Ntoukakis, V., & Pasqualini, S. (2019). An *Arabidopsis thaliana* leucine-rich repeat protein harbors an adenylyl cyclase catalytic center and affects responses to pathogens. Journal of Plant Physiology, 232, 12–22. https://doi.org/10.1016/J.JPLPH.2018.10.025

Boller, T., & Felix, G. (2009). A Renaissance of Elicitors: Perception of microbe-associated molecular patterns and danger signals by pattern-recognition receptors. Annual Review of Plant Biology, 60(1), 379–406. https://doi.org/10.1146/annurev.arplant.57.032905.105346

Boyes, D. C., Jaesung, N. *, & Dangl, J. L. (1998). The *Arabidopsis thaliana RPM1* disease resistance gene product is a peripheral plasma membrane protein that is degraded coincident with the hypersensitive response. Plant Biology, 95, 15849–15854.

Bramel-Cox, P. J., & Claflin, L. E. (1989). Selection for resistance to *Macrophomina phaseolina* and *Fusarium moniliforme* in sorghum. Crop Science, 29(6), 1468–1472. https://doi.org/10.2135/CROPSCI1989.0011183X002900060029X

Chalupska, D., Lee, H. Y., Faris, J. D., Evrard, A., Chalhoub, B., Haselkorn, R., & Gornicki, P. (2008). Acc homoeoloci and the evolution of wheat genomes. Proceedings of the National Academy of Sciences, 105(28), 9691-9696. https://doi.org/10.1073/pnas.080398110

Chittoor, J. M., Leach, J. E., & White, F. F. (1997). Differential induction of a peroxidase gene family during infection of rice by *Xanthomonas oryzae* pv. Oryzae. Molecular Plant-Microbe Interactions, 10(7), 861–871. https://doi.org/10.1094/MPMI.1997.10.7.861

Claflin, L. E., & Giorda, L. M. (2008). Stalk rots of sorghum. Sorghum and millets diseases, 185–190. https://doi.org/10.1002/9780470384923.ch33

Corwin, J. A., & Kliebenstein, D. J. (2017). Quantitative resistance: More than just perception of a pathogen. The Plant Cell, 29(4), 655. https://doi.org/10.1105/TPC.16.00915

Cui, Y., Chen, D., Jiang, Y., Xu, D., Balint-Kurti, P., & Stacey, G. (2021). Variation in gene expression between two sorghum bicolor lines differing in innate immunity response. Plants, 10(8). https://doi.org/10.3390/plants10081536

Dao, T. T. H., Linthorst, H. J. M., & Verpoorte, R. (2011). Chalcone synthase and its functions in plant resistance. Phytochemistry Reviews, 10(3), 397. https://doi.org/10.1007/S11101-011-9211-7

Das, I. K., Prabhakar, & Indira, S. (2008). Role of stalk-anatomy and yield parameters in development of charcoal rot caused by *Macrophomina phaseolina* in winter sorghum. Phytoparasitica, 36(2), 199–208. https://doi.org/10.1007/BF02981332

de Jesús-Pires, C., Ferreira-Neto, J. R. C., Pacifico Bezerra-Neto, J., Kido, E. A., de Oliveira Silva, R. L., Pandolfi, V., Wanderley-Nogueira, A. C., Binneck, E., da Costa, A. F., Pio-Ribeiro, G., Pereira-Andrade, G., Sittolin, I. M., Freire-Filho, F., & Benko-Iseppon, A. M. (2020). Plant Thaumatin-like proteins: Function, evolution and biotechnological applications. Current Protein & Peptide Science, 21(1), 36–51. https://doi.org/10.2174/1389203720666190318164905

de Sá, P. H. C. G., Guimarães, L. C., das Graças, D. A., de Oliveira Veras, A. A., Barh, D., Azevedo, V., da Costa da Silva, A. L., & Ramos, R. T. J. (2018). Next-generation sequencing and data analysis: Strategies, tools, pipelines and protocols. Omics Technologies and Bio-Engineering: Academic Press, 191–207. https://doi.org/10.1016/B978-0-12-804659-3.00011-7

Ding, L.-N., Li, T., Guo, X.-J., Li, M., Liu, X.-Y., Cao, J., & Tan, X.-L. (2021). *Sclerotinia* stem rot resistance in rapeseed: Recent Progress and Future Prospects. Journal of Agricultural and Food Chemistry, 69(10), 2965–2978. https://doi.org/10.1021/acs.jafc.0c07351

Dodds, P. N., & Rathjen, J. P. (2010). Plant immunity: Towards an integrated view of plant–pathogen interactions. Nature Reviews Genetics, 11(8). https://doi.org/10.1038/nrg2812

Engelsdorf, T., Gigli-Bisceglia, N., Veerabagu, M., McKenna, J. F., Vaahtera, L., Augstein, F., Van der Does, D., Zipfel, C., & Hamann, T. (2018). The plant cell wall integrity maintenance and immune signaling systems cooperate to control stress responses in

Arabidopsis thaliana. Science Signaling, 11(536). https://doi.org/10.1126/SCISIGNAL.AAO3070

Ferrari, S., Savatin, D., Sicilia, F., Gramegna, G., Cervone, F., & De Lorenzo, G. (2013). Oligogalacturonides: Plant damage-associated molecular patterns and regulators of growth and development. Frontiers in Plant Science, 4. https://www.frontiersin.org/articles/10.3389/fpls.2013.00049

Fracasso, A., Trindade, L. M., & Amaducci, S. (2016). Drought stress tolerance strategies revealed by RNA-Seq in two sorghum genotypes with contrasting WUE. BMC Plant Biology, 16(1), 1–18. https://doi.org/10.1186/s12870-016-0800-x

Fu, F., Girma, G., & Mengiste, T. (2020). Global mRNA and microRNA expression dynamics in response to anthracnose infection in sorghum. BMC Genomics, 21(1), 1–16. https://doi.org/10.1186/s12864-020-07138-0

Fukuoka, S., & Okuno, K. (2001). QTL analysis and mapping of *pi21*, a recessive gene for field resistance to rice blast in Japanese upland rice. Theoretical and Applied Genetics, 103(2), 185–190. https://doi.org/10.1007/s001220100611

Funnell-Harris, D. L., Sattler, S. E., O'Neill, P. M., Gries, T., Tetreault, H. M., & Clemente, T. E. (2019). Response of sorghum enhanced in monolignol biosynthesis to stalk rot pathogens. Plant Disease, 103(9), 2277–2287. https://doi.org/10.1094/PDIS-09-18-1622-RE

Garg, M. (2021). RNA sequencing. In Advances in Animal Genomics. Elsevier Inc. https://doi.org/10.1016/b978-0-12-820595-2.00005-9

Gechev, T. S., & Hille, J. (2005). Hydrogen peroxide as a signal controlling plant programmed cell death. The Journal of Cell Biology, 168(1), 17. https://doi.org/10.1083/JCB.200409170

Gelli, M., Duo, Y., Konda, A. R., Zhang, C., Holding, D., & Dweikat, I. (2014). Identification of differentially expressed genes between sorghum genotypes with contrasting nitrogen stress tolerance by genome-wide transcriptional profiling. BMC Genomics, 15(1), 1–16. https://doi.org/10.1186/1471-2164-15-179

Gelli, M., Konda, A. R., Liu, K., Zhang, C., Clemente, T. E., Holding, D. R., & Dweikat, I. M. (2017). Validation of QTL mapping and transcriptome profiling for identification of candidate genes associated with nitrogen stress tolerance in sorghum. BMC Plant Biology, 17(1), 1–18. https://doi.org/10.1186/s12870-017-1064-9

Gelli, M., Mitchell, S. E., Liu, K., Clemente, T. E., Weeks, D. P., Zhang, C., Holding, D. R., & Dweikat, I. M. (2016). Mapping QTLs and association of differentially expressed gene transcripts for multiple agronomic traits under different nitrogen levels in sorghum. BMC Plant Biology, 16(1). https://doi.org/10.1186/s12870-015-0696-x

Glazebrook, J. (2005). Contrasting mechanisms of defense against biotrophic and necrotrophic pathogens. Annual Review Phytopathology 43, 205–232. https://doi.org/10.1146/annurev.phyto.43.040204.135923

Govrin, E. M., & Levine, A. (2000). The hypersensitive response facilitates plant infection by the necrotrophic pathogen *Botrytis cinerea*. Current Biology, 10(13), 751–757. https://doi.org/10.1016/S0960-9822(00)00560-1

Gupta, A., Bhardwaj, M., & Tran, L.-S. P. (2020). Jasmonic acid at the crossroads of plant immunity and *Pseudomonas syringae* virulence. International Journal of Molecular Sciences, 21(20), 7482. https://doi.org/10.3390/ijms21207482

He, L., Du, C., Covaleda, L., Xu, Z., Robinson, A. F., Yu, J. Z., Kohel, R. J., & Zhang, H.-B. (2004). Cloning, characterization, and evolution of the NBS-LRR-encoding resistance gene analogue family in polyploid cotton (*Gossypium hirsutum* L.). Molecular Plant-Microbe Interactions, 17(11), 1234–1241. https://doi.org/10.1094/MPMI.2004.17.11.1234

Höfte, H., & Voxeur, A. (2017). Plant cell walls. Current Biology, 27(17), R865–R870. https://doi.org/10.1016/J.CUB.2017.05.025

Itoh, A., Schilmiller, A. L., McCaig, B. C., & Howe, G. A. (2002). Identification of a jasmonate-regulated allene oxide synthase that metabolizes 9-hydroperoxides of linoleic and linolenic acids. Journal of Biological Chemistry, 277(48), 46051–46058. https://doi.org/10.1074/jbc.M207234200

Jardine, D. J., & Leslie, J. F. (1992). Aggressiveness of *Gibberella fujikuroi* (*Fusarium moniliforme*) isolates to grain sorghum under greenhouse conditions. Plant Disease, 76(9), 897. https://doi.org/10.1094/pd-76-0897

Jemmat, A. M., Ranocha, P., Le Ru, A., Neel, M., Jauneau, A., Raggi, S., Ferrari, S., Burlat, V., & Dunand, C. (2020). Coordination of five class III peroxidase-encoding genes for early germination events of *Arabidopsis thaliana*. Plant Science, 298, 110565. https://doi.org/10.1016/J.PLANTSCI.2020.110565

Jones, J. D. G., & Dangl, J. L. (2006). The plant immune system. Nature, 444(7117). https://doi.org/10.1038/nature05286

Katilé, S. O., Perumal, R., Rooney, W. L., Prom, L. K., & Magill, C. W. (2010). Expression of pathogenesis-related protein PR-10 in sorghum floral tissues in response to inoculation with *Fusarium thapsinum* and *Curvularia lunata*. Molecular Plant Pathology, 11(1), 93–103. https://doi.org/10.1111/J.1364-3703.2009.00580.X

Kebede, A. Z., Johnston, A., Schneiderman, D., Bosnich, W., & Harris, L. J. (2018). Transcriptome profiling of two maize inbreds with distinct responses to *Gibberella* ear rot disease to identify candidate resistance genes. BMC Genomics, 19(1), 1–12. https://doi.org/10.1186/s12864-018-4513-4

Leslie, J. F. (1990). *Fusarium* spp. from corn, sorghum, and soybean fields in the central and eastern United States. Phytopathology, 80(4), 343. https://doi.org/10.1094/phyto-80-343

Leslie, J. F., Zeller, K. A., Lamprecht, S. C., Rheeder, J. P., & Marasas, W. F. O. (2005). Toxicity, pathogenicity, and genetic differentiation of five species of Fusarium from sorghum and millet. Phytopathology, 95(3), 275–283. https://doi.org/10.1094/PHYTO-95-0275

Li, Z., Huang, J., Wang, Z., Meng, F., Zhang, S., Wu, X., Zhang, Z., & Gao, Z. (2019). Overexpression of arabidopsis nucleotide-binding and leucine-rich repeat genes *RPS2* and *RPM1(D505V)* confers broad-spectrum disease resistance in rice. https://doi.org/10.3389/fpls.2019.00417

Liu, H., Du, Y., Chu, H., Shih, C. H., Wong, Y. W., Wang, M., Chu, I. K., Tao, Y., & Lo, C. (2010). Molecular dissection of the pathogen-inducible 3-deoxyanthocyanidin biosynthesis

pathway in sorghum. Plant & Cell Physiology, 51(7), 1173–1185. https://doi.org/10.1093/PCP/PCQ080

Liu, J. J., Sturrock, R., & Ekramoddoullah, A. K. M. (2010). The superfamily of thaumatin-like proteins: Its origin, evolution, and expression towards biological function. Plant Cell Reports, 29(5), 419–436. https://doi.org/10.1007/S00299-010-0826-8

Liu, W., Frick, M., Huel, R., Nykiforuk, C. L., Wang, X., Gaudet, D. A., Eudes, F., Conner, R. L., Kuzyk, A., Chen, Q., Kang, Z., & Laroche, A. (2014). The stripe rust resistance gene *Yr10* encodes an evolutionary-conserved and unique CC-NBS-LRR sequence in wheat. Molecular Plant, 7(12), 1740–1755. https://doi.org/10.1093/mp/ssu112

Lo, C., Coolbaugh, R. C., & Nicholson, R. L. (2002). Molecular characterization and in silico expression analysis of a chalcone synthase gene family in *Sorghum bicolor*. Physiological and Molecular Plant Pathology, 61(3), 179–188. https://doi.org/10.1006/PMPP.2002.0428

Lo, S. C. C., De Verdier, K., & Nicholson, R. L. (1999). Accumulation of 3-deoxyanthocyanidin phytoalexins and resistance to *Colletotrichum sublineolum* in sorghum. Physiological and Molecular Plant Pathology, 55(5), 263–273. https://doi.org/10.1006/PMPP.1999.0231

Lo, S. C. C., Hipskind, J. D., & Nicholson, R. L. (2007). cDNA cloning of a sorghum pathogenesis-related protein (PR-10) and differential expression of defense-related genes following inoculation with *Cochliobolus heterostrophus* or *Colletotrichum sublineolum*. Molecular Plant-Microbe Interactions, 12(6), 479–489. https://doi.org/10.1094/MPMI.1999.12.6.479

Lyons, R., Stiller, J., Powell, J., Rusu, A., Manners, J. M., & Kazan, K. (2015). *Fusarium oxysporum* triggers tissue-specific transcriptional reprogramming in *Arabidopsis thaliana*. PLoS ONE, 10(4). https://doi.org/10.1371/JOURNAL.PONE.0121902

Mace, E., Tai, S., Innes, D., Godwin, I., Hu, W., Campbell, B., Gilding, E., Cruickshank, A., Prentis, P., Wang, J., & Jordan, D. (2014). The plasticity of NBS resistance genes in sorghum is driven by multiple evolutionary processes. BMC Plant Biology, 14(1), 1–14. https://doi.org/10.1186/s12870-014-0253-z

Marla, S. R., Shiva, S., Welti, R., Liu, S., Burke, J. J., & Morris, G. P. (2017). Comparative transcriptome and lipidome analyses reveal molecular chilling responses in chilling-tolerant sorghums. The Plant Genome, 10(3), 1–16. https://doi.org/10.3835/plantgenome2017.03.0025

Marone, D., Russo, M. A., Laidò, G., De Leonardis, A. M., & Mastrangelo, A. M. (2013). Plant nucleotide binding site–leucine-rich repeat (NBS-LRR) genes: Active guardians in host defense responses. International Journal of Molecular Sciences, 14(4), 7302–7326. https://doi.org/10.3390/ijms14047302

Matić, S., Garibaldi, A., & Gullino, M. L. (2021). Combined and single effects of elevated CO_2 and temperatures on rice bakanae disease under controlled conditions in phytotrons. Plant Pathology, 70(4), 815–826. https://doi.org/10.1111/PPA.13338

McCormick, R. F., Truong, S. K., Sreedasyam, A., Jenkins, J., Shu, S., Sims, D., Kennedy, M., Amirebrahimi, M., Weers, B. D., McKinley, B., Mattison, A., Morishige, D. T., Grimwood, J., Schmutz, J., & Mullet, J. E. (2018). The *Sorghum bicolor* reference genome: Improved assembly, gene annotations, a transcriptome atlas, and signatures of genome organization. Plant Journal, 93(2), 338–354. https://doi.org/10.1111/tpj.13781

Mchale, L., Tan, X., Koehl, P., & Michelmore, R. W. (2006). Plant NBS-LRR proteins: Adaptable guards. Genome Biology, 7, 212. https://doi.org/10.1186/gb-2006-7-4-212

Miedes, E., Vanholme, R., Boerjan, W., & Molina, A. (2014). The role of the secondary cell wall in plant resistance to pathogens. Frontiers in Plant Science, 5. https://www.frontiersin.org/articles/10.3389/fpls.2014.00358

Mierziak, J., Kostyn, K., & Kulma, A. (2014). Flavonoids as important molecules of plant interactions with the environment. Molecules, 19(10), 16240. https://doi.org/10.3390/MOLECULES191016240

Monaghan, J., & Zipfel, C. (2012). Plant pattern recognition receptor complexes at the plasma membrane. Current Opinion in Plant Biology, 15(4), 349–357. https://doi.org/10.1016/j.pbi.2012.05.006

Natarajan, P., Ahn, E., Reddy, U. K., Perumal, R., Prom, L. K., & Magill, C. (2021). RNA-sequencing in resistant (QL3) and susceptible (Theis) sorghum cultivars inoculated with johnsongrass isolates of *Colletotrichum sublineola*. Frontiers in Genetics, 12. https://doi.org/10.3389/fgene.2021.722519

Nicaise, V., Roux, M., & Zipfel, C. (2009). Recent advances in PAMP-triggered immunity against bacteria: Pattern recognition receptors watch over and raise the alarm. Plant Physiology, 150(4), 1638–1647. https://doi.org/10.1104/pp.109.139709

Nida, H., Lee, S., Li, Y., & Mengiste, T. (2021). Transcriptome analysis of early stages of sorghum grain mold disease reveals defense regulators and metabolic pathways associated with resistance. BMC Genomics, 22(1), 1–17. https://doi.org/10.1186/s12864-021-07609-y

Niks, R. E., Qi, X., & Marcel, T. C. (2015). Quantitative resistance to biotrophic filamentous plant pathogens: Concepts, misconceptions, and mechanisms. Annual Review of Phytopathology, 53, 445–470. https://doi.org/10.1146/ANNUREV-PHYTO-080614-115928

Nishimura, N., Hitomi, K., Arvai, A. S., Rambo, R. P., Hitomi, C., Cutler, S. R., Schroeder, J. I., & Getzoff, E. D. (2009). Structural Mechanism of abscisic acid binding and signaling by dimeric *PYR1*. Science, 326(5958), 1373. https://doi.org/10.1126/SCIENCE.1181829

Pandian, B. A., Sathishraj, R., Djanaguiraman, M., Prasad, P. V. V., & Jugulam, M. (2020). Role of cytochrome P450 enzymes in plant stress response. Antioxidants, 9(5), 454. https://doi.org/10.3390/antiox9050454

Paniagua, C., Bilkova, A., Jackson, P., Dabravolski, S., Riber, W., Didi, V., Houser, J., Gigli-Bisceglia, N., Wimmerova, M., Budínská, E., Hamann, T., & Hejatko, J. (2017). Dirigent proteins in plants: Modulating cell wall metabolism during abiotic and biotic stress exposure. Journal of Experimental Botany, 68(13), 3287–3301. https://doi.org/10.1093/JXB/ERX141

Pant, S., & Huang, Y. (2021). Elevated production of reactive oxygen species is related to host plant resistance to sugarcane aphid in sorghum. Plant Signaling & Behavior, 16(2). https://doi.org/10.1080/15592324.2020.1849523

Pfeiffer, B. K., Pietsch, D., Schnell, R. W., & Rooney, W. L. (2019). Long-term selection in hybrid sorghum breeding programs. Crop Science, 59(1), 150–164. https://doi.org/10.2135/CROPSCI2018.05.0345

Pieterse, C. M. J., Van der Does, D., Zamioudis, C., Leon-Reyes, A., & Van Wees, S. C. M. (2012). Hormonal modulation of plant immunity. Annual Review of Cell and Developmental Biology, 28(1), 489–521. https://doi.org/10.1146/annurev-cellbio-092910-154055

Poland, J. A., Balint-Kurti, P. J., Wisser, R. J., Pratt, R. C., & Nelson, R. J. (2009). Shades of gray: The world of quantitative disease resistance. Trends in Plant Science, 14(1), 21–29. https://doi.org/10.1016/J.TPLANTS.2008.10.006

Radauer, C., Lackner, P., & Breiteneder, H. (2008). The Bet v 1 fold: An ancient, versatile scaffold for binding of large, hydrophobic ligands. BMC Evolutionary Biology, 8(1). https://doi.org/10.1186/1471-2148-8-286

Rajewski, J. F., & Francis, C. A. (1991). Defoliation effects on grain fill, stalk rot, and lodging of grain sorghum. Crop Science, 31(2), 353-359. https://doi.org/10.2135/cropsci1991.0011183X003100020026x

Rinerson, C. I., Rabara, R. C., Tripathi, P., Shen, Q. J., & Rushton, P. J. (2015). The evolution of WRKY transcription factors. BMC Plant Biology, 15(1). https://doi.org/10.1186/S12870-015-0456-Y

Robles-Barrios, F., Ramírez-Granillo, A., Medina-Canales, M. G., Gómez-Lim, M., Loske, A. M., Rodríguez-Tovar, A. V., & Pérez, N. O. (2022). *Fusarium temperatum* shows a hemibiotrophic infection process and differential pathogenicity over different maize breeds from Mexico. Journal of Phytopathology, 170(1), 21–33. https://doi.org/10.1111/JPH.13052

Roux, F., Voisin, D., Badet, T., Balagué, C., Barlet, X., Huard-Chauveau, C., Roby, D., & Raffaele, S. (2014). Resistance to phytopathogens e tutti quanti: Placing plant quantitative disease resistance on the map. Molecular Plant Pathology, 15(5), 427–432. https://doi.org/10.1111/MPP.12138

Santiago, J., Dupeux, F., Round, A., Antoni, R., Park, S. Y., Jamin, M., Cutler, S. R., Rodriguez, P. L., & Márquez, J. A. (2009). The abscisic acid receptor *PYR1* in complex with abscisic acid. Nature, 462(7273), 665–668. https://doi.org/10.1038/NATURE08591

Santiago, J., Rodrigues, A., Saez, A., Rubio, S., Antoni, R., Dupeux, F., Park, S. Y., Márquez, J. A., Cutler, S. R., & Rodriguez, P. L. (2009). Modulation of drought resistance by the abscisic acid receptor *PYL5* through inhibition of clade A PP2Cs. Plant Journal, 60(4), 575–588. https://doi.org/10.1111/J.1365-313X.2009.03981.X

Scully, E. D., Donze-Reiner, T., Wang, H., Eickhoff, T. E., Baxendale, F., Twigg, P., Kovacs, F., Heng-Moss, T., Sattler, S. E., & Sarath, G. (2016). Identification of an orthologous clade of peroxidases that respond to feeding by greenbugs (*Schizaphis graminum*) in C4 grasses. Functional Plant Biology, 43(12), 1134–1148. https://doi.org/10.1071/FP16104

Serba, D. D., Meng, X., Schnable, J., Bashir, E., Michaud, J. P., Vara Prasad, P. V., & Perumal, R. (2021). Comparative transcriptome analysis reveals genetic mechanisms of sugarcane aphid resistance in grain sorghum. International Journal of Molecular Sciences, 22(13). https://doi.org/10.3390/ijms22137129

Sharma, I., Kumari, N., & Sharma, V. (2014). Defense gene expression in *Sorghum bicolor* against *Macrophomina phaseolina* in leaves and roots of susceptible and resistant cultivars. Journal of Plant Interactions, 9(1), 315–323. https://doi.org/10.1080/17429145.2013.832425

Shetty, N. P., Jørgensen, H. J. L., Jensen, J. D., Collinge, D. B., & Shetty, H. S. (2008). Roles of reactive oxygen species in interactions between plants and pathogens. European Journal of Plant Pathology, 121(3), 267–280. https://doi.org/10.1007/S10658-008-9302-5/FIGURES/2

Singh, H., Kaur, J., Bala, R., Srivastava, P., Sharma, A., Grover, G., Dhillon, G. S., Singh, R. P., Chhuneja, P., & Bains, N. S. (2022). Residual effect of defeated stripe rust resistance genes/QTLs in bread wheat against prevalent pathotypes of *Puccinia striiformis* f. sp. *tritici*. PLoS ONE, 17(4), e0266482. https://doi.org/10.1371/journal.pone.0266482

Sinha, M., Singh, R. P., Kushwaha, G. S., Iqbal, N., Singh, A., Kaushik, S., Kaur, P., Sharma, S., & Singh, T. P. (2014). Current overview of allergens of plant pathogenesis related protein families. The Scientific World Journal, 2014. https://doi.org/10.1155/2014/543195

Smith, C. W., & Frederiksen, R. A. (2000). Sorghum: Origin, history, technology, and production. Wiley.

Springob, K., Nakajima, J. I., Yamazaki, M., & Saito, K. (2003). Recent advances in the biosynthesis and accumulation of anthocyanins. Natural Product Reports, 20(3), 288–303. https://doi.org/10.1039/B109542K

St. Clair, D. A. (2010). Quantitative disease resistance and quantitative resistance loci in breeding. Annual Review of Phytopathology, 48(1), 247–268. https://doi.org/10.1146/annurev-phyto-080508-081904

Sultana, M. M., Hachiya, T., Dutta, A. K., Nishimura, K., Suzuki, T., Tanaka, A., & Nakagawa, T. (2020). Expression analysis of genes encoding malectin-like domain (MLD)- and leucine-rich repeat (LRR)- containing proteins in *Arabidopsis thaliana*. Bioscience, Biotechnology, and Biochemistry, 84(1), 154–158. https://doi.org/10.1080/09168451.2019.1661769

Tena, G., Boudsocq, M., & Sheen, J. (2011). Protein kinase signaling networks in plant innate immunity. Current Opinion in Plant Biology, 14(5), 519–529. https://doi.org/10.1016/j.pbi.2011.05.006

Tesso, T. T., Claflin, L. E., & Tuinstra, M. R. (2004). Estimation of combining ability for resistance to Fusarium stalk rot in grain sorghum. Crop Science, 44(4), 1195–1199. https://doi.org/10.2135/cropsci2004.1195

Tesso, T. T., Ochanda, N., Little, C. R., Claflin, L., & Tuinstra, M. R. (2010). Analysis of host plant resistance to multiple *Fusarium* species associated with stalk rot disease in sorghum [*Sorghum bicolor* (L.) Moench]. Field Crops Research, 118(2), 177–182. https://doi.org/10.1016/j.fcr.2010.05.010

Treutter, D. (2005). Significance of flavonoids in plant resistance and enhancement of their biosynthesis. Plant Biology, 7(6), 581–591. https://doi.org/10.1055/S-2005-873009

Valério, L., De Meyer, M., Penel, C., & Dunand, C. (2004). Expression analysis of the Arabidopsis peroxidase multigenic family. Phytochemistry, 65(10), 1331–1342. https://doi.org/10.1016/J.PHYTOCHEM.2004.04.017

Wang, Z., Ma, L.-Y., Cao, J., Li, Y.-L., Ding, L.-N., Zhu, K.-M., Yang, Y.-H., & Tan, X.-L. (2019). Recent advances in mechanisms of plant defense to *Sclerotinia sclerotiorum*. Frontiers in Plant Science, 10. https://www.frontiersin.org/articles/10.3389/fpls.2019.01314

Wolf, S. (2017). Plant cell wall signaling and receptor-like kinases. The Biochemical Journal, 474(4), 471–492. https://doi.org/10.1042/BCJ20160238

Yahaya, M. A., & Shimelis, H. (2022). Drought stress in sorghum: Mitigation strategies, breeding methods and technologies—A review. Journal of Agronomy and Crop Science, 208(2), 127–142. https://doi.org/10.1111/jac.12573

Yang, J., Duan, G., Li, C., Liu, L., Han, G., Zhang, Y., & Wang, C. (2019). The crosstalks between jasmonic acid and other plant hormone signaling highlight the involvement of jasmonic acid as a core component in plant response to biotic and abiotic stresses. Frontiers in Plant Science, 10. https://www.frontiersin.org/articles/10.3389/fpls.2019.01349

Yang, Q., Balint-Kurti, P., & Xu, M. (2017). Quantitative disease resistance: dissection and adoption in maize. Molecular Plant, 10(3), 402–413. https://doi.org/10.1016/j.molp.2017.02.004

Yang, Q., Van Haute, M., Korth, N., Sattler, S. E., Toy, J., Rose, D. J., Schnable, J. C., & Benson, A. K. (2022). Genetic analysis of seed traits in *Sorghum bicolor* that affect the human gut microbiome. Nature Communications 2022 13:1, 13(1), 1–15. https://doi.org/10.1038/s41467-022-33419-1

Yang, X., & Wang, J. (2016). Genome-wide analysis of NBS-LRR genes in sorghum genome revealed several events contributing to NBS-LRR gene evolution in grass species. Evolutionary Bioinformatics, 12(9). https://doi.org/10.4137/EBO.S36433

Yu, C. K. Y., Springob, K., Schmidt, J., Nicholson, R. L., Chu, I. K., Wing, K. Y., & Lo, C. (2005). A Stilbene synthase gene (*SbSTS1*) is involved in host and nonhost defense responses in sorghum. Plant Physiology, 138(1), 393. https://doi.org/10.1104/PP.105.059337

Zhang, W., Zhao, F., Jiang, L., Chen, C., Wu, L., & Liu, Z. (2018). Different pathogen defense strategies in arabidopsis: More than pathogen recognition. Cells, 7(12). https://doi.org/10.3390/CELLS7120252

Zhang, Y., Lubberstedt, T., & Xu, M. (2013). The genetic and molecular basis of plant resistance to pathogens. Journal of Genetics and Genomics, 40(1), 23–35. https://doi.org/10.1016/j.jgg.2012.11.003

Zuo, W., Chao, Q., Zhang, N., Ye, J., Tan, G., Li, B., Xing, Y., Zhang, B., Liu, H., Fengler, K. A., Zhao, J., Zhao, X., Chen, Y., Lai, J., Yan, J., & Xu, M. (2015). A maize wall-associated kinase confers quantitative resistance to head smut. Nature Genetics, 47(2). https://doi.org/10.1038/ng.3170

CHAPTER 4 – GENETIC ANALYSIS BASED ON COMBINING ABILITY, CHARACTER ASSOCIATION AND HERITABLITY OF QUANTITATIVE TRAITS ASSOCIATED WITH FUSARIUM STALK ROT IN GRAIN SORGHUM (*Sorghum bicolor*)

4.1 Abstract

Stalks rot diseases are among the top biotic stressors affecting dryland sorghum production in the United States. A number of fungal pathogens are implicated with stalk rot diseases; the most important ones, however, are Fusarium stalk rot caused by various *Fusarium* spp and charcoal rot caused by *Macrophomina phaseolina.* This study aimed to evaluate the combining ability of stalk rot resistant and susceptible lines for various agronomic and stalk resistance parameters. Sixty-one lines were selected from the recombinant inbred line (RIL) of the BTx3042 (susceptible) × SC599 (resistant) developed for mapping a stalk rot resistance. They were crossed with three seed parents to generate 183 F_1 hybrids. The hybrids and 64 inbred parents were grown in an alpha lattice incomplete block design in three replications at two locations in Kansas during the 2019 and 2021 crop seasons. Data were collected on days to flowering, plant height, major lesion length, total lesion length, number of diseased nodes, grain yield, and stalk lodging. Mean squares due to entry, inbred, hybrid, and its components were significant for all traits. Lodging had a negative significant genotypic correlation with plant height and disease traits. Grain yield had a negative genotypic correlation with all disease traits and lodging in the hybrids and parents. The general and specific combing abilities were significant for disease parameters and yield.

Keys words*: Sorghum; General combining ability; Specific combining ability; Variance component*

4.2 Introduction

Sorghum is the world's fifth most widely cultivated cereal, primarily for human and animal consumption. In 2022, 58.03 million tons of sorghum was produced from 40 million hectares worldwide, with an average productivity of 1.6 t/ha (FAO, 2023). The US is the world's largest grain sorghum producer, with a total grain volume of 478.47 million tons harvested from 1.85 million hectares in 2022 (USDA, 2022). Kansas is the leading sorghum producer accounting for 56% of the national production, 59.1% of the area harvested (USDA, 2022). However, due to the severe drought, harvested acreage, total production, and productivity were significantly reduced in 2022 compared to 2020 and 2021 (USDA, 2022). The higher productivity of sorghum in the developed world seems to be largely due to adoption of hybrid technology and improved agronomic management. The genetic improvement in US sorghum was reported to have contributed more than 60% to the overall yield increases (Pfeiffer et al., 2019). Commercial hybrids using cytoplasmic male sterility have increased yield by 0.121 t/ha every year since the 1950s (Pfeiffer et al., 2019).

Sorghum is valued for its versatility and drought tolerance, making it a popular choice for farmers in Kansas, where drought is the major limitation to crop production (Carcedo et al., 2022). Sorghum is used for animal feed, ethanol production, and human consumption, among other applications (Duff et al., 2019). The economic impact of sorghum in Kansas is significant; it generates income for farmers, supports jobs in the agricultural industry, and contributes to the state's overall economy (Duff et al., 2019; O'Brien, 2019). However, this vital crop is affected by several factors, such as drought and associated biotic stresses, mainly stalk rot diseases. The disease causes significant damage to sorghum crop, reducing yield and quality, which in most

years go unnoticed (Jardine, 2006; Tesso et al., 2010, 2012). Infected plants become more susceptible to lodging, reducing yield and making harvest more difficult (Tesso et al., 2012). Despite higher genetic gains in the hybrid improvement, the yield loss through lodging in susceptible hybrids has been significant. Yield loss due to lodging can be as high as 60%, and no hybrid immune to stalk rot has been reported (Jardine, 2006). Both stalk strength and stalk rot incidence appear to be primarily influenced by genetics, so deliberate selection for these traits can reduce yield losses due to lodging.

Sorghum harbors rich genetic variability for almost every trait. Studying these variations and their use in breeding programs can lead to developing cultivars enhanced for the traits of interest. However, information on the performance of lines carrying traits of interest is necessary for devising a sound breeding method for their transfer or for direct use as hybrid parents.

Earlier studies have evaluated the combining ability of genotypes in an effort to understand the resistance mechanisms of the traits. Common agronomic parameters such as days to flowering, plant height, grain yield, and yield components have been evaluated in sorghum (Kenga et al., 2004; Tadesse et al., 2008; Makanda et al., 2010; Pfeiffer et al., 2010; Massaoudou et al., 2016; Pfeiffer et al., 2019; Bunphan et al., 2015; Mohammed et al., 2015; Mengistu et al., 2020; Maulana et al., 2021). However, only a few such studies on stalk rot were reported (Tesso et al., 2004, 2005). In the current study, we are interested in evaluating the combining ability of lines from the BTx3042 x SC599 recombinant inbred population selected based on their reaction to *F. thapsinum* infection. Field evaluation of the population revealed that a handful of the segregates had remarkably higher resistance than the resistant parent and were also superior in agronomic values. Documentation of combining ability on these superior lines is of value to the sorghum research

community interested in addressing this problem. Therefore, the objective of this study is to determine the mode of inheritance of stalk rot resistance and related agronomic traits in the selected set of recombinant inbred lines exhibiting resistance to *F. thapsinum* when evaluated as inbred per se. We hope the study will generate information on the value of the materials as breeding parents and also provide clues on designing a breeding scheme for transferring the resistance traits from these sources.

4.3 Materials and Methods

4.3.3 Genetic materials and mating design

A recombinant inbred line (RIL) population was developed between a stalk rot resistant line, SC599, and a susceptible line, BTx3042. The population was meant for mapping stalk rot resistance and other traits for which the two parents contrast. The F_8 population of the RIL consisting of 233 entries was evaluated for resistance against *F. thapsinum* on replicated plots in multiple seasons. Data were collected for stalk rot reaction, and the analysis of the results showed a handful of materials exhibiting remarkable resistance to the pathogen. The top 23 lines, along with 16 susceptible lines and 22 intermediates, were pooled and crossed to three seed parents, ARCH1105A, ATx623, and AOK11, using the design II mating scheme. A total of sixty-one RILs were included in the cross resulting in 183 hybrids. A total of 247 entries, comprised of the hybrids and the inbreds, were evaluated in four environments during the 2019 and 2021 main seasons.

4.3.4 Experimental design and field procedure

The entries were planted in two-row plots in alpha lattice design with three replications and four incomplete blocks. The same design and field procedure was used in all four environments,

Manhattan and Hays, in the 2019 and 2021 seasons. Fertilization and pre-plant weed control were applied as recommended. The field was closely supervised, and post-emergence weeds were manually removed as necessary. At flowering, six plants at uniform stages of development in each plot were tagged with two distinct tapes (three for each tape) for later inoculation.

Parallel to the fieldwork, preparation for pathogen inoculation continued in the laboratory. The pure culture of *F. thapsinum* was obtained from the Row Crop Pathology Laboratory, Kansas State University. The culture was grown on potato dextrose Agar to initiate inoculum suspension for field inoculation. Inoculum suspension was initiated by placing two pieces of approximately one square centimeter of the agar cultured pathogen into a liquid nutrient suspension potato dextrose broth in a 250ml flask. The suspension was then placed on a slow-moving orbital shaker and incubated at room temperature for three days. The inoculum suspension was then strained through multiple layers of KenAG non-gauze milk filters to separate the conidial suspension from the mycelial mass. A manual count under a microscope using a hemacytometer determined the number of conidia in the suspension. The inoculum was then adjusted to $5x10^4$ conidia ml^{-1} by diluting it with a PBS solution and kept on ice while transporting it to the field for inoculation. Field inoculation was performed 14 days after flowering. Three plants tagged with similar tape were injected with the inoculum suspension. The inoculum was administered to the basal stalks approximately 10 cm above the ground using a modified syringe and needle. The remaining three plants in a plot were inoculated with PBS solution as a control. On day 28 after inoculation, the plants were harvested by cutting at the base for disease scoring. Disease severity was scored using the procedure described in Tesso et al. (2009).

4.3.5 Data collection

Fusarium stalk rot disease was scored based on three disease parameters: total lesion length (TLL), major lesion length (MLL), and the number of diseased nodes (NDN). The disease scoring was done by splitting the stalks longitudinally through the points of inoculation up and down, and the length of the visible lesion was measured. Total lesion length (cm) was measured as the entire length of the visible lesion in the pith of the stalk, while major lesion length (cm) was measured as the length of the uninterrupted lesion on both sides of the inoculation site. In addition, phenotypic data were collected on days to flowering (DTF), plant height (PHT), grain yield (YLD), and lodging (LDG). Days to flowering was recorded as the number of days between planting and half-bloom. Plant height was measured as the total length of a mature plant from the base to the tip of the panicle. Grain yield was the weight of the kernels harvested at maturity from each plot expressed in tons per hectare. Lodging was scored using a scale of 1-5, where "1" represents complete resistance and "5" complete lodging.

4.3.6 Statistical analysis

The analysis of variance (ANOVA) was conducted using a PROC MIXED procedure in SAS (version 9.4). Factorial ANOVA (design II) was carried out using the procedure outlined by Bernardo (2010), where both parents and their crosses were considered as fixed effects while the environments and the replicated were treated as random effects. The total entry effect was partitioned into inbred and hybrid effects, and those were further partitioned into male, female components for the inbreds, and into male, female and male × female interaction components for the hybrids. The ANOVA also provided the interaction of each of these components with the environment. The significance of each component was tested using the appropriate tester assigned

using the test option in SAS. Significant means were separated using LSD method. The male and female effects represented the general combining ability (GCA) effect for male and female parents, respectively, while the female × male interaction effect represented the specific combining ability (SCA) effect for the hybrids in all the traits. The GCA estimates for each of the male and female parents were calculated as the difference between the marginal means of the parents and that of the grand mean of all the crosses. The significance of individual GCA was determined using a two-tailed t-test described by Cox and Fery (1984). The genotypic correlation coefficients were analyzed using PROC MIXED procedure in SAS (version 9.4) based on the formula provided by Dabholkar (1999).

Genotypic correlation coefficients were calculated using the formula:

$$r_{g_{xy}} = (Cov_{g_{xy}}) / \sqrt{\sigma^2_{g_x} \sigma^2_{g_y}}$$

Where: r_{gxy}= genotypic correlation coefficient between character *x* and *y*; Cov_{gxy}= genotypic covariance between character *x* and y; σ^2_{gx} = genotypic variance for character *x*; σ^2_{gy} = genotypic variance for character *y*

The coefficients of correlations at genotypic levels were tested for their significance by the formula described by Robertson (1959) as indicated below:

$t = r_{gxy} / SEr_{gxy}$, Where Ser_{gxy} = Standard error of genotypic correlation. The calculated "*t*" value was compared with the tabulated "*t*" value at (*n-2*) degree of freedom at 5% level of significance where *n* is the number of genotypes.

4.4 Results

4.4.7 Analysis of variance and mean performance of the genotypes for all traits

The across environment combined analysis of variance for all traits is presented in Table 4.1. The environment effect was highly significant for all traits indicating the variability across environments and the environment's impact on agronomic response and disease parameters. Similarly, the entry effect was highly significant for all agronomic and disease parameters measured, and further partitioning the entry effect into inbred and hybrid effects also showed that both components of the entry were highly significant for all parameters. However, the inbred vs. hybrid effect was significant only for plant height, number of diseased nodes, lodging, and grain yield. Partitioning the inbred effect into male and female components also showed a similar trend, except that the female effect was insignificant for total lesion length. The male vs. female effects were also significant except for days to flowering, major lesion length and the number of diseased nodes. Further partitioning the hybrid effect into male, female and male × female interaction effects showed that all components were highly significant for all traits. On the other hand, the interaction of the environment with the entry and its inbred and hybrid components was not significant, except the inbred vs. hybrid component for days to flowering and total lesion length were highly significant. The interaction of the environment with male and female components of the inbred as well as with the male vs. female component was not significant. Similarly, the interaction with male and male × female components of the hybrid was also not significant. However, the female-by-environment interaction effect was highly significant for days to flowering, total lesion length and grain yield (Table 4.1). The independent analysis of variance for the Manhattan and Hays locations showed similar results (Appendix B Tables B1 and B2).

Further analysis was carried out by splitting the environment into years and locations. A comparison of the mean performance of the inbreds and hybrids between years showed no significant difference for all traits (Table 4.1). However, there was a marked difference between inbreds and hybrids for days to flowering, plant height, and grain yield, where the hybrids were significantly larger than the inbreds. Disease parameters were slightly larger in the hybrids than in the inbreds. Disease severity was not significantly different between the two test seasons. On the other hand, agronomic characteristics, including grain yield, were higher at Manhattan for both inbred and hybrid entries. Disease parameters and lodging were slightly higher at Hays than in Manhattan, which was expected. However, the slightly longer days to flowering in the hybrids than the inbreds at both locations were not expected (Table 4.2).

Table 4.1. Mean squares of the combined analysis of variance for days to flowering, plant height, disease parameters, grain yield, and lodging for Manhattan and Hays in 2019 and 2021.

Source of variation	df	Mean Squares						
		DTF	PHT	MLL	TLL	NDN	LDG	GYLD
Environment (E)	3	12152***	56773***	57.8***	321.8***	36.7***	24.7***	124***
Block (E)	3	34.9	275.7	4.3	3.3	0.6	1.9	0.13
Entry	246	266.8***	5341.5***	100.1***	320.9***	20.4***	13.1***	13.9***
Inbred (I)	63	138.6***	5036.2***	94.4***	428.0***	6.2***	10.1***	5.2***
Male (M)	60	134.4***	4737.3***	98.1***	442.5***	6.3***	9.0***	4.8***
Female (F)	2	177.5***	3535.6**	10.5***	19.3	4.3**	24.2***	2.6***
M vs. F	120	228.0***	1749.2***	64.3***	185.6***	16.9***	5.6***	8.6***
Hybrid (H)	182	306.1***	4497.2***	99.8***	278.5***	24.2***	13.7***	15.6***
Male	60	314.8***	3276.3***	160.0***	445.5***	34.9***	6.0***	15.9***
Female	2	4834.3***	205979.9***	432.6***	920.7***	140.1***	733.4***	420.8***
M x F	120	228.0***	1749.2***	64.3***	185.6***	16.9***	5.6***	8.6***
I vs. H	1	1015.5	175981***	473.2	721.8	186.5***	74.2*	240***
Entry x E	738	26.66	80.1	4.1	13.3	0.4	0.1	0.1
Inbred x E	189	17.2	67.4	4.1	21.2	0.6	0.3	0.3
M x E	180	17.5	65.1	4.3	26.3	0.5	0.4	0.1
F x E	6	6.5	31.4	0.1	2.3	0.2	0.1	0.1
M vs. F x E	3	19.6	113.9	2.3	37.3	0.4	0.04	0.4
H x E	546	25.7	83.1	2.5	9.1	0.4	0	0.1
M x E	180	16.6	70.5	2.4	6.7	0.4	0.1	0.1
F x E	6	677.9***	582.2	21.6	148.8***	0.5	0.5	0.7**
M x F x E	360	19.14	81.6	2.2	8	0.3	0.1	0.1
I vs. H x E	3	786.5***	519.1	14.1	316.0***	0.05	1.5	1.0
Error	1959	30	204.9	7.5	37.4	1.31	0.6	0.2

[1]DTF = Days to flowering, PHT = Plant height (cm), MLL = Major lesion length (cm), TLL = Total lesion length (cm), NDN = Number of diseased nodes, YLD = Grain yield (t/ha) and LDG = Lodging (1-5). ***, **, * statistically significant at 0.001 0.005, and 0.01 levels of probability, respectively.

Table 4.2. Mean values of the locations and years of all traits for hybrids and inbreds.

Environment	[1]DTF		PHT		MLL		TLL		NDN		LDG		YLD	
	H	I	H	I	H	I	H	I	H	I	H	I	H	I
Year														
2019	62.1	61.8	122.8	105.1	6	5	13.6	11.9	3.8	3.2	2.7	2.4	2.9	2.4
2021	62.9	60.5	125.5	107.9	6.1	5.3	13.9	13.3	3.9	3.3	2.7	2.3	3	2.3
Mean	62.5	61.15	124.15	106.5	6.05	5.15	13.75	12.6	3.85	3.25	2.7	2.35	2.95	2.35
Location														
Hays	59.3	56.6	116.3	100.3	6.2	5.6	13.9	13.8	4	3.5	2.9	2.4	2.8	2.2
MHK	65.6	65.7	132	112.8	5.9	4.8	13.5	11.4	3.7	3.1	2.6	2.3	3.2	2.5
Mean	62.45	61.15	124.15	106.55	6.05	5.2	13.7	12.6	3.85	3.3	2.75	2.35	3	2.35

[1]DTF = Days to flowering, PHT = Plant height (cm), MLL = Major lesion length (cm), TLL = Total lesion length (cm), NDN = Number of diseased nodes, YLD = Grain yield (t/ha) and LDG = Lodging (1-5), MHK = Manhattan.

4.4.8 Genotypic Trait Correlation

Genotypic correlation reflects the underlying genetic basis of traits, and phenotypic correlation is influenced by a combination of genetic and environmental factors (Dabholkar, 1999). Thus, while two traits may be strongly genetically correlated, their phenotypic correlation may be weaker or non-existent if environmental factors obscure the relationship between them (Falconer, 1996).

In this study, the genotypic correlation analysis was carried out separately for the parents and hybrids; the results were presented in Table 4.3. The genotypic correlation between the traits for the parents and hybrids did not show a pattern, it was similar between certain traits and not in others. The only significant correlation among agronomic traits was between plant height and lodging in the parents(r=0.73) and the hybrids (0.79). All other associations between agronomic parameters were not significant.

Correlation with the disease traits, such as plant height vs. major lesion length and total lesion length, had a significant positive association in the parents. In addition, major lesion length was significantly correlated with total lesion length and lodging percentage in the parents. Similarly, plant height vs. lodging and major lesion length vs. total lesion length were correlated significantly in the hybrids.

Table 4.3. Genotypic correlation of parents (above the diagonal) and hybrids (below the diagonal) for the traits studied.

Traits	DTF	PHT	MLL	NDN	TLL	LDG	YLD
DTF		0.11	0.13	-0.15	0.13	-0.04	-0.02
PHT	0.11		0.83**	0.12	0.85**	0.73	0.07
MLL	0.08	0.09		0.37	0.88**	0.78**	-0.16
NDN	-0.15	0.26	0.46		0.39	0.28	-0.14
TLL	0.10	0.28	0.83**	0.52		0.75	-0.09
LDG	0.38	0.79**	0.19	0.25	0.30		-0.25
YLD	0.11	-0.17	0.14	-0.04	0.02	0.08	

DTF = Days to flowering, PHT = Plant height (cm), MLL = Major lesion length (cm), TLL = Total lesion length (cm), NDN = The number of diseased nodes, YLD = Grain yield (t/ha) and LDG = Lodging (1-5).

4.4.9 Combining ability

In Table 4.1, the hybrid effect was partitioned into male, female and the male and female interaction components. The male and female components represent the GCA effect for males and females, respectively, and the male × female component represents the SCA effect. From Table 4.1, the male and female GCA and SCA effects were highly significant for all traits. Among the males, the marginal mean for days to flowering ranged from as early as 55.6 days in the stalk rot resistant line RIL158 to 68 days in the intermediate line RIL37 (Table 4.4). Similarly, plant height ranged from 100 cm to 154 cm, lodging score ranged from 1.5 to 3.33, and grain yield from 1.5 to 4.13 t/ha. The total and major lesion length of disease traits ranged from 9.4 m in RIL220 and 2.93 cm in RIL73 to 15.03 to 25.9 cm both in RIL130. The mean number of diseased nodes ranged from 2.27 in RIL73 to 6.17 in RIL158. The range among the females was expected to be narrow for days to flowering, ranging from 59.49 in female line AOK11 to 64.06 in ARC1105A. Mean plant height ranged from 113.07 again in AOK11 to 143.54cm in Tx623. The minimum score for lodging was recorded in AOK11, while the highest in Tx623. Grain yield was the least (2.42 t/ha) in AOK11 and highest (3.84 t/ha) in ARC1105A (Table 4.4).

Of the total of 61 males included in the test hybrid synthesis, 29 had significant GCA for days to flowering, with the most significant positive GCA being 5.55 and 5.52 in RIL37 and RIL95, respectively. Negative and significant GCA of -6.15 and -5.67 was recorded in early maturing lines RIL26 and RIL113, respectively. For plant height, the highest positive GCA was 34.36, recorded in RIL87, followed by 21.11 in RIL113, while the highest negative GCA, -19.96 and -13.15, obtained in RIL161 and RIL207, respectively. GCA for lodging score based on the scale of 1-5 was significant for 40 of the 61 lines included in the test, with the highest negative GCA (lodging resistance) being -1.14 and the highest positive GCA of 0.70. For grain yield, the resistant line RIL213 had the highest positive GCA for yield, followed by RIL158. RIL213 also had among the highest negative GCA for disease parameters lodging, indicating that it combines multiple desirable traits. The lowest GCA for yield was obtained in RIL15. Most of the lines behaved according to their resistance designations for disease traits. Seventy-five percent of the resistant lines had negative GCA for all disease parameters, and 75% of the susceptible lines had positive GCA for the same parameters (Table 4.4). Among lines designated to have intermediate stalk rot reaction, 64% were shown to have negative GCA for major lesion length, 55% for total lesion length, and 50% for the number of nodes diseased. Overall, the highest negative GCA for total and major lesion length were -5.25 and -2.37 cm out of the overall mean of 13.74 and 6.08 cm, respectively. The highest negative GCA for the number of nodes diseased was -1.46. On the other hand, the highest and significant positive GCA was 12.45 cm, 9.18 cm for total and major lesion length, respectively, both in RIL 130 and 2.45 for the number of nodes diseased in RIL158 (Table 4.4). Among the female parents, AR1105 and Tx623 had positive and significant GCA for all traits except for plant height and number of diseased nodes that were negative and significant in AR1105 and negative nonsignificant for major lesion length and significant negative for grain

yield for Tx623. GCA for OK11 was negative and significant for all traits except number of diseased nodes (Table 4.4).

Heritability due to the male and female parents followed a similar trend with additive and dominance variances (data not shown). The broad sense heritability was higher for all traits except DTF and PHT due to higher environmental variances. The heritability due to the female parent was higher than that due to the male parent for days to flowering, plant height, lodging, and grain yield showing that the female parent had a greater influence on the expression of these traits. On the other hand, the heritability of disease parameters was higher in the males.

Table 4.4. Means and GCA for days to flowering, plant height, disease parameters, lodging, and grain yield.

Parents	Days to flowering		Plant height (cm)		Major lesion length (cm)		Total lesion length (cm)		Number of diseased nodes		Lodging (1-5)		Grain yield (t/ha)	
	Mean	GCA	Mean	GCA	Mean	GCA	Mean	GCA	Mean	GCA	Mean	GCA	Mean	GCA
Females														
ARC1105A	64.06	1.9***	114.99	-4.58***	6.95	1.12***	14.54	1.10***	3.55	-0.16**	2.77	0.15***	3.84	1.04***
ATx623	63.86	1.7***	143.54	23.97***	5.73	-0.1	14.22	0.78**	4.35	0.64***	3.7	1.08***	2.64	-0.16***
AOK11	59.49	-2.63***	113.87	-5.70***	5.53	-0.30**	12.44	-1.00***	3.65	-0.06	1.69	-0.93***	2.42	-0.38***
Mean	**62.47**		**124.13**		**6.07**		**13.73**		**3.85**		**2.72**		**2.97**	
Males														
RIL100(I)	61.2	-0.95	118.63	-0.94	4.3	-1.52**	11.6	-1.84	3.53	-0.18	2.57	-0.06	3.03	0.24**
RIL104(I)	59.7	-2.43**	132.1	12.52***	3.73	-2.09***	11.23	-2.20*	2.63	-1.07***	2.77	0.13	2.97	0.17*
RIL127(I)	61.77	-0.37	127.47	7.91**	9.23	3.39***	17.87	4.41***	4.6	0.92***	2.83	0.2	3.9	1.09***
RIL135(I)	58	-4.15***	116.8	-2.76	4.43	-1.40**	11.13	-2.34*	3.93	0.23	2.57	-0.04	3	0.19**
RIL141(I)	61.47	-0.65	119.9	0.32	3.9	-1.94***	10	-3.46***	3.17	-0.52**	2.57	-0.06	2.7	-0.1
RIL155(I)	60.93	-1.23	118.27	-1.28	5.63	-0.22	13.77	0.32	4.73	1.02***	2.73	0.11	3.43	0.61***
RIL158(I)	55.63	-6.51***	118.97	-0.59	5.57	-0.24	12.93	-0.5	6.17	2.45***	2.67	0.05	4.33	1.49***
RIL161(I)	60.63	-1.51	99.6	-19.96***	6.67	0.81	14.47	0.98	3.57	-0.16	1.5	-1.14***	3.17	0.37***
RIL178(I)	61.7	-0.45	120.8	1.23	6.83	1.00*	13.83	0.4	3.37	-0.32	3.03	0.39**	3.37	0.57***
RIL211(I)	66.9	4.80***	126.47	6.91**	4.07	-1.74**	11.1	-2.32*	3.47	-0.26	2.63	-0.01	2.8	-0.03
RIL212(I)	61.53	-0.56	109.43	-10.16***	8.43	2.60***	16.87	3.41**	4.07	0.35	2.5	-0.11	2.3	-0.53***
RIL216(I)	61.87	-0.26	114.27	-5.31*	7.6	1.75**	19.73	6.26***	5.2	1.47***	2.4	-0.24*	3.1	0.27**
RIL218(I)	61.97	-0.18	120.9	1.31	4.13	-1.71**	10.07	-3.38**	3.97	0.26	2.23	-0.40**	3.03	0.22**
RIL219(I)	61.37	-0.76	123.97	4.38	10.23	4.38***	18.63	5.18***	4.37	0.65**	3.33	0.71***	2.93	0.13
RIL231(I)	64.27	2.16*	129.07	9.48**	5.57	-0.3	13.8	0.37	3.8	0.1	2.97	0.35**	3.53	0.72***
RIL37(I)	67.67	5.55***	114.73	-4.87	6.03	0.18	9.9	-3.57**	3.03	-0.70**	1.83	-0.76***	3	0.20**
RIL44(I)	62.67	0.55	116.07	-3.51	6.43	0.61	12.2	-1.27	2.97	-0.71**	2.13	-0.50***	3.5	0.71***
RIL51(I)	60.9	-1.2	133.67	14.06***	3.47	-2.37***	9.6	-3.85***	2.9	-0.83***	2.67	0.06	2.93	0.1
RIL53(I)	62.3	0.16	126.57	7.01**	5.03	-0.83	14.43	0.99	3.2	-0.50**	2.87	0.21	2.57	-0.24**
RIL80(I)	63.8	1.69	121.63	2.04	5.5	-0.35	11.87	-1.54	2.8	-0.91***	2.73	0.12	1.77	-1.05***
RIL93(I)	62.37	0.24	120.87	1.26	5.8	-0.04	13.57	0.12	3.97	0.25	2.7	0.09	3.2	0.39***
RIL95(I)	67.63	5.52***	123.5	3.92	4.67	-1.18*	12.17	-1.27	3.87	0.15	3.1	0.48***	3.93	1.11***
RIL1(R)	65.47	3.4**	130.1	10.52***	6.17	0.33	13.13	-0.32	4.3	0.55**	2.8	0.19	2.33	-0.49***

Parents	Days to flowering		Plant height (cm)		Major lesion length (cm)		Total lesion length (cm)		Number of diseased nodes		Lodging (1-5)		Grain yield (t/ha)	
	Mean	GCA	Mean	GCA	Mean	GCA	Mean	GCA	Mean	GCA	Mean	GCA	Mean	GCA
RIL113(R)	56.37	-5.76***	140.67	21.11***	4.93	-0.89	12.8	-0.63	4.57	0.85***	2.9	0.31**	3.8	1.02***
RIL14(R)	63.3	1.16	134.43	14.86***	8	2.18***	16.47	3.05**	3.13	-0.61**	3.2	0.60***	2.67	-0.16*
RIL146(R)	67.5	5.38***	136.03	16.43***	5.4	-0.45	14.27	0.81	2.8	-0.91***	2.97	0.36**	2.13	-0.64***
RIL162(R)	63.33	1.21	124.6	4.99*	6.3	0.47	13.3	-0.15	3.53	-0.19	2.8	0.2	3.27	0.48***
RIL166(R)	63.2	1.1	109.13	-10.45***	4.93	-0.91	11.53	-1.9	3.2	-0.51**	2.03	-0.55***	2.63	-0.18*
RIL19(R)	63.23	1.1	131.07	11.51***	6.73	0.88	13.93	0.49	4.17	0.44*	2.93	0.33**	3.13	0.33***
RIL207(R)	61.9	-0.23	106.4	-13.15***	3.93	-1.92***	8.93	-4.48***	3.43	-0.3	1.97	-0.65***	2.87	0.05
RIL209(R)	63.53	1.44	120.37	0.78	5.87	0.02	11.83	-1.59	3.2	-0.52**	2.2	-0.42**	3.17	0.37***
RIL213(R)	64.23	2.13*	112.87	-6.71**	3.8	-2.02***	8.2	-5.25***	2.87	-0.85***	2.2	-0.44**	4.8	2.00***
RIL217(R)	57.07	-5.06***	116.27	-3.31	5.53	-0.29	12.4	-1.05	5.27	1.55***	3.07	0.47***	3.4	0.61***
RIL220(R)	66.53	4.44***	116.5	-3.07	3.4	-2.41***	9.4	-4.04***	3.03	-0.67**	2.37	-0.25*	2.6	-0.21**
RIL222(R)	61.67	-0.45	130.7	11.15***	9.2	3.34***	15	1.58	4.47	0.75***	3.33	0.70***	1.67	-1.15***
RIL229(R)	58	-4.12***	130.57	10.99***	5	-0.83	11	-2.47*	2.7	-1.02***	2.8	0.19	3.63	0.79***
RIL230(R)	65.33	3.21**	127.7	8.11**	5.77	-0.06	12.63	-0.82	2.63	-1.09***	2.97	0.33**	3.77	0.94***
RIL24(R)	67.27	5.13***	123.6	4.03	5.07	-0.79	11.87	-1.59	2.77	-0.95***	3.1	0.45***	2.5	-0.33***
RIL26(R)	56	-6.15***	127.37	7.80**	3.73	-2.09***	11.17	-2.28*	3.97	0.24	2.33	-0.29*	2.6	-0.21**
RIL4(R)	65.7	3.57***	123.7	4.13	5.07	-0.77	12.03	-1.38	2.6	-1.14***	3.1	0.48***	2.33	-0.45***
RIL40(R)	62.63	0.49	116.27	-3.32	5.23	-0.61	12.03	-1.43	3.77	0.03	2.83	0.17	2.2	-0.59***
RIL43(R)	63.03	0.88	134.2	14.63***	5.43	-0.4	10.33	-3.11**	2.93	-0.79***	2.93	0.32**	4.13	1.31***
RIL50(R)	63.03	0.91	108.87	-10.72***	5.6	-0.24	14.2	0.77	3.93	0.23	2.67	0.06	3.4	0.63***
RIL56(R)	57.97	-4.15***	131.77	12.23***	6.97	1.12*	18.23	4.77***	3.87	0.17	2.9	0.28*	2.73	-0.06
RIL73(R)	63.6	1.46	116.03	-3.55	2.93	-2.92***	9.47	-4.00***	2.27	-1.46***	2	-0.62***	2.1	-0.73***
RIL130(S)	59.63	-2.51**	115.47	-4.1	15.03	9.18***	25.9	12.45***	6.13	2.42***	2.03	-0.61***	3.37	0.54***
RIL136(S)	64.83	2.71**	121.3	1.71	4.77	-1.06*	11.67	-1.78	3.8	0.1	2.6	-0.04	2.67	-0.13
RIL15(S)	61.83	-0.31	135.57	16.04***	6	0.18	16.63	3.21**	2.73	-0.98***	2.97	0.31**	1.5	-1.32***
RIL167(S)	60.57	-1.56	140.07	20.49***	6.77	0.91	16.97	3.53**	5.67	1.96***	3.17	0.55***	3.03	0.26**
RIL175(S)	62.17	0.05	130.27	10.66***	9.6	3.77***	16.2	2.75**	5.07	1.33***	3.07	0.45***	3.4	0.62***
RIL176(S)	67.17	5.05***	135.13	15.55***	7.2	1.34**	16.37	2.94**	5.07	1.35***	3.1	0.50***	3.13	0.32***
RIL208(S)	60	-2.15*	126.77	7.18**	6.6	0.76	15.07	1.62	6.03	2.33***	3.23	0.58***	2.87	0.04
RIL32(S)	57.47	-4.68***	124.37	4.79	5.03	-0.78	11.63	-1.78	4.2	0.51**	2.73	0.12	3.13	0.32***

Parents	Days to flowering		Plant height (cm)		Major lesion length (cm)		Total lesion length (cm)		Number of diseased nodes		Lodging (1-5)		Grain yield (t/ha)	
	Mean	GCA	Mean	GCA	Mean	GCA	Mean	GCA	Mean	GCA	Mean	GCA	Mean	GCA
RIL39(S)	64.1	1.96*	125.57	5.98*	7.37	1.54**	24.4	10.97***	3.47	-0.26	3.3	0.67***	2.47	-0.33***
RIL6(S)	62.53	0.41	115.87	-3.69	4.57	-1.29**	10.9	-2.56**	4.13	0.45*	2.83	0.21	2.97	0.17*
RIL83(S)	65.6	3.46**	130.73	11.16***	4.9	-0.92	12.67	-0.76	4.63	0.93***	2.9	0.26*	2.23	-0.58***
RIL84(S)	66.33	4.21***	125.57	5.98*	6.27	0.43	13.73	0.32	3.97	0.23	3.13	0.53***	2.1	-0.72***
RIL85(S)	64.6	2.46**	135.6	16.03***	8.03	2.21***	15.1	1.68	3.4	-0.32	3	0.37**	3.43	0.62***
RIL86(S)	61.83	-0.29	116.5	-3.09	11.73	5.89***	21.47	7.99***	6.13	2.40***	2.03	-0.59***	3.27	0.46***
RIL87(S)	62.17	0.05	153.93	34.36***	6.77	0.92	16.57	3.13**	5.27	1.55***	3.03	0.42**	3.97	1.14***
RIL88(S)	64.17	2.05*	136.83	17.27***	7.87	2.01***	17.8	4.36***	3	-0.73**	3.03	0.41**	1.57	-1.26***
Mean	**62.48**		**124.14**		**6.08**		**13.74**		**3.86**		**2.72**		**2.97**	0

The designation of disease reaction in the bracket: I = intermediate; R = resistant and S = susceptible. ***, **, * statistically significant at 0.001 0.005, and 0.01 levels of probability, respectively.

4.5 Discussion

Information on the inheritance of a trait is of prime importance for parental selection and designing appropriate breeding schemes to improve the trait (Jain & Patel, 2014). Information for selecting parents for population development and hybrid synthesis relies heavily on combining ability of the parental sources (Harer & Bapat, 1982). Sprague & Tatum (1942) emphasized the importance of both specific and general combining ability, SCA, and GCA, respectively. Sprague & Tatum (1942) and Hallauer et al. (2010) interpreted the high GCA effect as a signal for an additive action to be a major player in determining the trait, while higher SCA is a sign of dominance and epistatic effects affecting the trait. Hallauer et al. (2010) suggested the importance of some level of dominance and epistasis to have heterosis and stated the importance of a higher percentage of better parent heterosis commercially. Heritability indicates that the success rate of improvement in the trait would be possible through selection (Falconer, 1996). In this study, sixty-one lines selected from an F_8 RIL population were crossed to three diverse tester females. The resulting hybrids were evaluated with the goal of determining the combining ability of the selected lines with respect to resistance to Fusarium stalk rot.

The result revealed significant variability among the entry and components of the entry for all traits. This was consistent with previous similar studies but in completely different backgrounds (Tesso et al., 2004, 2005). The result also showed a significant effect of the environment on all traits. The effect of the environment on the agronomic performance of crops is well established, and so is the effect of the environment on diseases such as stalk rot. Past studies have shown that the severity of stalk rot diseases is highly confounded with the environment such that the pathogens can cause diseases to cause economic loss only when the environment is conducive to their

development. Stalk rot infection occurs at an early vegetative stage, but the pathogen cannot overtake the host until the host condition is weakened by stresses such as drought or physiological stresses associated with maturity and a combination of the two (Bandara et al., 2017; Perumal et al., 2020). Hence the significant environmental effect simply confirms the importance of these variations. The significant genotype by environment interaction effect simply shows that the test entries were genetically diverse and carry variable fitness potential to environments. A low GCA value, positive or negative, shows that the mean of a parent in crossing with the other does not vary largely from the general mean of the crosses. In contrast, a high GCA value shows that the parental mean is superior or inferior to the general mean. This indicates potent evidence of desirable gene flow from parents to offspring at high intensity and represents information regarding the concentration of predominantly additive genes (Caixeta Franco et al., 2001).

The significant GCA for male and female for disease parameters indicates that additive genes play a significant role in genotypic response to stalk rot infection. Previous studies have reported similar results, and the pattern of variation among genotypes also suggests that several genes of moderate to minor effect contribute to resistance to the disease (Tesso et al., 2004). Dominance genetic effect also appears to have a significant role in affecting stalk rot disease development. Top lines with significant GCA for resistance come from the resistance group, and those with highest GCA for susceptibility come from the susceptible group. No lines from the resistant group showed a susceptible reaction in hybrid combination and vice versa (Table 4.4), indicating that multiple genes with dominance effects condition resistance. A high GCA estimate indicates higher heritability and less environmental effects. It may also result in less gene interactions and higher achievement in selection (Topal et al., 2004; Tyagi & Lal, 2005; Chigeza et al., 2014). One of the main features of the elite parent with high GCA effect is its large adaptability.

Correlation refers to the statistical association between two traits in a population (Lynch & Walsh, 1998). It measures the degree to which two traits co-vary in their expression (Houle, 1992; Dabholkar, 1999). In this study the genotypic correlation between plant height and lodging was highly significant and positive (Tables 4.3). This agrees with a common observation and the law of physics that longer objects are more prone to breakage. The torque produced as a result of head weight tends to be higher taller plants than in shorter plants. Plant height also had significant and positive correlation with lesion lengths (Table 4.3) perhaps not because taller plants are susceptible to the disease but because they have longer internodes through which the pathogen can spread easily compared to shorter plants with short and compact internodes. The correlation between disease parameters in both inbreds and hybrids was highly significant primarily because they are interrelated parameters and were also recorded on exactly same plants.

The correlation between disease parameters and lodging and between disease parameters and grain yield are of great interest. Although both lodging score and grain yield data were recorded on intact plants (not pathogen inoculated), the correlation between these traits and disease parameters was nonsignificant and positive in the hybrids (Tables 4.4). But it was negative in the parents, shows that genotypes that showed susceptible reaction when studied using artificial inoculation are also prone to infection by natural processes that may compromise yield and stalk strength. Although disease incidence was not surveyed among uninoculated plants in the plots, there are chances that pathogen inoculums exist in the soil to cause natural infection given that the environment is conducive for stalk rot pathogens, especially of Fusarium stalk rots.

4.6 Conclusion

We aimed to see the combining ability of the lines randomly drawn from the population developed for mapping Fusarium stalk resistance. The study revealed the presence of significant variability for all traits, including disease parameters. Genotypic responses to disease were different for different environments resulting in significant genotype-by-environment interaction. Although yield data was collected from open plots and disease data from inoculated plants only, the significant negative correlation between disease and yield shows that sorghum yield may suffer from stalk rot infection in almost all years. Since different environments may also harbor different strains of the pathogen, and it will be practically challenging to breed resistant hybrids for specific environments and pathogen strains, future work along this line should emphasize varietal selection across a range of environments or the use of stable resistance sources in the breeding program to capture resistance genes that are stable across environments. The existing screening procedure for resistance to stalk rot diseases is cumbersome and not applicable in breeding nurseries. A high throughput phenotyping procedure for scoring disease severity must be developed to exploit the wide genetic variability for the trait fully.

References

Bandara, Y. M. A. Y., Weerasooriya, D. K., Tesso, T. T., Prasad, P. V. V., & Little, C. R. (2017). Stalk rot fungi affect grain sorghum yield components in an inoculation stage-specific manner. Crop Protection, 94, 97–105. https://doi.org/10.1016/j.cropro.2016.12.018

Bunphan, D., Jaisil, P., Sanitchon, J., Knoll, J. E., & Anderson, W. F. (2015). Heterosis and combining ability of F1 hybrid sweet sorghum in Thailand. Crop Science, 55(1), 178–187.

Caixeta Franco, M., Tulio Cassini, S., Rodrigues Oliveira, V., Vieira, C., Mui Tsai, S., & Damiao Cruz, C. (2001). Combining ability for nodulation in common bean (*Phaseolus vulgaris* L.) genotypes from Andean and Middle American gene pools. Euphytica, 118(3), 265–270. https://doi.org/10.1023/A:1017560118666

Carcedo, A. J. P., Mayor, L., Demarco, P., Morris, G. P., Lingenfelser, J., Messina, C. D., & Ciampitti, I. A. (2022). Environment Characterization in Sorghum (*Sorghum bicolor* L.) by Modeling Water-Deficit and Heat Patterns in the Great Plains Region, United States. Frontiers in Plant Science, 13. https://www.frontiersin.org/articles/10.3389/fpls.2022.768610

Chigeza, G., Mashingaidze, K., & Shanahan, P. (2014). Advanced cycle pedigree breeding in sunflower: Combining ability for oil yield and its components. Euphytica, 195, 183–195.

Dabholkar, A. (1999). Elements of biometrical genetics (revised and enlarged edition). Concept publishing company.

Duff, J., Bice, D., Hoeffner, I., & Weinheimer, J. (2019). The sorghum industry and its market perspective. In Sorghum (pp. 503–514). John Wiley & Sons, Ltd. https://doi.org/10.2134/agronmonogr58.c23

Falconer, D. S. (1996). Introduction to quantitative genetics. Pearson Education India.

FAO, (2021). Food and Agricultural Organization. Crops data 2019, http://www.fao.org/faostat/en/#data/QC.

Hallauer, A. R., Carena, M. J., & Miranda Filho, J. B. (2010). Quantitative genetics in maize breeding, 3rd ed. Handbook of Plant Breeding Volume 6. Springer.

Harer, P., & Bapat, D. (1982). Line X tester analysis of combining ability in grain sorghum. Journal of Maharashtra Agricultural Universities.

Jain, S., & Patel, P. (2014). Combining ability and heterosis for grain yield, fodder yield and other agronomic traits in Sorghum [*Sorghum bicolor* (L.) Moench]. Electronic Journal of Plant Breeding, 5(2), 152–157.

Jardine, D. J. (2006). Stalk rots of corn and sorghum (p. 6). Kansas State University.

Kenga, R., Alabi, S., & Gupta, S. (2004). Combining ability studies in tropical sorghum *(Sorghum bicolor* (L.) Moench). Field Crops Research, 88(2–3), 251–260.

Lynch, M., & Walsh, B. (1998). Genetics and analysis of quantitative traits (Vol. 1). Sinauer.

Makanda, I., Tongoona, P., Derera, J., Sibiya, J., & Fato, P. (2010). Combining ability and cultivar superiority of sorghum germplasm for grain yield across tropical low-and mid-altitude environments. Field Crops Research, 116(1–2), 75–85.

Massaoudou, H., Ba, M., Kapran, I., Danquah, E. Y., Ofori, K., & Gracen, V. (2016). Combining ability for yield and resistance to midge *Stenodiplosis sorghicola* (coquillett) in sorghum (*Sorghum bicolor* (L.) Moench). Journal of Plant Breeding and Genetics, 4(2), 19–33.

Maulana, F., Perumal, R., & Tesso, T. (2021). Hybrid performance as related to genomic diversity and population structure in public sorghum inbred lines. Crop Science, 61(1), 357–371.

Mengistu, G., Shimelis, H., Laing, M., Lule, D., & Mashilo, J. (2020). Combining ability and heterosis among sorghum (*Sorghum bicolor* [L.] Moench) lines for yield, yield-related traits, and anthracnose resistance in western Ethiopia. Euphytica, 216, 1–21.

Mohammed, R., Are, A. K., Bhavanasi, R., Munghate, R. S., Kavi Kishor, P. B., & Sharma, H. C. (2015). Quantitative genetic analysis of agronomic and morphological traits in sorghum, *Sorghum bicolor*. Frontiers in Plant Science, 6, 945.

O'Brien, D. (2019). Domestic and international sorghum marketing. In Sorghum (pp. 477–502). John Wiley & Sons, Ltd. https://doi.org/10.2134/agronmonogr58.c22

Perumal, R., Tomar, S. S., Bandara, A., Maduraimuthu, D., Tesso, T. T., Prasad, P. V. V., Upadhyaya, H. D., & Little, C. R. (2020). Variation in stalk rot resistance and physiological traits of sorghum genotypes in the field under high temperature. Journal of General Plant Pathology, 86(5), 350–359. https://doi.org/10.1007/s10327-020-00940-4

Pfeiffer, B. K., Pietsch, D., Schnell, R. W., & Rooney, W. L. (2019). Long-term selection in hybrid sorghum breeding programs. Crop Science, 59(1), 150–164. https://doi.org/10.2135/CROPSCI2018.05.0345

Pfeiffer, T., Bitzer, M., Toy, J., & Pedersen, J. F. (2010). Heterosis in sweet sorghum and selection of a new sweet sorghum hybrid for use in syrup production in Appalachia. Crop Science, 50(5), 1788–1794.

Robertson, A. (1959). The sampling variance of the genetic correlation coefficient. Biometrics, 15(3), 469–485.

Sprague, G. F., & Tatum, L. A. (1942). General vs. specific combining ability in single crosses of corn. Journal of the American Society of Agronomy.

Tadesse, T., Tesso, T., & Ejeta, G. (2008). Combining ability of introduced sorghum parental lines for major morpho-agronomic traits. Journal of SAT Agricultural Research 6

Tesso, T. T., Claflin, L. E., & Tuinstra, M. R. (2004). Estimation of combining ability for resistance to Fusarium stalk rot in grain sorghum. Crop Science, 44(4), 1195–1199. https://doi.org/10.2135/cropsci2004.1195

Tesso, T. T., Claflin, L. E., & Tuinstra, M. R. (2005). Analysis of stalk rot resistance and genetic diversity among drought tolerant sorghum genotypes. Crop Science, 45(2), 645–652. https://doi.org/10.2135/cropsci2005.0645

Tesso, T. T., Ochanda, N., Claflin, L., & Tuinstra, M. (2009). An improved method for screening Fusarium stalk rot resistance in grain sorghum (*Sorghum bicolor* [L.] Moench.). African Journal of Plant Science, 3(11), 254–262.

Tesso, T. T., Ochanda, N., Little, C. R., Claflin, L., & Tuinstra, M. R. (2010). Analysis of host plant resistance to multiple *Fusarium* species associated with stalk rot disease in sorghum [*Sorghum bicolor* (L.) Moench]. Field Crops Research, 118(2), 177–182. https://doi.org/10.1016/j.fcr.2010.05.010

Tesso, T. T., Perumal, R., Little, C. R., Adeyanju, A., Radwan, G. L., Prom, L. K., & Magill, C. W. (2012). Sorghum pathology and biotechnology—A fungal disease perspective: Part II. Anthracnose, stalk Rot, and downy mildew. The European Journal of Plant Science and Biotechnology, 6, 31–44.

Topal, A., Aydın, C., Akgün, N., & Babaoglu, M. (2004). Diallel cross analysis in durum wheat (*Triticum durum* Desf.): Identification of best parents for some kernel physical features. Field Crops Research, 87(1), 1–12.

Tyagi, A. P., & Lal, P. (2005). Line x tester analysis in sugarcane (*Saccharum officinarum*). The South Pacific Journal of Natural and Applied Sciences, 23(1), 30–36.

USDA. (2022). National Agricultural Statistics Service (NASS), Agricultural Statistics Board, United States Department of Agriculture (USDA).

Appendix A Figures and Tables for Chapter Three

Appendix A Figure A.1. Generalized flow chart of the RNA-Seq experiment and data analysis

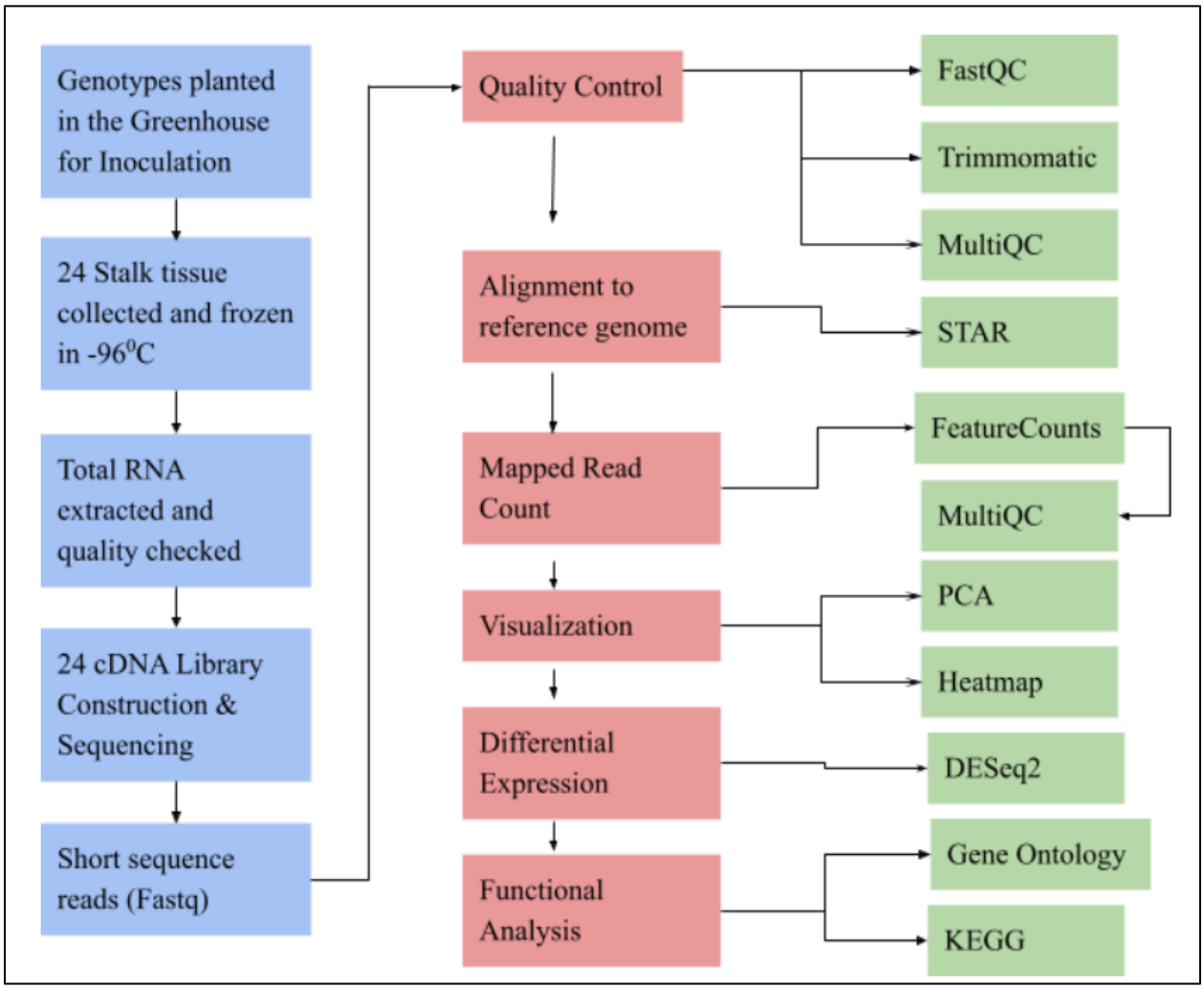

Appendix A Figure A.2. FastQC Plots of different quality parameters

Appendix A Figure A.3. Significant GO:BP terms of DEGs between control and pathogen-treated BTx3042 (Susceptible) at 24 and 48 hpi. (A) downregulated DEG at 24 hpi; (B). downregulated DEG at 48 hpi; and (C) upregulated DEGs at 48 hpi Y-axis=GO pathways, X-axis=Number of genes (Blue) and Fold Enrichment (Orange).

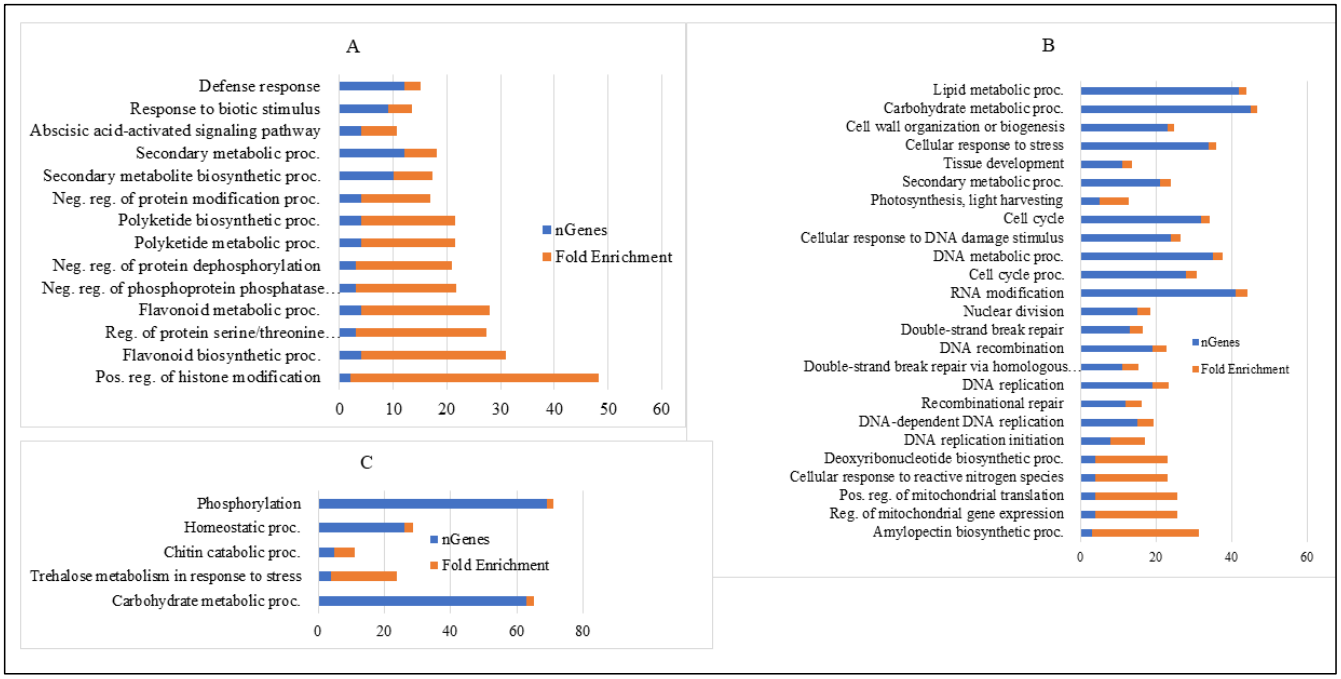

Appendix A Figure A.4. Significant GO:BP terms of DEGs between control and pathogen-treated SC599 (Resistant) at 24 and 48. (A) Downregulated DEGs at 24 hai; (B) Upregulated DEGs at 24 hai; (C) Downregulated DEGs at 48 hai. Y-axis=GO pathways, X-axis=Number of genes (Blue) and Fold Enrichment (Orange).

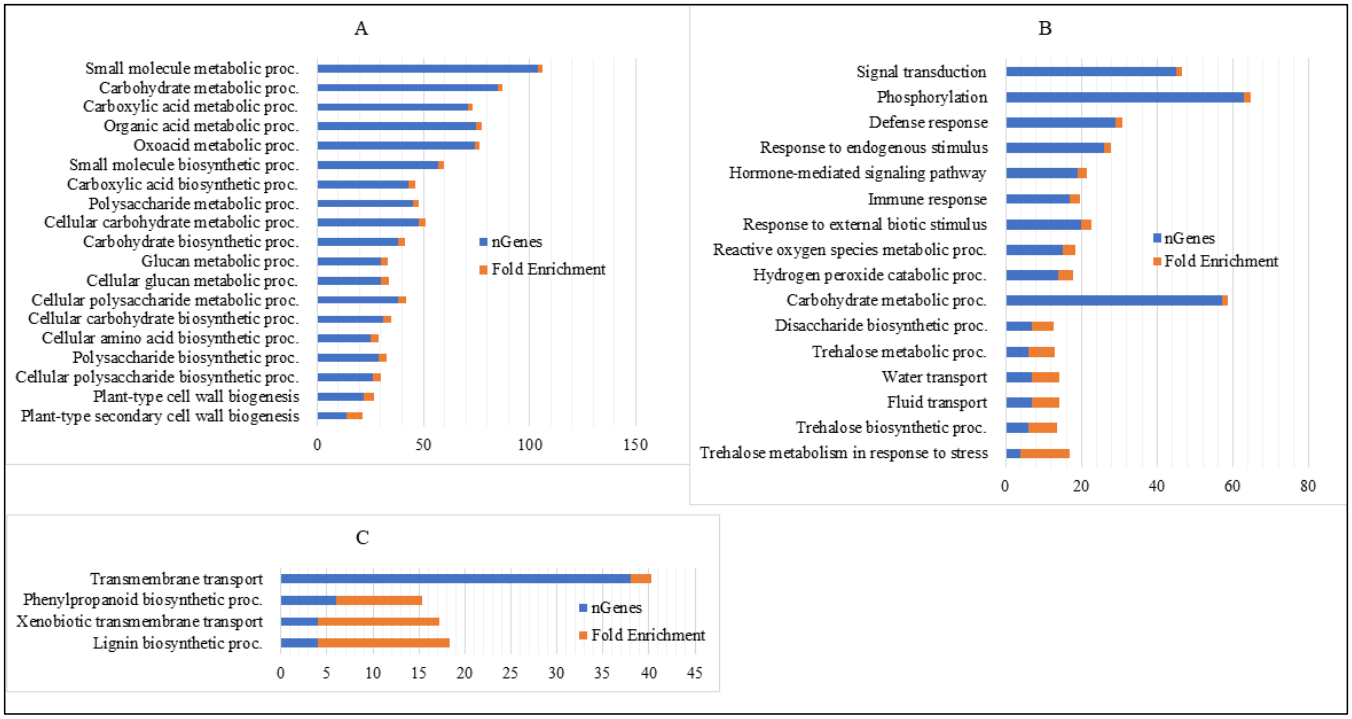

Appendix A Table A.1. Illumina Truseq RNA CD Indexes (96 indexes) and adapter sequences

Sample	Plate layout	i7 Index Name	i5 Index Name	i7 bases	i5 bases
BC24.1	A11	D711	D501	TCTCGCGC	AGGCTATA
BC24.2	B11	D711	D502	TCTCGCGC	GCCTCTAT
BC24.3	C11	D711	D503	TCTCGCGC	AGGATAGG
BC48.1	B12	D712	D502	AGCGATAG	GCCTCTAT
BC48.2	C12	D712	D503	AGCGATAG	AGGATAGG
BC48.3	D12	D712	D504	AGCGATAG	TCAGAGCC
BP24.1	G11	D711	D507	TCTCGCGC	ACGTCCTG
BP24.2	H11	D711	D508	TCTCGCGC	GTCAGTAC
BP24.3	A12	D712	D501	AGCGATAG	AGGCTATA
BP48.1	D11	D711	D504	TCTCGCGC	TCAGAGCC
BP48.2	E11	D711	D505	TCTCGCGC	CTTCGCCT
BP48.3	F11	D711	D506	TCTCGCGC	TAAGATTA
SC24.1	D1	D701	D504	ATTACTCG	TCAGAGCC
SC24.2	E1	D701	D505	ATTACTCG	CTTCGCCT
SC24.3	F1	D701	D506	ATTACTCG	TAAGATTA
SC48.1	F12	D712	D506	AGCGATAG	TAAGATTA
SC48.2	G12	D712	D507	AGCGATAG	ACGTCCTG
SC48.3	H12	D712	D508	AGCGATAG	GTCAGTAC
SP24.1	A1	D701	D501	ATTACTCG	AGGCTATA
SP24.2	B1	D701	D502	ATTACTCG	GCCTCTAT
SP24.3	C1	D701	D503	ATTACTCG	AGGATAGG
SP48.1	G1	D701	D507	ATTACTCG	ACGTCCTG
SP48.2	H1	D701	D508	ATTACTCG	GTCAGTAC
SP48.3	E12	D712	D505	AGCGATAG	CTTCGCCT

Appendix A Table A.2. Raw sequence fastqc general statistics and quality parameters (report generated by multiqc)

Sample	Total seq. (M)	Dup. (%)	GC (%)	Avg. seq. length	Poor qual. Seq.	Seq. length	Total dedup. %	Per base seq. qual.	Per seq qual scores	Per base seq cont	Per seq gc cont	Per base n cont	Seq length distr	Seq dup levels	Overrep seq	Adap cont.
BC24.1	404.7	88.25	48	74.55	0	35-75	11.75	pass	pass	fail	warn	pass	warn	fail	pass	pass
BC24.2	208.5	85.20	48	74.54	0	35-75	14.80	pass	pass	fail	warn	pass	warn	fail	pass	pass
BC24.3	39.4	76.57	48	74.55	0	35-75	23.43	pass	pass	fail	warn	pass	warn	fail	pass	pass
BC48.1	42	77.79	49	74.55	0	35-75	22.21	pass	pass	fail	warn	pass	warn	fail	pass	pass
BC48.2	38.9	78.24	48	74.55	0	35-75	21.76	pass	pass	fail	warn	pass	warn	fail	pass	pass
BC48.3	39	81.33	48	74.54	0	35-75	18.67	pass	pass	fail	warn	pass	warn	fail	pass	pass
BP24.1	42.3	79.97	47	74.55	0	35-75	20.03	pass	pass	fail	warn	pass	warn	fail	pass	pass
BP24.2	39.7	81.54	48	74.55	0	35-75	18.46	pass	pass	fail	warn	pass	warn	fail	pass	pass
BP24.3	36.5	78.31	48	74.55	0	35-75	21.69	pass	pass	fail	warn	pass	warn	fail	pass	pass
BP48.1	39.9	78.05	48	74.55	0	35-75	21.95	pass	pass	fail	warn	pass	warn	fail	pass	pass
BP48.2	38.2	80.41	48	74.55	0	35-75	19.59	pass	pass	fail	warn	pass	warn	fail	warn	pass
BP48.3	33.8	78.82	47	74.54	0	35-75	21.18	pass	pass	fail	warn	pass	warn	fail	pass	pass
SC24.1	36.6	77.70	49	74.55	0	35-75	22.30	pass	pass	fail	warn	pass	warn	fail	pass	pass
SC24.2	31.9	75.31	49	74.55	0	35-75	24.69	pass	pass	fail	fail	pass	warn	fail	pass	pass
SC24.3	31.4	76.19	48	74.55	0	35-75	23.81	pass	pass	fail	warn	pass	warn	fail	warn	pass
SC48.1	40.6	78.25	49	74.55	0	35-75	21.75	pass	pass	fail	warn	pass	warn	fail	pass	pass
SC48.2	34.2	78.07	49	74.54	0	35-75	21.93	pass	pass	fail	warn	pass	warn	fail	pass	pass
SC48.3	36.3	75.52	49	74.55	0	35-75	24.48	pass	pass	fail	warn	pass	warn	fail	pass	pass
SP24.1	28	78.63	48	74.54	0	35-75	21.37	pass	pass	fail	warn	pass	warn	fail	pass	pass
SP24.2	36.4	78.09	49	74.54	0	35-75	21.91	pass	pass	fail	warn	pass	warn	fail	pass	pass
SP24.3	37.6	78.55	49	74.54	0	35-75	21.45	pass	pass	fail	warn	pass	warn	fail	pass	pass
SP48.1	39.1	79.14	48	74.54	0	35-75	20.86	pass	pass	fail	warn	pass	warn	fail	pass	pass
SP48.2	34.5	78.94	48	74.54	0	35-75	21.06	pass	pass	fail	warn	pass	warn	fail	pass	pass
SP48.3	30.4	76.70	49	74.54	0	35-75	23.30	pass	pass	fail	warn	pass	warn	fail	pass	pass

Appendix A Table A.3. Total raw and Trimmomatic quality trimmed Million(M) reads of the 24 single end sequencing libraries

Single-end sequencing libraries	Total Raw Reads M	Trimmomatic		
		Trimmed Reads M	% Survived	%GC
BC24.1	404.7	393.7	97.28	48
BC24.2	208.5	202.1	96.94	48
BC24.3	39.4	38.5	97.48	48
BC48.1	42	40.9	97.5	49
BC48.2	38.9	37.9	97.4	48
BC48.3	39	38.1	97.85	48
BP24.1	42.3	41.3	97.67	47
BP24.2	39.7	38.8	97.68	48
BP24.3	36.5	35.6	97.59	48
BP48.1	39.9	38.9	97.56	48
BP48.2	38.2	37.3	97.75	48
BP48.3	33.8	32.9	97.37	46
SC24.1	36.6	35.5	97.01	49
SC24.2	31.9	31	97.23	49
SC24.3	31.4	30.3	96.63	48
SC48.1	40.6	39.5	97.29	49
SC48.2	34.2	33.1	96.83	49
SC48.3	36.3	35.3	97.06	49
SP24.1	28	27	96.63	48
SP24.2	36.4	35.3	96.94	48
SP24.3	37.6	36.5	97.13	48
SP48.1	39.1	37.9	97.06	48
SP48.2	34.5	33.4	96.76	48
SP48.3	30.4	29.3	96.44	48
Total	1419.9	1380.1		

Appendix A Table A.4. STAR uniquely aligned and feature counts assigned reads of the single end sequencing libraries

Single-end sequencing libraries	Total M reads	STAR		Feature Counts			
		Uniquely Aligned reads M	% Uniquely Aligned	M Assigned	% Assigned	Unassigned M - NoFeatures	Unassigned M- Ambiguity
BC24.1	393.7	348.5	88.5	226.7	65.1	21.4	100.4
BC24.2	202.1	177.8	88	113.5	63.8	11	53.4
BC24.3	38.5	33.9	88.1	22.6	66.6	1.8	9.5
BC48.1	40.9	36.5	89.2	23.9	65.5	2.4	10.2
BC48.2	37.9	33.4	88.3	22.3	66.8	2.1	9
BC48.3	38.1	34.1	89.5	22.8	66.8	2	9.3
BP24.1	41.3	36.4	88.1	23.9	65.6	2	10.5
BP24.2	38.8	34.3	88.6	22.3	64.9	2.2	9.8
BP24.3	35.6	31.6	88.6	20.4	64.6	2	9.1
BP48.1	38.9	34.6	88.8	22	63.5	2.3	10.3
BP48.2	37.3	33.3	89.2	21.2	63.7	2.4	9.7
BP48.3	32.9	28.9	87.6	18.6	64.3	2.1	8.2
SC24.1	35.5	31.5	88.7	21	66.8	1.6	8.9
SC24.2	31	27.5	88.7	18.1	66.1	1.5	7.9
SC24.3	30.3	26.6	87.8	17.9	67.4	1.5	7.2
SC48.1	39.5	34.9	88.5	22.2	63.6	2.2	10.5
SC48.2	33.1	29.1	87.9	18.5	63.4	2	8.7
SC48.3	35.3	31.2	88.5	20.4	65.4	1.9	8.9
SP24.1	27	23.9	88.4	15.3	64	1.6	7.1
SP24.2	35.3	31.1	88	19.6	63.1	2.1	9.4
SP24.3	36.5	32.1	87.9	20.4	63.6	2.1	9.6
SP48.1	37.9	33.5	88.3	20.9	62.4	2.3	10.3
SP48.2	33.4	29.1	87.3	18.7	64.1	1.7	8.8
SP48.3	29.3	25.6	87.5	16.3	63.7	1.5	7.8

Appendix B Tables for Chapter Four

Appendix B Table B.1. Mean squares for days to flowering, plant height, disease parameters, grain yield, and lodging for Hays in 2019 and 2021

Source of variation	df	Mean Squares						
		[1]DTF	PHT	MLL	TLL	NDN	LDG	GYLD
Year (E)	1	172.6***	1012.7***	0.8**	15.7***	0.5***	0.4***	0.01
Block (E)	3	47.5	463.9	2.4	15.4	0.6	0.1	0.1
Entry	246	196.3***	2509.3***	54.3***	179.0***	11.1***	7.1***	6.1***
Inbred	63	97.3***	2292.4***	66.1***	302.5***	4.8***	5.4***	2.1***
Male	60	85.3***	2168***	68.9***	308.4***	4.9***	4.9***	2.0***
Female	2	67.4	297.9	5.3**	5.0	1.0	6.1***	0.5**
Hybrid	182	219.3***	2128***	49.3***	134.4***	12.7***	7.3***	7.0***
Male	60	198.5	1732.7*	90.1***	232.3***	19.5***	3.1	7.3***
Female	2	4463.9***	87330.9***	84.2	308.8	80.6***	389.3***	180.8***
Male x Female	120	160.6	995.7***	28.0***	82.4***	8.2***	2.9***	3.9***
Entry x E	246	4.4	22.2	0.1	0.7	0.03	0.01	0.03
Inbred x E	63	3.6	19.3	0.1	1.0	0.02	0.03	0.1
Male x E	60	3.9	19.8	0.2	1.0	0.02	0.03	0.1
Female x E	2	4.2	975.2	0.04	7.1**	0.2	0.002	0.01
Hybrid x E	182	5.3	25.0	0.1	0.8	0.04	0.01	0.02
Male x E	60	5.8	37.0	0.1	1.0	0.1	0.01	0.02
Female x E	2	1.8	9.0	0.1	1.1	0.1	0.03	0.0
Male x Female x E	120	5.2	19.7	0.1	0.8	0.04	0.02	0.02
Error	975	44.5	234.3	9.1	44.5	1.5	0.6	0.23

[1]DTF = number of days to flowering, PHT = plant height (cm), MLL = major lesion length (cm), TLL = total lesion length (cm), NDN = number of nodes the disease crossed, GYLD = grain yield (t/ha) and LDG = lodging (1-5). ***, **, * statistically significant at 0.001 0.005, and 0.01 levels of probability, respectively.

Appendix B Table B.2. Mean squares for days to flowering, plant height, disease parameters, grain yield, and lodging for Manhattan in 2019 and 2021

Source of variation	df	Mean Squares						
		[1]DTF	PHT	MLL	TLL	NDN	LDG	GYLD
Year (E)	1	18.6	5213.5***	14.8*	297.8***	3.2***	0.1	0.02
Block (E)	3	3.6	380.0	11.7	24.2	0.7	0.3	0.2
Entry	246	127.3***	2988.6***	52.3***	168.8	10.1***	6.2***	7.9***
Inbred	63	77.5***	2767.5***	32.3***	141.4***	2.0**	4.7***	3.1***
Male	60	76.2***	2578.9***	33.4***	147.2***	1.9**	4.3***	2.9***
Female	2	105.5	1735.9	6.6	9.1	1.2	14.1	1.9
Hybrid	182	144.2***	2471.0***	57.1***	168.7***	12.4***	6.5***	8.8***
Male	60	146.3	1618.4*	74.6**	225.2**	16.3*	2.8	8.8**
Female	2	2242.9***	119801.6***	416.2***	1085.9***	60.6**	344.7***	237.5***
Male x Female	120	109.6***	935.6***	42.4***	125.4***	9.6***	2.7***	4.9***
Entry x E	246	15.0	54.2	1.9	11.3	0.3	0.2	0.02
Inbred x E	63	18.5***	79.4**	7.2***	35.4	0.9	0.7	0.02
Male x E	60	18.4***	80.3***	7.5***	36.6	0.9	0.7	0.02
Female x E	2	3.7	47.8	0.3	4.5	0.3	0.03	0.002
Hybrid x E	182	7.3	47.5	0.1	0.8	0.03	0.02	0.02
Male x E	60	8.2	45.8	0.1	0.9	0.04	0.02	0.02
Female x E	2	14.9	344.7***	0.5	3.4	0.01	0.02	0.01
Male x Female x E	120	6.8	43.1	0.2	0.8	0.04	0.02	0.02
Error	975	15.6	175.1	5.9	30.4	1.1	0.5	0.3

[1]DTF = Days to flowering, PHT = plant height (cm), MLL = major lesion length (cm), TLL = total lesion length (cm), NDN = number of nodes the disease crossed, GYLD = grain yield (t/ha) and LDG = lodging (1-5). ***, **, * statistically significant at 0.001 0.005, and 0.01 levels of probability, respectively.